Western Australia School of Mines

Unplanned Dilution and Ore-Loss Optimisation in Underground Mines via Cooperative Neuro-Fuzzy Network

Hyong Doo Jang

This thesis is presented for the Degree of

Doctor of Philosophy
of
Curtin University

July 2014

DECLARATION

To the best of my knowledge and belief this thesis contains no material previously published by any other person except where due acknowledgment has been made.

This thesis contains no material which has been accepted for the award of any other degree or diploma in any university.

Signature: 

Date: *29 October 2014*

To my wife Soyeon and daughter Jinwon

For their endurance, understanding, and love

ACKNOWLEDGEMENTS

I would like to express my appreciation to Professor Erkan Topal for his invaluable supervision, support, and encouragement. Without his support, this research would not have come to its current stage of development.

I wish to express my gratitude to Dr. Youhei Kawamura who served as a co-supervisor. His support, guidance, and inspiration were greatly supportive during the course of research.

I also want to give my thanks to Dr. Takeshi Shibuya (University of Tsukuba, Japan), who shears ideas through discussions, and provides invaluable technical supports about soft computing technologies.

I am very grateful to all of academic and support staffs of the Western Australian School of mines (WASM) in Kalgoorlie campus and thanks to my co-research fellows, Mr. Yu Li, Mr. Don Sandanayake, Miss. Ayako Kusui, Mr. Ushan Zoysa, Mr. Zhao Fu, Mr. Mohammad Moridi, and Mr. Mai Ngoc Luan.

Special thanks to my mother and in-laws for their encouragements and devotions.

Last but not least, thanks to my father in the Heaven.

PUBLICATIONS INCORPORATED INTO THIS THESIS

Some of papers have been published during the period of thesis preparation and details of previous publications are listed below.

- *Jang, H., & Topal, E. (2013). Optimizing overbreak prediction based on geological parameters comparing multiple regression analysis and artificial neural network. Tunnelling and Underground Space Technology, 38, 161-169.*

- *Jang, H., & Topal, E. (2013). Underground Blasting Optimization by Artificial Intelligence Techniques. In Y. Agusta (Ed.), The 3rd International Workshop on Soft Computing and Disaster Control, held in Stikom Bali, Indonesia, November 2013 (pp. 34-35). STMIK STIKOM BALI.*

- *Jang, H. (2013). Maximise underground mine profitability by predicting stope overbreak using artificial intelligence technologies, Akita University Leading Program 2013 workshop delivered at Akita University, Japan, 25 September 2013.*

- *Boxwell, D., Jang, H., & Topal, E. (2014). Using Artificial Neural Networks to Predict Stope Overbreak at Plutonic Underground Gold Mine. Mining Education Australia, 21.*

- *Jang, H., & Topal, E. (2014). A review of soft computing technology applications in several mining problems. Applied Soft Computing, 22, 638-651.*

- *Jang, H., Topal, E., & Kawamura, Y. (2014). Unplanned dilution and ore-loss prediction in long-hole stoping via a multiple regression and conjugate gradient artificial neural network analysis. Journal of the South African Institute of Mining and Metallurgy. (Submitted)*

- *Jang, H., Topal, E., & Kawamura, Y. (2014). Optimisation of unplanned dilution and ore-loss in underground stoping operations using a concurrent neuro-fuzzy system. Applied Soft Computing. (Submitted).*

- *Jang, H., & Yang, H. (2014). A Case Study of Prediction and Analysis of Unplanned Dilution in an Underground Stoping Mine using Artificial Neural Network, Tunnel and Underground Space, 22-4, 282-288.*

ABSTRACT

Unplanned dilution and ore-loss due to underground stope production may be the greatest negative cost factor for the viability of mining operations and can also threaten the safety of both the workforce and the machinery. These phenomena are inevitable when underground stopes are being excavated via drilling and blasting methods. Many studies have been conducted on unplanned dilution and ore-loss, but their precise mechanisms have yet to be clarified. The set of empirical approaches currently used to predict and manage unplanned dilution and ore-loss are unsatisfactory in their predictive performance. Furthermore, these methods offer a qualitative analysis and are limited to predicting unplanned dilution. Thus, the demand for a proper countermeasure to minimise unplanned dilution and ore-loss has arisen.

The aim of this study is to establish a proper unplanned dilution and ore-loss management system. To achieve this, unplanned dilution prediction and consultation systems are proposed and a total management system is established by unifying the prediction and consultation systems. Unplanned dilution and ore-loss prediction models are established using two approaches. Initially, multiple linear and nonlinear regression analyses (MLRA and MNRA) are employed as conventional statistical approaches. Then, a conjugate gradient artificial neural network (CG-ANN) is utilised as an innovative soft computing approach. These unplanned dilution and ore-loss prediction models are established based on 1,067 datasets with ten causative factors via a thorough review of approximately over 30,000 historical documents from three underground stoping mines in Western Australia. Evaluation of the prediction performances of the MLRA, MNRA, and CG-ANN models returned correlation coefficients (R) of 0.419, 0.438, and 0.719, respectively. Given that the unplanned dilution and ore-loss prediction performance for the investigated mines had an *R* of 0.088, the CG-ANN model result is remarkable.

Attempts have also been made to illuminate the mechanisms behind unplanned dilution and ore-loss. The contributions of potential influence factors are scrutinised

using the connection weight algorithm (CWA) and profile method (PM). It was found that the adjusted Q-value (AQ) and the average horizontal-to-vertical stress ratio (K) are significant contributors compared with other factors. Furthermore, some essential trends of unplanned dilution and ore-loss were discovered during the investigation, information that will be helpful not only in underground stope planning but also in the management of stope production.

In succession, a fuzzy expert system (FES) is proposed as an unplanned dilution and ore-loss consultation system based on a survey of 15 mining experts. This system uses adjusted Q-value and the percentage of predicted unplanned dilution and ore-loss as inputs, and the new terminologies of the powder factor (Pf) and ground support (GS) control rates (PFCR and GSCR) are set as outputs. Ultimately, an integrated uneven break and ore-loss management system was achieved by establishing a cooperative neuro fuzzy system via combining the proposed prediction and consultation systems.

TABLE OF CONTENTS

LIST OF FIGURES

LIST OF TABLES

LIST OF ABBREVIATIONS

AE: *Acoustic emission method*
AF_i: *Air pressure impulse*
AF_p: *Air pressure pulse*
AHP: *Analytic hierarchy process*
AHW: *Angle difference between hole and wall*
ANFIS: *Adoptive network based fuzzy inference system*
ANN: *Artificial neural network*
AQ: *Adjusted Q rate*
AsR: *Aspect ratio*
BAO: *Blasting-induced air overpressure*
BBB: *Blasting-induced backbreak*
BD: *Blastability designation*
Bdia *Blasthole diameter*
BFQ: *Blasting-induced frequency*
BFR: *Blasting-induced flyrock*
BID: *Blasting induced damage*
Blen: *Average length of blasthole*
BOB: *Blasting-induced overbreak*
BP: *Blasting parameters*
BRF: *Blasting-induced rock fragmentation*
BTBL: *Stope either breakthrough to a nearby drift and/or stope or not*
CGA: *Conjugate gradient algorithm*
CMS: *Cavity monitoring system*
CNFS: *Concurrent neuro-fuzzy system*
COG: *Centre of gravity method*
CWA: *Connection weight approach*
DG: *Displacements and/or ground settlement*
DOE: *Design of experiments technique*
E_d: *Modulus of deformation*
E_{el}: *Modulus of elasticity*
EHT: *Equotip hardness Tester*
ES: *Engineering state (either stable or unstable)*
ESP: *Equipment selection problem*
FA: *Fuzzy algorithm*
FC: *Failure criteria*
FDAHP: *Fuzzy Delphi analytic hierarchy process*
FDM: *Finite difference method*
FES: *Fuzzy expert system*
FIS: *Fuzzy inference system*
FM: *Failure modes*
FSMLP: *On-line feature selection net*
FWA: *Fuzzy weighted average*
GA: *Genetic algorithm*
GEP: *Genetic programming*

GSCR: *Ground support control rate*
GSI: *Geological Strength Index*
GU: *Gu's rock classification*
HI: *Hollow Inclusion cell over-coring method*
HR: *Hydraulic radius*
I_s***:*** *Point load strength*
K: *Average horizontal to vertical stress ratio*
LDA: *Linear discriminant analysis*
LM: *Levenberg-Marquardt algorithm*
logsig: *Log sigmoid function*
MADM: *Multiple-attribute decision-making*
MD: *Mahalanobis distance*
MLP: *Multi-layer perceptron*
MLRA: *Multiple linier regression analysis*
MMS: *Mining method selection*
MNRA: *Multiple nonlinear regression analysis*
MPL: *Muck pile ratio*
MWC: *Modified Wiebols-Cook criterion*
NH-A: *Nonlinear hydrocodone – Autodyn*
PaD: *Partial derivatives method*
PCA: *Principal component analysis*
Pf: *Powder factor*
PFCR: *Powder factor control rate*
PM: *Profile method*
PPA: *Peak particle acceleration*
PPV: *Peak particle velocity*
P_t***:*** *Tonnes of stope planned*
PUB: *Predicted uneven break*
PWV: *P-wave velocity*
RA: *Simple and/or multiple regression analysis*
RAC: *Rafiai criterion*
RME: *Rock mass excavability*
RMR: *Rock mass rating*
RMSE: *Root Mean Square Error*
RSE: *Relative Strength of Effect*
SA: *Sensitivity analysis*
SbR: *Space and burden ratio*
SC: *Soft computing*
SS: *Subsidence*
tansig: *Hyperbolic tangent*
TC: *Tunnel convergence*
TEX: *Total explosive required*
TOPSIS: *Technique for order performance by similarity to ideal*
TSP230: *Tunnel seismic prediction*
UB: *Uneven break*

UCS:	*Uniaxial compressive stress*
VIDS ///	*A high resolution semi-automatic image analysis system*
VIF	*Variance Inflation Factor*
YAM:	*Yagar's method*
σ_t	*Tensile strength*

CHAPTER 1. INTRODUCTION

Mining is one of the primitive industries of human civilisation (Hartman, 2007). The significance of the mining industry has always been emphasised due to its enormous ripple effects on other industries. In comparison with past centuries, contemporary mining productivity has improved significantly along with the remarkable evolution of mining-related technologies. Through the constant efforts of engineers and scholars, numerous advanced theories and innovative mining methods have been introduced and adopted in various mining industries. Recently, automated machinery has begun to take on dangerous, labour-intensive tasks, drilling has become much faster and more accurate, explosives have become more powerful, and planning has become more systematic and effective through the use of numerous innovative mine design software packages. In fact, the overall processes of mining that are used today are better optimised than ever before.

Nevertheless, there are still many issues to be overcome in actual mining activities. In the field, mining engineers frequently encounter situations requiring them to make decisions without adequate and detailed information. Because an improper decision can directly cause irretrievable damage to not only the mine economy but also to the miners themselves, proper countermeasure systems are indispensable.

Limiting the scope of recurring mining issues to the production of underground stope mining, one of the most complex conundrums is unplanned dilution and ore-loss, a pair of notoriously inevitable and unpredictable phenomena that occur when drilling and blasting methods are used to excavate the ore. In spite of the significant efforts of previous engineers, the majority of underground stoping mines continue to suffer from unplanned dilution and ore-loss. Some of the extent empirical approaches to predicting unplanned dilution have been employed in mines, but existing prediction performance is both unsatisfactory and unable to predict ore-loss. Therefore, the necessity of creating a proper management system to minimise potential unplanned dilution and ore-loss has arisen.

Considering the complexity of the problem, the proposed system must take into account the geological condition of the mine, the mine's blasting scheme and

geometry, factors related to stope design, and human error. This information can be obtained by a thorough review of the planning and reconciliation processes in underground stoping mines. Figure 1-1 demonstrates an example of the stope production process.

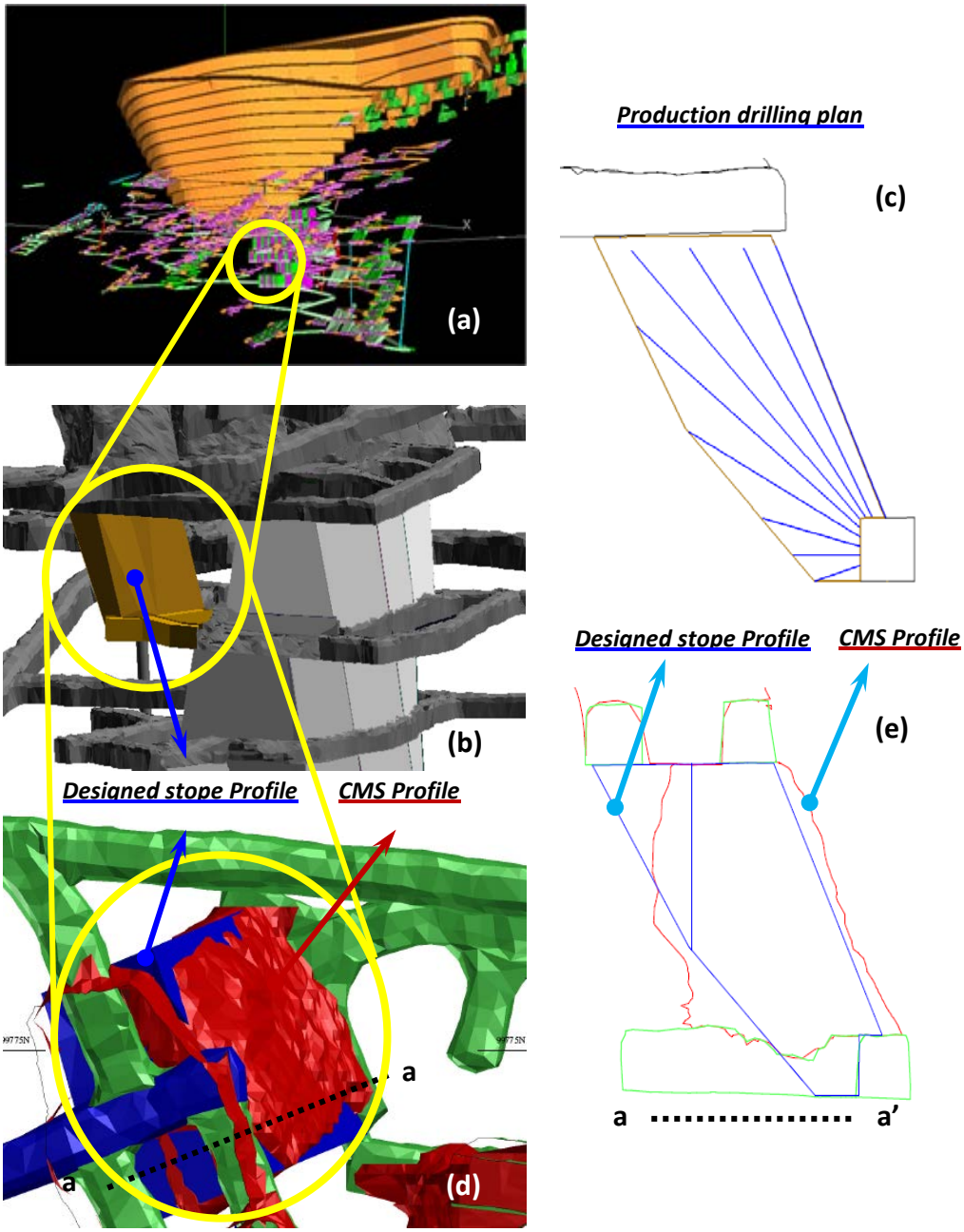

Figure 1-1 Overview of typical underground stope production and reconciliation using a cavity monitoring system (CMS)

As shown in Figures 1-1a and 1-1b, a stope is first planned out in a production stage. To determine the shape and production sequence of the stope, numerous conditions such as the grade of ore, geology, and stress must be considered. After

determining the shape of the stope, the production basting pattern will be planned to fit as the shape of the stope, as shown in Figure 1-1c. After the production blasting, the excavated space will be monitored by a cavity monitoring system (CMS) (Miller & Jacob, 1993) which is a three dimensional laser scanning apparatus specialised for surveying of underground cavities. Figures 1-1d and 1-1e demonstrate a reconciliation process comparing a designed stope profile with an actual stope profile after the production process captured by CMS.

1.1 PROBLEM STATEMENT

In addition to the longstanding awareness of the significance of unplanned dilution and ore-loss, they have further been recognised as highly unpredictable due to their complex occurrence mechanisms. The complexity of unplanned dilution and ore-loss mechanisms, i.e., the over- and under-break, can be explained by features of the object material, the rock mass and dynamic breaking forces, i.e., the shock wave and gas pressure from explosions. The rock mass is one of the complex materials in the earth. The inherent features of the rock mass are that it is anisotropic and inhomogeneous and consists of a group of randomly distributed geological discontinuities. Furthermore, it is stressed by both gravitational and tectonic forces. Thus, the elastic-plastic fracture mechanism of the rock mass itself is complex. The fracture mechanism of the rock mass becomes more complex when it is placed under force by dynamic shockwaves and gas pressure via an explosion, and the complexity increases further when considering the different conditions and designs of underground stopes.

In fact, the majority of underground stoping mines suffer from severe unplanned dilution and ore-loss, which may lead to mine closures. Thus, an appropriate management system for unplanned dilution and ore-loss is desperately needed. The proposed management system must be capable of predicting unplanned dilution and ore-loss and providing appropriate recommendations to mining engineers.

1.2 OBJECTIVES

As a remedy for the difficulties and problems described in the problem statement section, the main objectives of this study are the following:

- Review the existing methodologies for managing unplanned dilution and ore-loss.
- Establish a practical unplanned dilution and ore-loss prediction and consultation systems.
- Implement and validate the proposed system.
- Analyse the contribution of causative factors on the unplanned dilution and ore-loss phenomena to illuminate the occurring mechanism.

1.3 SCOPE

Dilution can be classified in four domains: planned dilution, unplanned dilution, planned ore-loss, and unplanned ore-loss. Planned dilution, also referred as primary or internal dilution, is the low grade material contaminated within the ore reserve block. Planned ore-loss is the ore outside of ore reserve block. These planned dilution and ore-loss are part of stope planning but does not relate to actual production activities. Unplanned dilution, also referred as external or secondary dilution, and unplanned ore-loss can be referred to as over- and under-breaks in underground stope production. These phenomena can be classified into dynamic and quasi-static types (Mandal & Singh, 2009). The quasi-static type occurs at a distance of time after blasting, while the dynamic type occurs immediately. This study focuses on dynamic unplanned dilution and ore-loss, identified by the new term, 'uneven break' (UB). An uneven break (UB) can be defined as the tonnes of mined unplanned dilution (over-break) or unmined ore-loss (under-break) per tonnes of planned stope to be mined and can be calculated as a percentage as follows:

$$UB\ rate = (tonnes\ of\ unplanned\ dilution\ or\ oreloss \div tonnes\ of\ planned\ stope) \times 100 \quad \text{Eq. 1-1}$$

1.4 SIGNIFICANCE AND RELEVANCE

The study proposes a new unplanned dilution and ore-loss management system that will play a significant role in both the planning and production processes of stope mining. Uneven break (UB) can be the main cause of a mine closure, and thus, their proper management with the proposed system can greatly enhance not only mining profits but also the safety of the human workforce and mining machinery. The significance of this research can be summarised as:

- The proposed uneven break (UB) prediction system is the first practical model that can provide a quantitative percentage of potential over- and under-break prior to actual production.
- It is the first successful application of artificial neural networks (ANNs) to predict uneven break (UB) in underground stope production.
- In contrast with previous empirical models that are limited to unplanned dilution, the proposed system covers both unplanned dilution (over-break) and ore-loss (under-break).
- It is the first practical UB control system that provides quantitative values for UB controlling criteria, the powder factor and the ground support control rate (PFCR and GSCR).
- It also attempts to illuminate the mechanism behind UB.

This system gives mining engineers the ability to intuitively recognise the magnitude of unfavourable over and under-breaks in planned stopes. Moreover, the proposed UB consultation system will be performing as a great guide system to minimise the potential UB. Furthermore, some essential trends in the causative factors of UB were revealed through the investigation. These important findings will allow us to gain better understanding of the complex UB phenomenon.

1.5 THESIS OVERVIEW

This thesis is organised into eight chapters. In chapter 1, the representation of the critical conundrum in underground stoping mines, unplanned dilution and ore-loss, is stated. This chapter also includes the objectives and the scope of the research

and demonstrates the significant contributions of the research to the mining industry.

Chapter 2 provides an overview of unplanned dilution and ore-loss in underground stoping mines. In this chapter, the definition, significance, and limitations of current unplanned dilution and ore-loss management systems are critically reviewed.

Chapter 3 comprises a comprehensive review of previous applications of artificial neural networks (ANNs) and fuzzy expert systems (FES) to several mining conundrums.

In chapter 4, the processes of data collection and management of unplanned dilution and ore-loss prediction and consultation models are described.

In chapter 5, UB prediction models are established via two approaches. As a conventional statistical approach, multiple linear and nonlinear regression analyses are employed, and the ANN model is utilised as an innovative soft computing approach.

To illuminate the unplanned dilution and ore-loss mechanism, parameter contributions are investigated in Chapter 6. The investigation was conducted based on the UB prediction systems and provides not only the intensity of potential UB causative factors but also the influential directions.

Chapter 7 presents the concept of a UB consultation system using the fuzzy expert system (FES). Moreover, the details of the integrated UB management system are provided.

Chapter 8 concludes the research by representing the essential findings, limitations and future research directions.

CHAPTER 2. OVERVIEW OF UNPLANNED DILUTION AND ORE-LOSS IN UNDERGROUND STOPING

2.1 INTRODUCTION

Stoping methods have recently been recognised as the most prevalent method of underground hard rock mining. According to Pakalnis et al. (1996), 51% of underground metal mines in Canada utilise open stoping methods, and approximately 70% of underground metalliferous mines in Australia operate by various stoping methods, i.e., open-stoping, sublevel-stoping, narrow-stoping, and other types of stoping (Austrade, 2013). A survey of eight major underground mines in Australia revealed that seven of those eight mines were operating using the sublevel, long-hole, and open stoping methods. In fact, stoping methods have been acknowledged as one of the most efficient and stabilised mining methods for underground metalliferous mining.

Despite the advantages of stoping methods, many mines suffer from severe unplanned dilution and ore-loss, which are often the main cause of mine closures. Furthermore, many mines have reported both direct and indirect damage from unplanned dilution and ore-loss. For instance, Pakalnis (1986) stated that 47% of the open stoping mines in Canada suffered from more than 20% dilution. Moreover, Henning and Mitri (2007) reported that approximately 40% of open stoping operations continue to suffer from 10 to 20 % of dilution. In spite of expeditiously advanced mining technologies, unplanned dilution and ore-loss remain the most critical issue.

This chapter provides an overview of unplanned dilution and ore-loss in underground stoping. The importance of properly managing unplanned dilution and ore-loss is discussed through a review of the features of influential factors in dilution according to previous studies. In addition, several current unplanned dilution and ore-loss management systems are reviewed.

2.2 Definition of dilution

Dilution in mining refers to the contamination of ore with inferior grade ore and/or waste and backfill material. Generally, dilution is categorised in three subgroups: planned, unplanned and ore-loss. Figure 2-1 shows a graphical overview of dilution and ore-loss in an underground stoping operation.

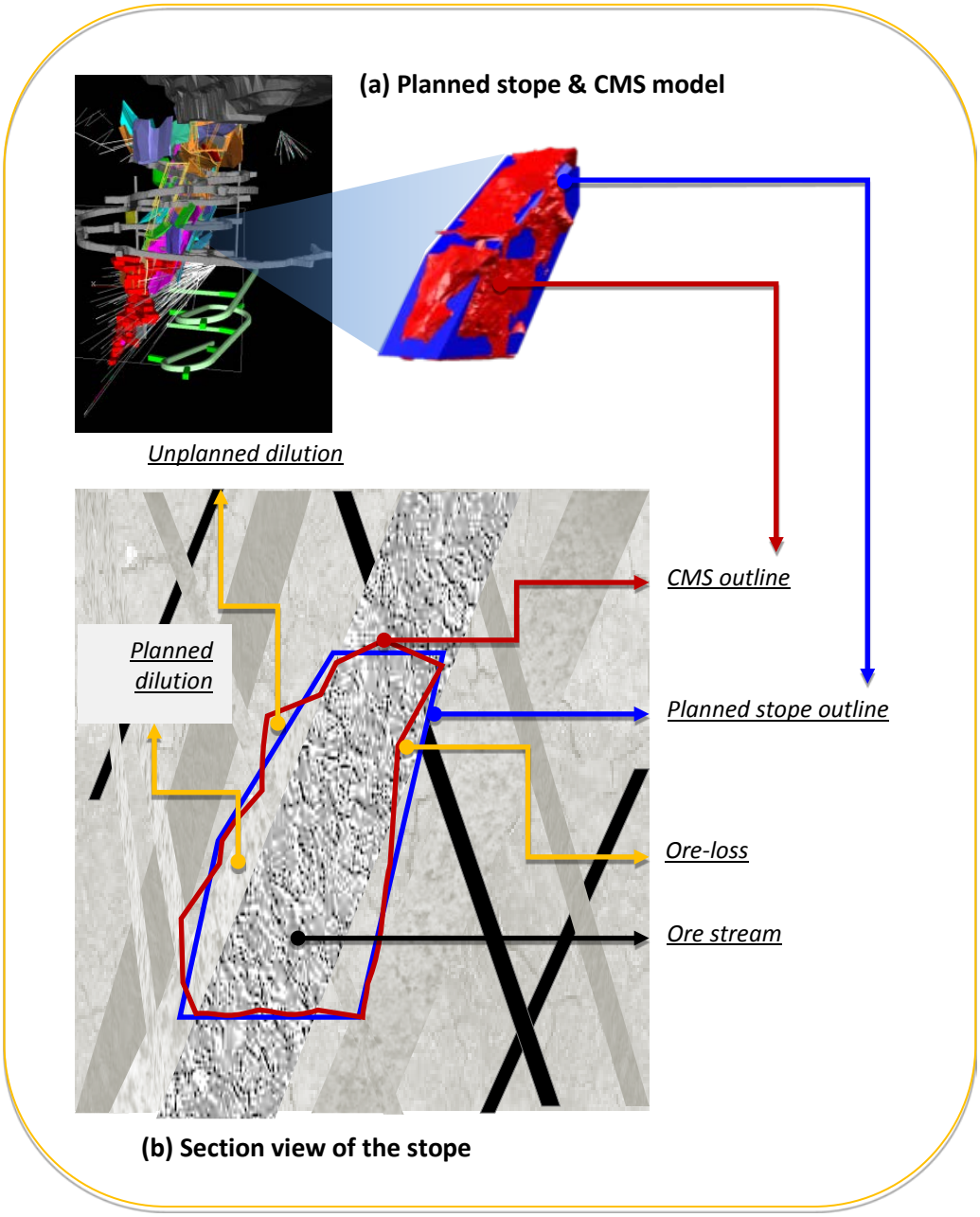

Figure 2-1 Overview of dilution and ore-loss in a stope

As shown in Figure 2-1a, the performance of a stope mine can be assessed by comparing the planned void model to the actual three-dimensional excavated void

model, which can be obtained using a CMS. Figure 2-1b illustrates a sectional view of a monitored stope that clearly shows the formulation of dilutions and ore-loss.

Planned dilution, also called primary or internal dilution, occurs when lower grade material, below cut-off grade, is present within an ore reserve block that contaminates its overall grade. From a different perspective, unplanned dilution, also referred as secondary or external dilution, occurs when a lower grade ore or waste material on the exterior of the ore reserve block intrudes into the produced pure ore stream. Ore-loss can be defined as a missed ore block that remains in the stope after the conclusion of production.

2.3 SIGNIFICANCE OF UNPLANNED DILUTION AND ORE-LOSS

Mining projects always pose inherent uncertainties such as commodity prices and resource models including mining factors. To enhance revenue of mine, dilution and ore-loss are roughly predicted and their global factors are normally included in geostatistical block model and cut-off grade calculation on the feasibility stage of a mining project. These factors have critical importance because they can directly increase operating and opportunity costs that impact on a short term plan as well as the global mine economy. Although a mine has an optimised plan, the mentioned inherent uncertainties make a discrepancy in reconciliation between planned and actual operation. Furthermore, the discrepancy becomes higher in production stages because of inevitable unplanned dilution and ore-loss. In fact, unplanned dilution and ore-loss are the most critical issues for underground stoping mines, directly influencing the productivity of underground stopes and the profitability of entire mining operations.

The significance of unplanned dilution and ore-loss management has been emphasised in numerous studies. Indeed, minimising unplanned dilution is the most effective method of increasing mine profits (Tatman, 2001). The influence of unplanned dilution on the productivity of mining operations has also been emphasised by Henning and Mitri (2008), whose study showed the severe negative economic impact of unplanned dilution and the opportunity costs incurred from additional mucking, haulage, crushing, hoisting, milling and process of waste

required. Unplanned dilution and ore-loss also severely affect profitability of a mine. According to a report on typical narrow vein mines from Stewart and Trueman (2008), unplanned dilution costs 25 AUD/tonne, which is much higher than the typical mucking and haulage cost of 7 AUD/tonne and milling costs of 18 AUD/tonne. Furthermore, the ore-loss also incurs extra opportunity costs which would decrease the net present value of current cash flow of mine. An analysis of financial loss due to unplanned dilution at Kazansi mine in South Africa was conducted by Suglo and Opoku (2012). The study concluded that the economic loss from unplanned dilution from 1997 to 2006 was as high as 45.95 million USD. Likewise, Konkola Mine in Zambia spent 11.30 million USD to manage unplanned dilution in 2002 alone (Mubita, 2005).

Evaluating the productivity of underground stoping methods can be achieved by comparing the amount of unplanned dilution and ore-loss to the amount of planned stopes (Cepuritis et al., 2010), which implies that the inevitable and unpredictable unplanned dilution and ore-loss can not only threaten the safety of the workforce and machinery but also severely impact the productivity of overall mining processes.

Indeed, unplanned dilution and ore-loss are the most critical and negative phenomena associated with the stoping method, and the most effectual way to enhance a mine's productivity is to minimise the amount of unplanned dilution and ore-loss (Tatman, 2001).

2.4 FACTORS INFLUENCE TO UNPLANNED DILUTION AND ORE-LOSS

Unplanned dilution and ore-loss are one of the most complex phenomena in underground stoping operations, and accordingly, numerous known and unknown factors as well as their mutual interactions contribute their occurrence. Thus, the mechanisms underlying unplanned dilution and ore-loss cannot be properly analysed based on a single causative factor or a group of factors; rather, it is imperative to consider the entire range of possible contributing factors together. As shown in Figure 2-2, the causative factors of unplanned dilution and ore-loss can be divided into three core groups with one subsidiary group: stope design factors, blasting factors, geological factors, and human error and other factors.

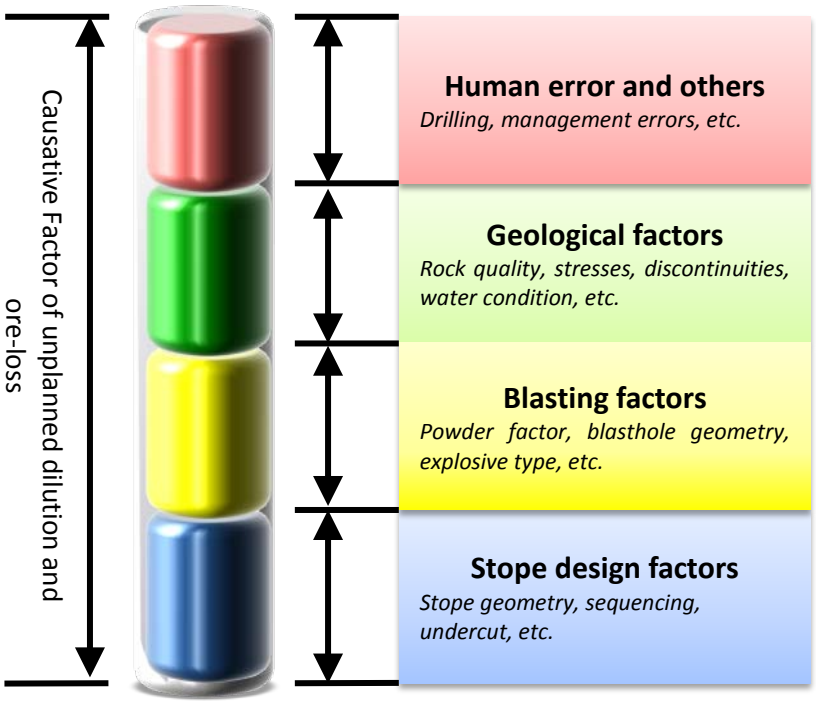

Figure 2-2 Categories of causative factors of unplanned dilution and ore-loss

2.4.1 *Geological factors*

Many researchers have contributed to defining the contributing geological factors to unplanned dilution and ore-loss. However, the anisotropic and heterogeneous features of the rock mass are inherently complex, and defining the geological factors and their effect weights is a difficult task. Figure 2-3 demonstrates the several geological factors behind unplanned dilution and ore-loss in underground stopes.

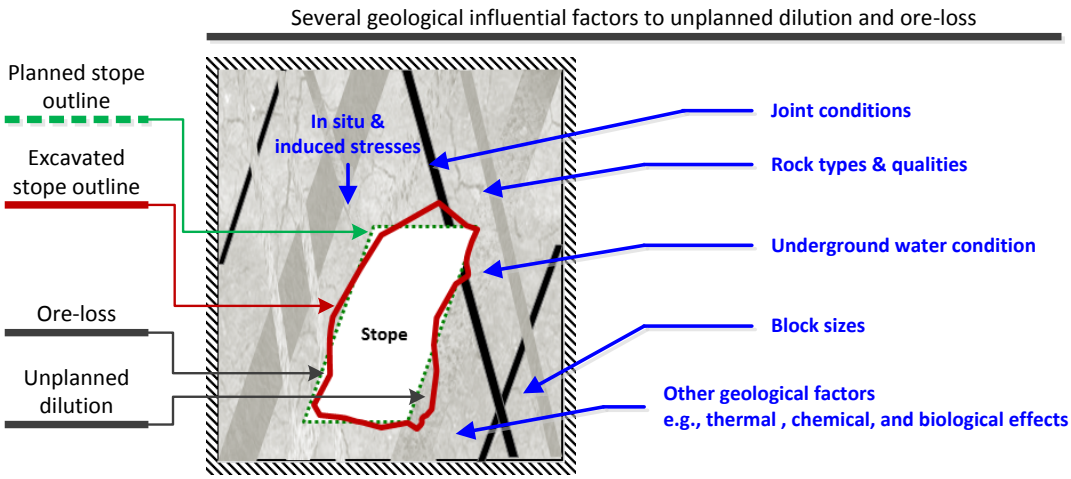

Figure 2-3 Geological factors influencing unplanned dilution and ore-loss

As shown in Figure 2-3, many geological factors influence unplanned dilution and ore-loss, but a group of studies has indicated several essential geological factors in unplanned dilution and ore-loss; these are summarised in Table 2-1 with a comparison to the factors employed in this study.

Table 2-1 Summary of representative geological factors for unplanned dilution and ore-loss and factors employed in this study

Researcher	Geological factors	Employed factors in this study
Potvin (1988)	• *Block size, stress, joint orientation & gravity* • *Support*	*I.* Adjusted Q rate *II.* Average horizontal to vertical stress ratio (K)
Villaescusa (1998)	• *Poor geological control* • *Inappropriate support schemes*	
Clark (1998)	• *Rock quality & major structures* • *Stress*	
Tatman (2001)	• *Less-than-ideal wall condition*	
Mubita (2005)	• *Inadequate ground condition*	
Stewart (2005)	• *Stress damage* • *Pillars*	

As seen in Table 2-1, the majority of the geological circumstances surrounding stopes and their variations have a significant influence on unplanned dilution and ore-loss phenomena. Accordingly, many studies seeking to define the relationship between geological conditions and unplanned dilution and ore-loss have been conducted.

Germain and Hadjigeorgiou (1997) studied the influential factors in stope over-break at the Louvicourt mine in Canada. The excavated stope void was obtained using a CMS and compared with the initial planned stope model. The stope production performances were analysed via linear regression to examine the relationships of the stope geometries and blasting patterns with stope over-break. The correlation coefficients (R) of the powder factor and Q-value compared to the stope performance were found to be -0.083 and 0.282, respectively. The study concluded by reconfirming the complex mechanism of stope over-break.

Suorineni et al. (1999a) conducted a study on the influence of faults in open stopes using numerical analysis. Faults increase the relaxation zone around open stopes, which increases the chance of slough. This study showed the significance of geological factors in dilution phenomena and stope stability.

The influence of stress effects on stope dilution was studied at Bousquet mine in Quebec, Canada by (Henning et al., 2001). The authors investigated the relationship between the profile of sequentially excavated stopes and the attenuation of blasting vibrations with hanging wall deformations. In addition, the rock mass damage extensions on primary and secondary excavated stopes were evaluated via Hook-Brown brittle parameters. The study discovered the important role played by redistributed stress in the extension of the dilution.

As the stress distribution attracted attention as an important contributor to dilution, a case study was conducted in the Kundana gold mines in Western Australia (Stewart et al., 2005). In this study, the authors observed the magnitude of over-break on 410 stopes considering their stress conditions. They found that more than 50% of over-break was observed on the stope wall where stress had exceeded the damage criterion.

Henning and Mitri (2007) conducted a study to examine the influence of stopes' depth, in situ stress, and geometry on the over-break of stope walls. An elastic-plastic numerical analysis program (Map3D) was employed to simulate the behaviour of stope walls under different circumstances, and various aspects of dilution were observed by a comprehensive range of parametric studies. The study found that the stope aspect ratio and major principal stresses have a significant influence on the over-break.

Consecutively, Henning and Mitri (2008) studied the influence of the sequence of stope production on stope dilution. After investigating 172 differently sequenced long-hole stopes, the authors found an increasing magnitude of over-break as the number of backfilled walls escalated.

2.4.2 *Blasting factors*

Drilling and blasting are two of the core activities in both the development and production stages of metalliferous underground mines, and both are still recognised as the most cost effective methods. On the flip side of their cost effectiveness, however, is that rock breakage by blasting is often highly unpredictable. One of the reasons behind this difficulty is in the intrinsic attribute of the dynamic explosion.

Dynamic shock waves and gas pressure will be generated within several milliseconds after the exothermic chemical reaction of the explosion.

The generated dynamic shock waves will promptly propagate into the surrounding material at a rate of several thousand meters per second, and extraordinarily high gas pressures, in the approximate range 20 GPa or more, will directly follow. These energies will easily melt, pulverise, crush, and fracture the surrounding rock mass highly. Furthermore, the dynamic fracture behaviour of the rock mass is influenced by numerous parameters, such as the type and magnitude of the explosives used, the blasting geometries, the geological and geotechnical characteristics of rock masses, the regional climate, and so on. Considering the intersections of the aforementioned parameters, the dynamic rock mass fracture mechanism is extremely complex.

To define the blasting factors that contribute to unplanned dilution and ore-loss, blasting-induced damage must be investigated. Numerous studies have been conducted to define a blast induced damage model; however, the exact rock breakage mechanism has not yet been clearly identified. In fact, the dominant mechanisms for blasting-induced damage (BID), i.e., the effect of blasting-induced shock waves and gas pressures, has been debated for the last 40 years. Some of representative studies of BID are listed in Table 2-2.

Table 2-2 Summary of representative studies of blasting-induced damage

Blasting-induced damage (BID) research priorities concerning shock waves	
Taylor et al. (1986)	• *Uses the continuum damage mechanism (Krajcinovic, 1983) to develop a computational constitutive model that simulates stress wave induced rock failure.*
Yang et al. (1996)	• *Demonstrates a constitutive BID model is demonstrated based on the impulsive loading from stress waves.*
Liu and Katsabanis (1997)	• *Introduces a constitutive BID model based on continuum mechanics and statistical fracture mechanics.*
Zhang et al. (2003)	• *Introduces a BID model for predicting dynamic anisotropic damage and fragmentation*
Wei et al. (2009)	• *Proposes a new BID criterion of peak particle velocity (PPV) damage considering RMR and charge loading density.*

Blasting-induced damage (BID) research priorities concerning gas pressure	
McHugh (1983)	• *Models the act of internal gas and tensile pressures by GASLEAK code (Cagliostro & Romander, 1975) and NAG-FRAG (Seaman, 1980) respectively.*
Paine and Please (1994)	• *Introduces a fracture propagation model by gas.*
Ning et al. (2011)	• *Simulates the explosion gas pressure loading on a jointed rock mass by discontinuous deformation analysis*
García Bastante et al. (2012)	• *Introduces a BID model based on Langefors' theory incorporating the energy load in borehole, coupling factor, and the mean gas isentropic expansion factor*

As demonstrated in Table 2-2, the precise mechanism of blasting-induced damage (BID) has yet to be clarified, and these ongoing studies demonstrate the complexity of over- and under-break mechanisms.

Although rock breakage caused by dynamic explosion forces is exceedingly complex and the influential factors and their intensities are difficult to define, several noticeable blasting factors have been described in existing studies. Table 2-3 demonstrates some of the representative blasting factors in unplanned dilution and ore-loss, as well as the blasting factors employed in this study.

Table 2-3 Summary of representative blasting factors for unplanned dilution and ore-loss and employed factors in this study

Researcher	**blasting factors**	**Employed factors in this study**
Potvin (1988)	• *Blasting practice*	
Villaescusa (1998)	• *Poor initial blast geometry* • *Incorrect blast patterns* • *Sequences of explosive types*	
Clark (1998)	• *Blasthole geometry* • *Up- & down-holes* • *Breakthroughs* • *Parallel & fanned holes* • *Explosive types* • *Blast sequences*	*III. Length of blasthole* *IV. Powder factor* *V. Angle difference between hole & wall* *VI. Blasthole diameter* *VII. Space & burden ratio* *(continuous numbering from table 2-1)*
Tatman (2001)	• *High powder factor*	
Mubita (2005)	• *Poor blasting results*	
Stewart (2005)	• *Blasting damage*	

As shown in Table 2-3, different expressions have been used in different studies, but the fundamental ideas concerning the relationship of blasting factors and unplanned dilution and ore-loss phenomena are the same. To sum up, the geometry of blasting plans and the powder factor appear to be the dominant blasting factors. Regarding suggestions from previous studies, five factors, i.e., the diameter and length of the blasthole, the powder factor, the angle difference between the blasthole and the wall, and the space-to-burden ratio were selected as the blasting factors to be examined here.

2.4.3 *Stope design factors*

Inappropriate stope design, i.e., the shape, size, and sequence of excavation, can cause extreme unplanned dilution and ore-loss. Thus, the geological, geotechnical, and rock-mechanical analyses that are preliminary to stope design should be undertaken with extreme care.

Many studies have examined the relationship between stope design and unplanned dilution. Pakalnis et al. (1995) reported the dilution relationship between the average depth of the slough and the width of the stope after surveying Detour Lake mine in Canada. Figure 2-4 shows a particular tendency: the narrower the stope, the higher the dilution.

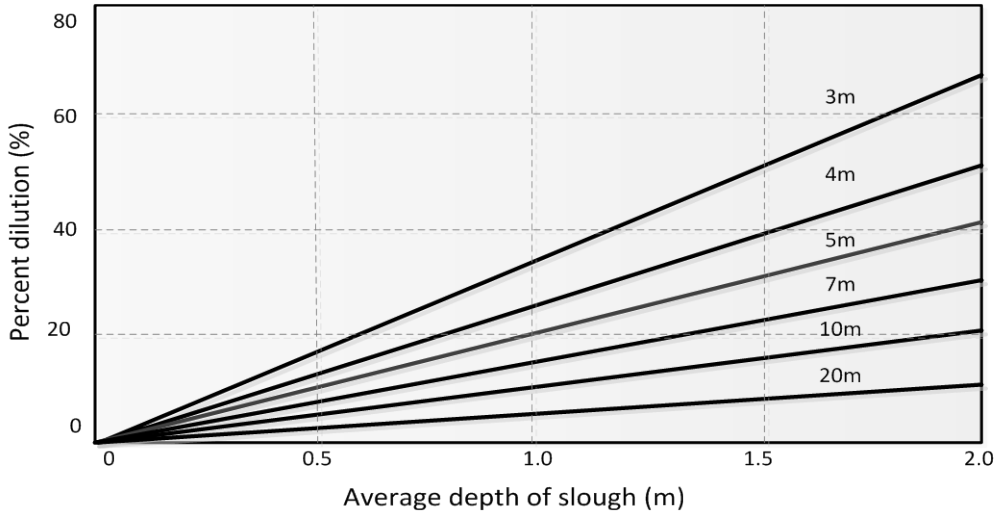

Figure 2-4 Percent of dilution as a function of stope width after Pakalnis et al. (1995)

Hughes et al. (2010) conducted a case study to define the influence of stope strike length on unplanned dilution at Lapa Mine in Canada. The tendency of dilution

subject to different stope strike lengths was evaluated through 2D finite element numerical analysis. The study concluded that unplanned dilution can be significantly reduced by decreasing stope strike length.

The undercutting and/or overcutting of stopes can significantly decrease the stability of the stope hanging wall. The volume of the stress relaxation zone will increase with the undercut (Diederichs & Kaiser, 1999), which can cause massive dilution. Figure 2-5 shows three examples of increasing the relaxation zone by undercutting.

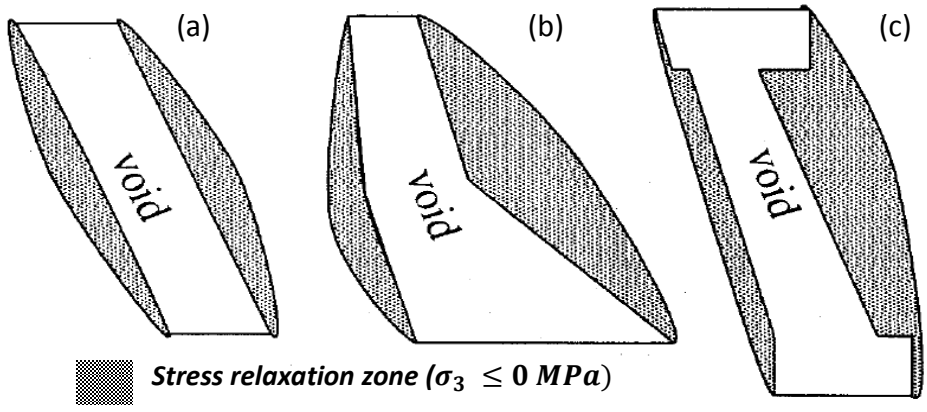

Figure 2-5 Influence of geometry on the stress relaxation zone after Hutchinson and Diederichs (1996)

Wang (2004) conducted a study examining the influence of undercutting on the stability of the stope hanging walls based on historical data from HBMS's mines in Canada. The undercut factor (UF), which compared the degree of undercut with actual dilution, was introduced to qualify the scale of undercutting. The author sought to propose a relationship between unpredicted dilution and UF; however, a typical trend was not found due to limitations in the datasets.

Many published studies have warned of the significant influence of stope height and dip on unplanned dilution. Perron (1999) emphasised the sensitivity of unplanned dilution to the stope height in a field study of Langlois mine in Canada. The instability of the stope wall was perceived in an initial stope design of 60 m high and 20 m wide. The stope was redesigned to increase stability and reduce dilution by developing an additional sub-level that reduced the stope height to 30 m, taking a lower production rate.

The dip of a stope can significantly influence unplanned dilution. As the dip of the stope decreases, a larger relaxation zone will develop around the stope, which can increase the dilution on the stope wall. The relationship between hanging wall dip and unplanned dilution was studied by Yao et al. (1999), who demonstrated that the stope over-break tends to decrease when the dip in the hanging wall is higher. Several suggestions concerning possible stope design factors influencing unplanned dilution and ore-loss are tabulated and compared with the list of factors employed in this study in Table 2-4.

Table 2-4 Summary of representative stope design factors influencing unplanned dilution and ore-loss and employed factors in this study

Researcher	Stope design factors	Employed factors in this study	
Potvin (1988)	• *Stope geometry and Inclination*		
Villaescusa (1998)	• *Poor stope design* • *Lack of proper stope sequencing*	*VIII.*	*Planned tonnes of stope*
		IX.	*Aspect ratio*
Clark (1998)	• *Stoping sequence, supports, & geometry* • *Hydraulic radius and slot raise location*	*X.*	*Stope either breakthrough to a nearby drift and/or stope or not*
Tatman (2001)	• *Improperly aligned drill holes*		
Mubita (2005)	• *Stope boundary inconsistencies* • *Inappropriate mining methods*	*(continuous numbering from table 2-3)*	
Stewart (2005)	• *Undercutting and extraction sequences*		

2.4.4 *Human error and other factors*

All of the procedures of stope production should be executed as closely as possible to the planned design, but of course, mistakes can occur at any stage of production. For example, mining engineers are often forced to make ad-hoc decisions concerning the dimensions of the stope, sequencing of stope developments, and the timing of backfill. To carry out prompt and precise determinations, the engineer should have sufficient experience in the field coupled with a broad understanding of geological and geotechnical ideas.

Human error is also a regular occurrence in field exercises. Although contemporary mining machinery, for instance, drilling machines, are far more advanced than their

older counterparts, drilling precisely as planned remains nearly impossible. In fact, the complex geological features of natural rock impedes many drilling activities, including posing precise collaring location, straight line drilling without any deviations, and reaching exact depths.

The influence of human error on unplanned dilution and ore-loss can be magnified when it is accompanied by other unfavourable geological conditions. Many researchers have noted the importance of human error and other factors, and Table 2-5 provides a summary of several representative comments.

Table 2-5 Summary of representative human errors and other factors in unplanned dilution and ore-loss

Researcher	Stope design factors	Employed factors in this study
Potvin (1988)	• *Backfill & adjacent stope* • *Timing*	*Indirectly implied blasthole deviation through the average blasthole length*
Villaescusa (1998)	• *Deviation of blastholes* • *Lack of supervision & communication* • *Hushed stope planning & lack of stope performance review*	
Clark (1998)	• *Realistic collar location* • *Blasthole deviation* • *Communication between engineers*	
Tatman (2001)	• *Excessive equipment limitations*	
Mubita (2005)	• *Poor mining discipline*	
Stewart (2005)	• *Backfill abutment* • *Damage to cemented fill*	

Although the expressions differ, the underlying considerations are similar. As the data collection for the present study relied on historical documents, data on the human error and other factors were impossible to obtain. To include human error factors in the proposed models, the average blasthole length was collected because the accuracy of drilling is generally expressed as a percentage of the blasthole depth (Stiehr & Dean, 2011).

2.5 CURRENT MANAGEMENT OF UNPLANNED DILUTION AND ORE-LOSS

Unplanned dilution and ore-loss are the most critical problem in underground hard rock mines and are considered to be inevitable during the process of stope excavation. Thus, the goal in creating a management system for unplanned dilution and ore-loss is not absolute prevention but minimisation. In spite of the contributions of many researchers, the majority of unplanned dilution and ore-loss management still relies on historical stope reconciliation information and experts' knowledge. Some of these methods are demonstrated in the following sections.

2.5.1 *Stability graph method*

Notwithstanding efforts by numerous researchers, a model for unplanned dilution and ore-loss that considers the overall range of causative factors has not been introduced. The majority of existing unplanned dilution and ore-loss studies have attempted to discover the relationship of dilution and ore-loss with a few particular causative factors.

Recently, the stability graph method (Mathews et al., 1981; Potvin, 1988) has become the most frequently used approach for managing unplanned dilution and stope stability. This method has distinguished itself as adequate to estimate stope dilution and has been promoted by both industry and academia accordingly (Diederichs & Kaiser, 1996; Pakalnis et al., 1996). The stability graph method charts a stability number (N) against a hydraulic radius (HR: area/perimeter of the stope wall) of the stope wall. The stability number (N) was modified by Potvin (1988) and is defined as:

$$N' = Q' \times A \times B \times C \qquad \text{Eq. 2-1}$$

Where N' is the modified stability number, Q' is the modified Q ratio (Barton, 1974), A is the stress factor, B is the joint orientation factor, and C is the gravity factor. Figure 2-6, Figure 2-7, and Figure 2-8 demonstrate the graphical determination of the A, B, and C factors.

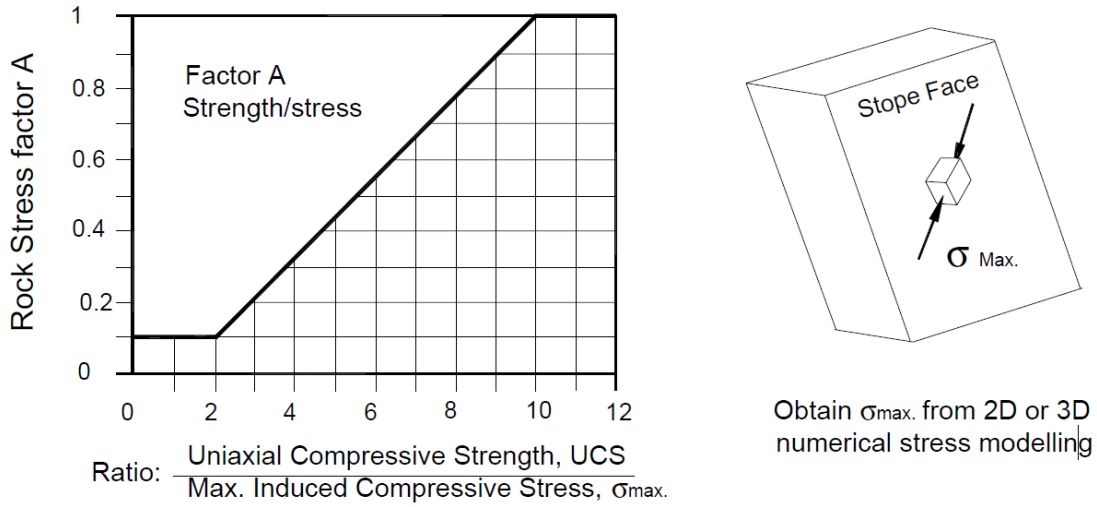

Figure 2-6 Graphical determination of stress factor (A) after Potvin (1988) from Wang (2004)

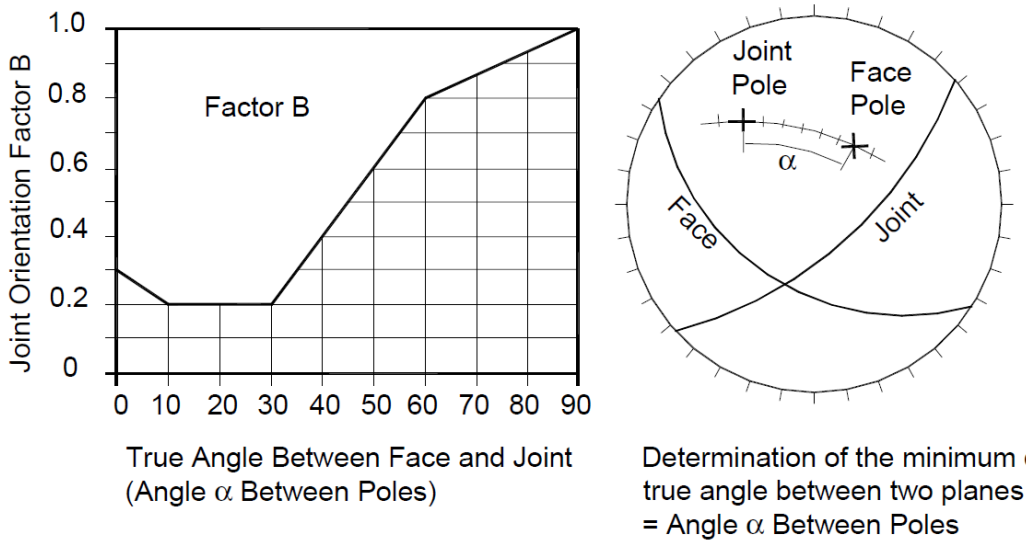

Figure 2-7 Graphical determination of joint orientation factor (B) after Potvin (1988) from Wang (2004)

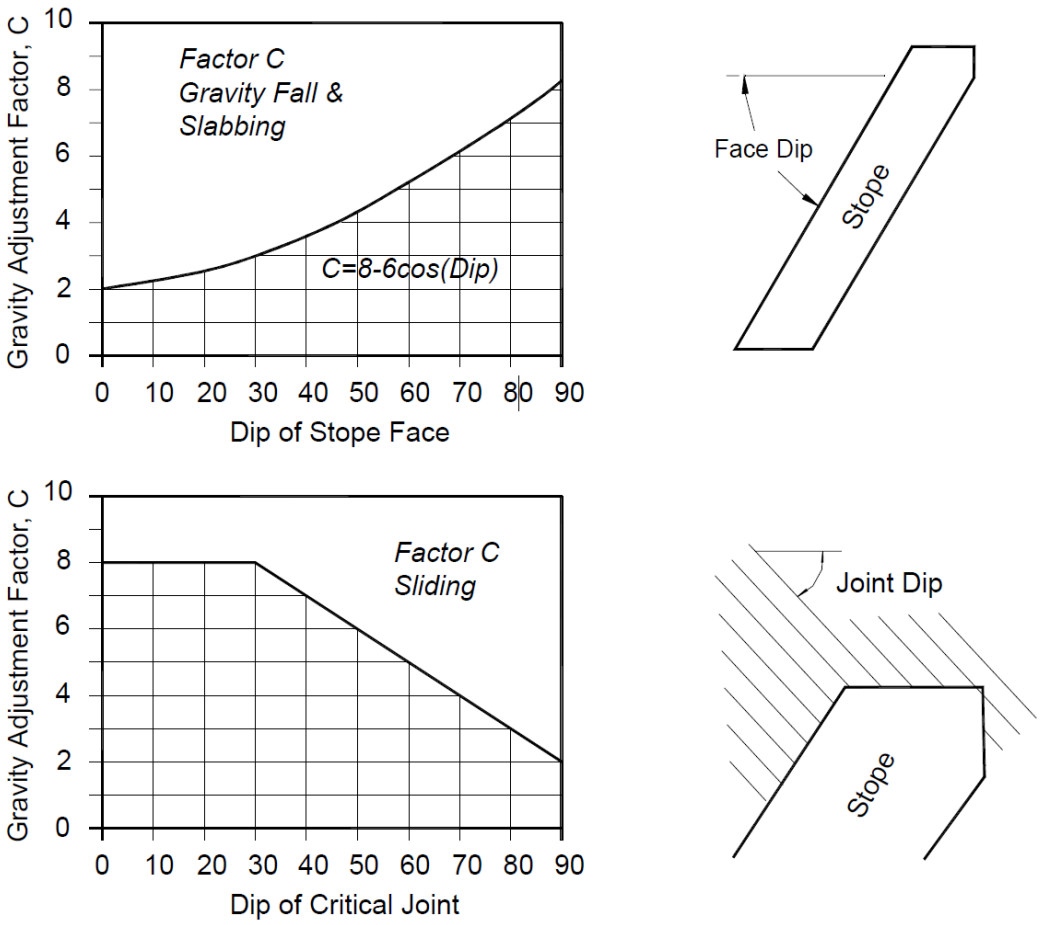

Figure 2-8 Graphical determination of gravity adjustment factor (C) after Potvin (1988) from Wang (2004)

Since Mathews first introduced the stability graph method in 1981, it has been modified and improved upon by various authors. Significant modifications include:

- Nickson (1992) – Introduced and incorporated cable bolt effects on the stability of the stope wall.
- Scoble and Moss (1994) – Proposed dilution lines.
- Clark (1998) - Proposed an empirical stope design approach with new terminology, ELOS (equivalent to linear over-break/slough).
- Hadjigeorgiou et al. (1995) and Clark and Pakalnis (1997) - Modified the gravity factor.
- Suorineni et al. (1999b) - Introduced a new factor for faults.

In the stability graph method, the delineation of a stable or caved zone is determined using logistic regression. Figure 2-9 demonstrates the stability graph method as suggested by Mathews et al. (1981) and Nickson (1992).

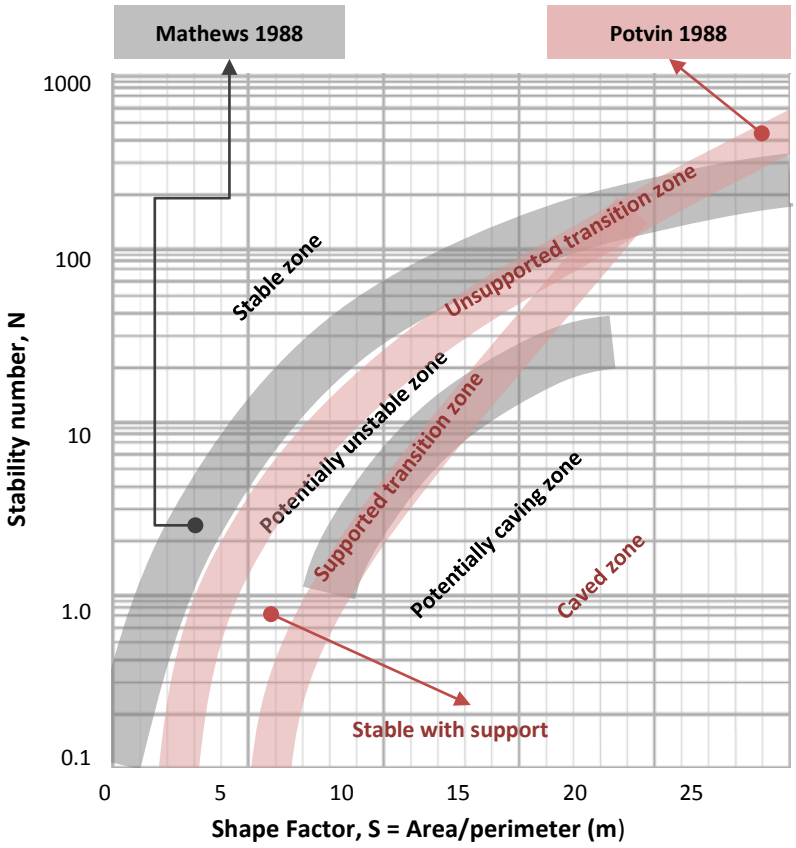

Figure 2-9 Stability graph proposed by Mathews et al. (1981) and Nickson (1992)

In spite of the reputation of the stability graph method, certain limitations have been noted by several researchers, including:

- The method does not consider the far field stress relative to the stope orientation. (Martin et al., 1999)
- It is not applicable to rock-busting conditions (Potvin & Hadjigeorgiou, 2001)
- Because the stability graph method was developed based on ranges from a particular database, its application can be limited within those original ranges.
- It does not account for the exposure period of the stope wall.
- It does not consider the alteration of induced stress via stope sequencing.
- It does not consider blasting factors.

Concerning the limitations of stability graph method, predicting unplanned dilution and ore-loss appears to be a rather difficult task. Indeed, the complex occurrence mechanism of unplanned dilution and ore-loss is a significant impediment to its predictability.

2.5.2 *Other empirical approaches*

Other empirical methods have been adopted to evaluate stope design. The critical span curve method was first introduced in 1994 for back stability analysis in cut and fill mines (Lang, 1994). The initial method has been improved upon by researchers at the University of British Colombia by expanding the datasets up to 292 case studies (Wang et al., 2000). The definition of the 'critical span' is the diameter of the largest circle of unsupported back in the stope, and the stability of the stope back is related to the designed unsupported span. The method comprises three domains, i.e., stable, potentially unstable, and unstable. The span design coves formulated by the 292 datasets are shown in Figure 2-10.

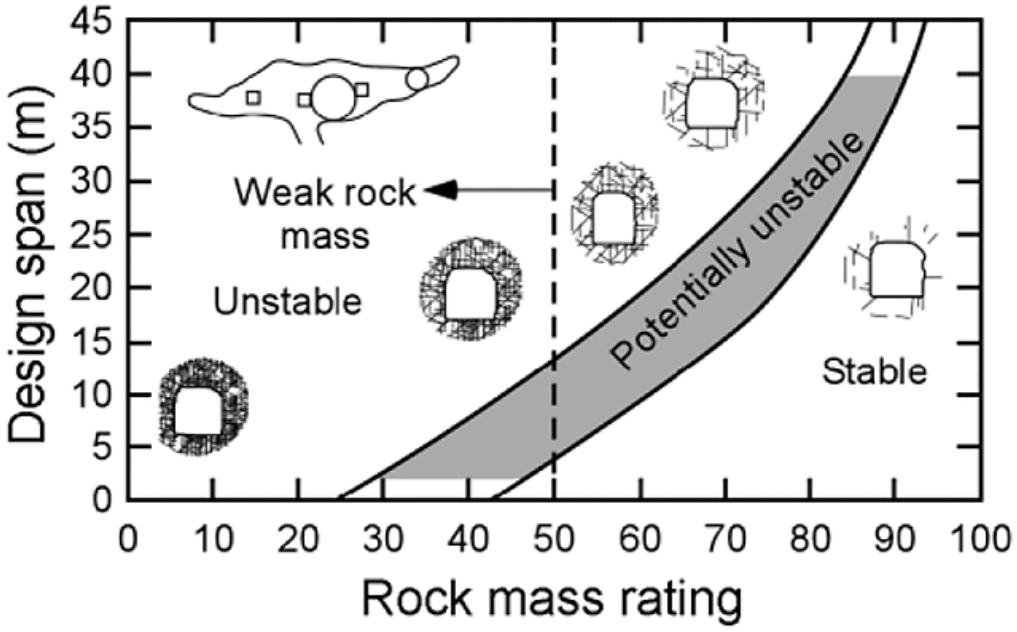

Figure 2-10 Span curve method after Brady et al. (2005)

A quantitative dilution estimation model was introduced by Pakalnis (1986) based on historical data from the HBMS Ruttan mine. Stopes were categorised in three groups: isolated, adjacent rib, and echelon. The hydraulic radius and rock mass rating (RMR) were used as parameters to determine the percentage of dilution. For example, the dilution estimation model for an isolated stope is shown in Figure 2-11.

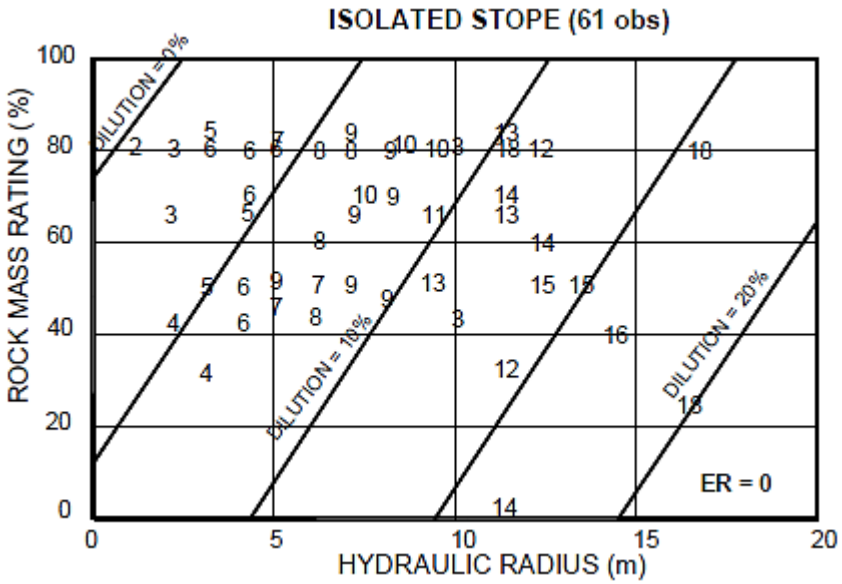

Figure 2-11 A quantitative dilution estimation approach for an isolated stope after Pakalnis (1986)

2.5.3 *Numerical analysis*

Recently, numerical analysis has become prevalent in the mining industry to analyse stope stability. Indeed, numerical methods have become an essential procedure in analysis and a fundamental process in rock engineering design (Jing, 2003). Figure 2-12 shows some of the representative numerical analysis methods used in mines.

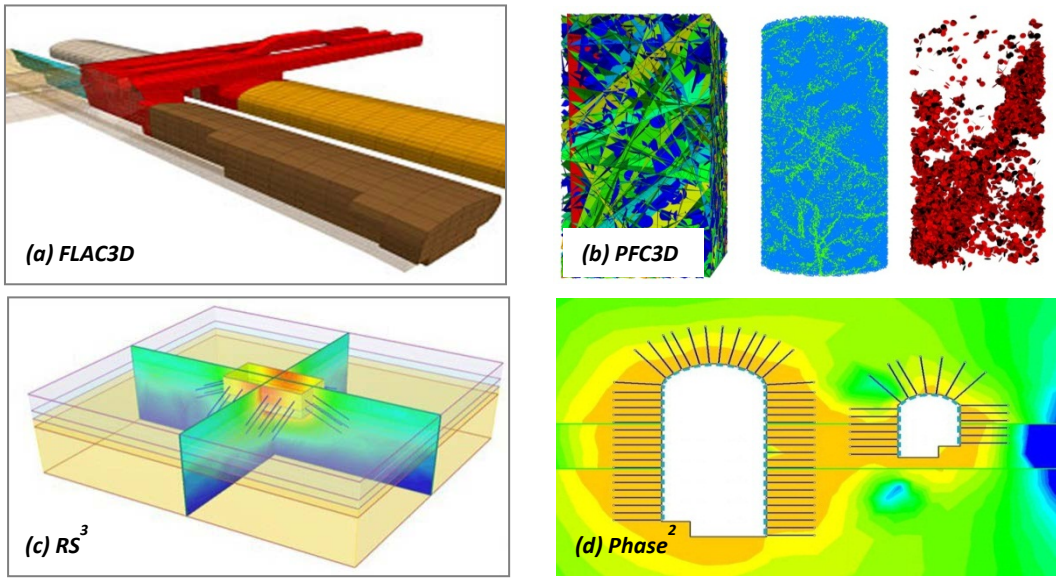

Figure 2-12 Schematic view of representative numerical analysis methods

Many methods have been developed to create simulations that are as close as possible to natural rock conditions. Figures 2-12a and 2-12b show the FLAC3D (3D

continuum modelling analysis) and PFC3D (3D dis-continuum particle flow analysis) models from Itasca Consulting Group (2013), and Figures 2-12c and 2-12d show the RS3 (3D finite element stress analysis) and Phase2 (Elastic-plastic finite element stress analysis) models from Rocscience inc (2014). These numerical analysis models have continued to evolve with the rapid technological advances in computer science.

Many mines today use these numerical analysis methods to verify stopes' stability and attempt to predict the occurrence of an over-break on the stope wall. However, the dynamic fracture and failure mechanisms of over- and under-breaks on the anisotropic and heterogeneous features of rock mass remain a herculean task.

2.6 SUMMARY AND DISCUSSION

This chapter concentrates on three topics. First, the significance of unplanned dilution and ore-loss in underground stoping mine was examined through a comprehensive review of previous publications. Second, potential causative factors of unplanned dilution and ore-loss were reviewed and ultimately categorised as being due to geological factors, blasting factors, stope design factors, and human error and other factors. Finally, several unplanned dilution and ore-loss management models were reviewed.

Current management systems for unplanned dilution, ore-loss and stope stability have been improved by various statistical, empirical, and numerical modelling methods. However, no extant model specifically considers the geological, blasting, stope design and human error factors simultaneously.

In general, it appears to be impractical to consider all of these factors simultaneously due to the complexity of the mechanisms behind unplanned dilution and ore-loss. Additionally, although numerical analysis has further potential as computer technology continues to advance, anticipating all possible causative factors remain beyond its capacity.

A novel innovation in unplanned dilution and ore-loss prediction and consultation models is established in this study by the use of artificial neural network and fuzzy

algorithms. The proposed models include ten causative factors that cover the majority of the possible roots of unplanned dilution and ore-loss.

CHAPTER 3. OVERVIEW OF ARTIFICIAL NEURAL NETWORK AND FUZZY ALGORITHM AND APPLICATIONS IN MINING

3.1 INTRODUCTION

As mentioned in earlier chapters, the uneven break (UB) is one of the most complex phenomena in underground stope production and has severe negative effects on both the productivity and profitability of entire mining processes. Furthermore, due to its complexity, it is impossible to create a straightforward prediction model via conventional statistic and stochastic models.

To overcome these difficulties, advanced soft computing technologies have been employed to establish uneven break (UB) prediction and consultation models. Soft computing is distinct concept from hard computing, which operates on the basis of binary values. Soft computing can be defined as 'a collection of methodologies that aim to exploit tolerance for imprecision and uncertainty to achieve tractability, robustness, and low solution cost' (Zadeh, 1994), and fuzzy algorithms, artificial neural networks, supporting vector machines, evolutionary communication, machine learning, and probabilistic reasoning are its core principles. Soft computing technologies have been successfully employed in a broad range of industries and have attracted attention from mining engineers and scholars. Consequently, SC has been applied to many of mining's most challenging problems since the 1980s.

Among various SC principles, this study employs artificial neural networks (ANNs) and fuzzy algorithms (FAs) to establish an uneven break (UB) prediction and consultation program. ANN has been recognised as a powerful tool in nonlinear approximation, which is suitable for modelling the uneven break (UB) prediction system. Moreover, fuzzy algorithms (FAs) have the advantage of treating imprecision and uncertainty data, which is appropriate for modelling the uneven break (UB) consultation system. This chapter contains a brief overview of ANNs and FAs. In addition, previous ANN and FA applications in mining-related subjects are reviewed.

3.2 ARTIFICIAL NEURAL NETWORK

The artificial neural network (ANN) is a parallel computational inference model whose functionality is a simple imitation of a biological neuron. As demonstrated in Figure 3-1, the ANN model is comprised of input, hidden, and output layers, with each layer consisting of a number of artificial neurons, a simple mathematical element (referred to as a neuron).

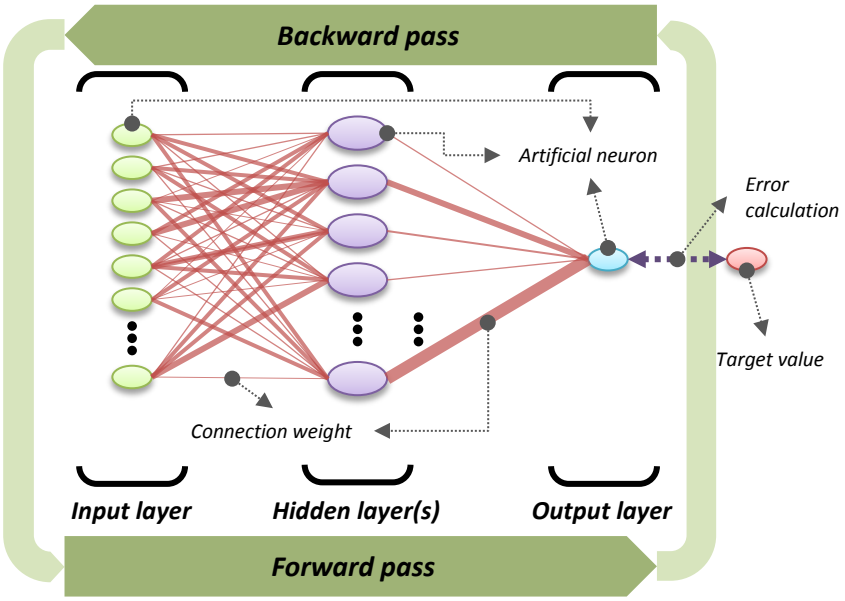

Figure 3-1 Architecture of the multilayer feed-forward ANN

As shown in Figure 3-1, the neurons are completely interconnected to nearby layers and the connection intensity is expressed by the numerical weight. The ANN has three processes: training, validation, and testing. In the training stage, the optimum weights of all connections can be achieved via forward and backward calculations. The forward process computes a predicted output and compares it with an actual target value to calculate the error of the iteration; the forward process then updates all prior connection weights based on the error. Indeed, the ANN is optimised by discovering the optimum weight values of the model connections.

3.2.1 *How ANN works as a human brain*

In spite of the advancement of technology, the human brain, which has more than 10 billion neurons and 6 trillion synapse combinations, is a better processor than a digital computer. Neurons use biochemical reactions to receive, process, and

transmit information through synapses, and this complex network allows us to handle perceptual and cognitive matters, as well as providing us with the capacity to process imprecise information. In fact, the most fascinating aspect of the brain is that it can learn. The artificial neuron network (ANN) is a mathematical model of the biological nervous system. Like a biological brain, neurons receives signals from other neurons, which can be intensified and weakened by proper activation functions, and the connection weights modulate the input signals just as synapsis does in the brain. An ANN's learning ability can be activated by adjusting the weights with the applied learning algorithm.

3.2.2 *Types of ANN learning algorithms*

ANN learning can be generally classified as supervised, unsupervised, and reinforcement learning. This study focuses on supervised learning, which must occur through paired input and output data.

3.2.2.1 Initial ANN learning algorithm

The first authorised ANN study was presented by McCulloch and Pitts (1943). In their model, each neuron was assumed to be in a binary state. Later, Rosenblatt (1958) introduced the perceptron (a procedure-type training algorithm), which is the simplest form of the current ANN model. Figure 3-2 shows a single layer perceptron with multiple input nodes.

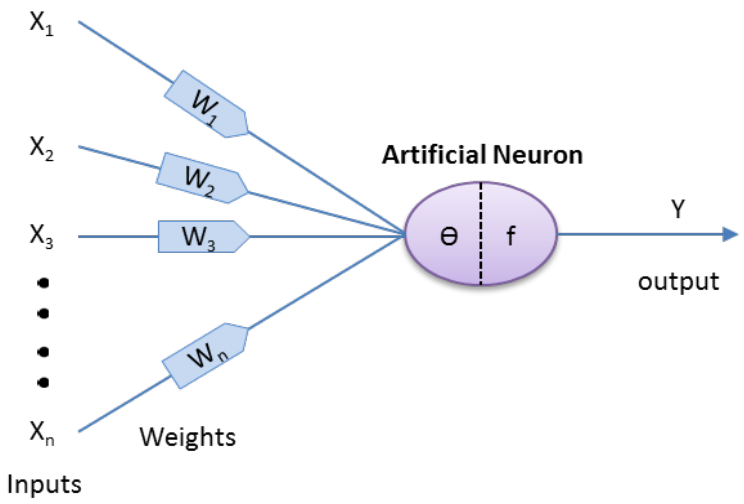

Figure 3-2 Structure of a single layer perceptron

The purpose of the perceptron is to classify inputs. Figure 3-2 shows a basic perceptron that will classify n dimensional spaces into two classes using a hyper-plane, which can be determined as a linearly separable function as below:

$$Y^p = \sum_{i=1}^{n} x_i^p w_i^p - \theta = 0 \qquad \text{Eq. 3-1}$$

where Y^p is the outputs, x_i^p and w_i^p are the i^{th} input and connection weight, and θ is a threshold of the neuron of p step. The learning process of perceptrons minimises the errors between the target (Y_d^p) and actual output (Y^p), which can be defined as:

$$e^p = Y_d^p - Y^p \qquad \text{Eq. 3-2}$$

If the error e^p is positive, then the output Y^p needs to be increased, and vice versa. This process of output adjustment is activated by updating weights during the training process, as below:

$$w_i^{p+1} = w_i^p + \Delta w_i^p \qquad \text{Eq. 3-3}$$

$$\Delta w_i^p = \alpha \times x_i^p \times e^p \qquad \text{Eq. 3-4}$$

where Δw_i^p represents the weight adjustment in p step using the delta rule (Eq. 3-4), w_i^{p+1} is the updated weight for $p+1$ step, and α is the learning rate, which is a positive constant less than one.

3.2.2.2 Back-propagation and higher order learning algorithms

The perceptron can only perform linear separation and cannot solve any nonlinear problems, limitations that were overcome by the innovative back-propagation algorithm (Bryson & Ho, 1969). Certainly, the back-propagation algorithm in the multilayer feed-forward ANN facilitates any nonlinear approximation. In the forward process of the back-propagation algorithm, all of the input vectors ($x_{1,2\cdots n}$) will be multiplied by randomly assigned corresponding connection weights, and the algorithm will be activated by the appointed transfer function as follows:

$$Y^p = f\left(\sum_{i=1}^{n} x_i^p w_i^p - \theta\right) \qquad \text{Eq. 3-5}$$

where p is the number of steps, Y^p is the output from the p step, w_i^p is the weight of the p step of the i^{th} input, θ is the bias (initial threshold), and f is the allocated transfer function. The calculated Y^p will be compared to the target, Y_d^p, and the error e^p will be back-propagated to update the connection weights for the next iteration.

The steepest descent algorithm is frequently used to adjust the weights in a basic back-propagation ANN, which searches for the global minima in the error space that directs the negative of the error gradient. The steepest descent is known as a stable algorithm, but its slow convergence is less than ideal.

As a countermeasure to the slow convergence of the steepest decent algorithm, the Gauss-Newton algorithm (Osborne, 1992), which performs a more rapid convergence, can be applied. However, the algorithm will only accelerate when the error function is appropriate for generating a quadratic approximation (Yu & Wilamowski, 2011). Furthermore, the convergence is very unstable.

These problems may be surmounted by the Levenberg-Marquardt (LM) algorithm. In fact, the LM algorithm is a unified algorithm comprising the steepest descent and Gauss-Newton algorithms. The algorithm activates with the steepest decent algorithm and converts to the Gauss-Newton algorithm when the error function curvature becomes quadratic (Levenberg, 1944; Marquardt, 1963). Nevertheless, the LM algorithm often grows comparatively slow and struggles to reach the global minima, which may be caused by the built-in steepest decent algorithm.

Another innovative algorithm, the conjugate gradient algorithm (CGA) (Hestenes & Stiefel, 1952), can serve as an alternative to the LM algorithm. In the CGA, the direction of the search for the global minima in error space is resolved with a conjugate direction that normally yields a more rapid convergence than that of the steepest descent algorithm (Møller, 1993). Various combination coefficients (β) were introduced, and a well-known Fletcher and Reeves (1964) algorithm was selected to model the UB prediction ANN. The β for p+1 step in the model can be calculated as follows:

$$\beta^{p+1} = (g^{p+1,T} g^{p+1})/(g^{p,T} g^{p}) \qquad \text{Eq. 3-6}$$

where, β^{p+1} is the conjugate gradient algorithm constant at $p+1$step, g^{p} and $g^{p,T}$ are the error gradient ($g = \partial E(x,w)/\partial w$) and its transposed matrix at p step, and g^{p+1} and $g^{p+1,T}$ are the error gradient ($g = \partial E(x,w)/\partial w$) and its transposed matrix at $p+1$ step.

The weight update rules for the steepest descent, Gauss-Newton, Levenberg-Marquardt and conjugate gradient algorithms are tabulated in Table 3-1.

Table 3-1 Weight update rules for representative ANN learning algorithms, modified from Yu and Wilamowski (2011)

Algorithm	Weight update rules	Convergence
Steepest descent	$w^{p+1} = w^{p} - \alpha g^{p}$	Stable, slow
Gauss-Newton	$w^{p+1} = w^{p} - (J^{p,T} J^{p})^{-1} J^{p} e^{p}$	Unstable, fast
Levenberg-Marquardt	$w^{p+1} = w^{p} - (J^{p,T} J^{p} + \mu I)^{-1} J^{p} e^{p}$	Stable, fast
Conjugate Gradient	$w^{p+1} = -g w^{p+1} + \beta^{p+1} e^{p}$	Stable, fast

w^{p+1} is the updated weight for p+1 step, α is the learning rate, g is the error gradient ($g = \partial E(x,w)/\partial w$), J^{p} is the Jacobian matrix for the P step, μ is the combination coefficient, and β^{p+1} is the conjugate gradient algorithm constant.

3.2.3 *Types of ANN transfer function*

The transfer function influences the performance of ANN, and thus, an appropriate function should be used for the goal of a model. Selected representative transfer functions are illustrated in Figure 3-3.

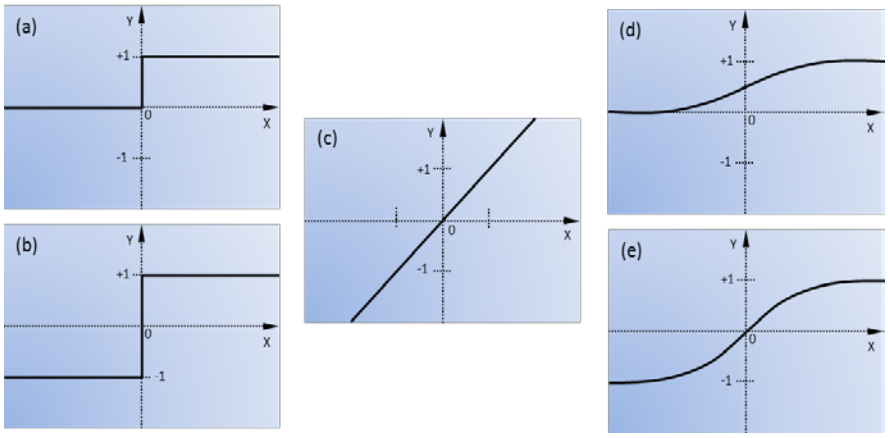

Figure 3-3 Various transfer functions of ANN

The hard limit functions (Figure 3-3a and b) are usually used for classification and pattern recognition, and the linear activation function (Figure 3-3c) performs well in linear approach problems. The sigmoid (Figure 3-3d) and hyperbolic tangent (Figure 3-3e) functions transfer an input from 0 to 1 and 1 to -1, respectively, and are typically used for nonlinear approximations. The equations for activation functions are listed from Eq. 3-7 to Eq. 3-10.

$$Y^{step} = \begin{cases} 1, & if\ X \geq 0 \\ 0, & if\ X < 0 \end{cases} \quad \text{Eq. 3-7}$$

$$Y^{linear} = X \quad \text{Eq. 3-8}$$

$$Y^{sigmoid} = \frac{1}{1 + e^{-X}} \quad \text{Eq. 3-9}$$

$$Y^{tanh} = \frac{e^{x} - e^{-x}}{e^{x} + e^{-x}} \quad \text{Eq. 3-10}$$

3.2.4 *ANN applications in several mining conundrums*

The ANN model has been applied to various mining-related problems over the last 25 years. Moreover, with the help of advanced computer technologies, much of the ANN and mining-related research has been converted to practical applications. Numerous ANN applications can be found in the field of rock mechanics and blasting-related subjects.

3.2.4.1 ANN applications in rock mechanics

Rock mechanics are of essential importance in mining because all mining plans and activities are processed based on rock masses. This subject is fundamental to generating an appropriate mine design and planning for a certain mineral deposit, but the complex formation of the natural rock mass can be rather difficult to investigate.

Uniaxial compressive stress (UCS) and the deformation modulus are vital parameters for rock mechanics, and while they can be obtained through in situ tests,

such testing necessitates substantial costs. Thus, laboratory rock sample tests and various empirical equations have been introduced to achieve these parameters (Bieniawski, 1978; Hoek & Brown, 1997; Nicholson & Bieniawski, 1990). Laboratory tests, however, represent only a tiny portion of the investigated rock mass. Additionally, the test results are hypersensitive to the condition of the specimens, and the test processes (Hoek, 2000) and empirical equations are problematic due to uncertainties surrounding the heterogeneous nature of the rock, the variability of rock types, and limited data availability (Kayabasi et al., 2003).

As countermeasures to these difficulties, various rock classification methods such as the rock mass rating (RMR) system (Bieniawski, 1973, 1974), Q-system (Barton et al., 1974), and Geological Strength Index (GSI) (Hoek, 1994), have been introduced to offer appropriate guidelines for rock engineering. With the aid of these rock classification methods, mine design and planning has grown more systematic. Empirical rock classification methods are not without their problems, however. While these methods are certainly suitable for the original rock conditions from which samples were taken, they cannot be generally applied without adjustments. Furthermore, the qualitative analysis of rock conditions is rather subjective.

Certainly, the complexity and uncertainty of the rock mass is an enormous impediment to the advancement of mining, and several studies have sought to use ANNs to overcome the difficulties previously described.

An ANN was applied to predict UCS by Meulenkamp and Grima (1999). The ANN was formulated with two hidden layers, and the Levenberg-Marquardt algorithm was employed as a training function. The authors allocated Equotip-determined hardness, density, porosity, grain size, and rock types as the input parameters to predict UCS based on thirty-four rock samples. As a result, the UCS prediction ANN demonstrates a more accurate performance than conventional multi-regression analysis predictions.

ANN is also employed to predict the stability states of an underground opening by Yang and Zhang (1997). The authors obtained data from a coal mine roadway from Sheorey (1991). In this study, the span and depth of the roadway, USC, RQD, J_n, J_r, J_a,

J_w, SRF, dry density, rock type, and joint orientation were set as the inputs and the stability states as the output. The goal of the study was to examine the contribution of inputs to outputs. To achieve this goal, the Relative Sensitivity of Effect (RSE) was defined for inputs on output, which can demonstrate the relative importance of the effect of input parameters on output units. The authors concluded the study by indicating the RQD and rock type as the most sensitive parameters for the stability of the roadway.

Darabi et al. (2012) attempted to predict convergence and subsidence in a tunnel in the Tehran No. 3 subway line using various approaches, including, empirical models, numerical analysis, regression analysis, and ANN. Among these approaches, ANN showed better prediction performance than other methods.

Analytical solutions for tunnel convergence prediction have been proposed by many researchers, e.g., Morgan (1961), Wood (1975), and Einstein and Schwartz (1979). Rafiai and Moosavi (2012) demonstrated the limitations of these analytical solutions due to the assumptions of elastic behaviour and isotropic in situ fields and employed ANN to surmount those defects. Data were initially generated through numerical simulations by FLAC (Itasca, 2002) and were reproduced using the design of experiments (DOE) technique (Antony, 2003).

ANN was also employed to predict tunnel convergence by Mahdevari and Torabi (2012). The authors indicated the difficulty of TBM jamming during the excavation of a weak rock area and accentuated the importance of predicting tunnel convergence. The authors established tunnel convergence prediction models by regression analysis, back-propagated ANN, and a radial-based ANN system, and the ANN models demonstrated results superior to those of regression analysis. The ANN model also performed better than conventional analytical and numerical analyses. Several representative ANN applications in rock mechanics and related subjects are tabulated in Table 3-2.

Table 3-2 ANN applications in rock mechanics and related subjects

Field of study	Author	Objects	SC methods			Auxiliary methods	
			ANN	FA	GA		
Rock mechanics (Identifying the strengths and the deformation modulus of rock masses)	Lee and Sterling (1992)	FM	●				
	Meulenkamp and Grima (1999)	UCS	●			EHT	RA
	Singh et al. (2001)	I_s, UCS, σ_t	●			VIDS ///	
	Gokceoglu et al. (2004)	E_d	●	●			
	Sonmez et al. (2006)	E_{el}	●				
	Majdi and Beiki (2010)	E_d	●		●	PCA	
	Beiki et al. (2010)	E_d	●			SA	
	Rafiai et al. (2013)	FC	●				
Rock mechanics (predicting rock mass performance and estimating stability)	Yang and Zhang (1997)	ES	●			RSE	
	Deng and Lee (2001)	DG	●		●	FEM	
	Kim et al. (2001a)	DG	●			RSE	SA
	Li et al. (2006)	DG	●	●			
	Alimoradi et al. (2008)	RMR	●			TSP230	
	Darabi et al. (2012)	TC, SS	●			FDM	RA
	Rafiai and Moosavi (2012)	TC	●			FDM	DOE
	Mahdevari and Torabi (2012)	TC	●			SA	RA

SC: *Soft computing,* ***ANN:*** *Artificial neural network,* ***FA:*** *Fuzzy algorithm,* ***GA:*** *Genetic algorithm (Holland, 1975),* ***FM:*** *Failure modes,* ***UCS:*** *Unconfined compressive strength,* I_s*:* *Point load strength,* σ_t***:*** *Tensile strength,* E_d***:*** *Modulus of deformation* E_{el}***:*** *Modulus of elasticity,* ***FC:*** *Failure criteria,* ***ES:*** *Engineering state (either stable or unstable),* ***DG:*** *Displacements and/or ground settlement,* ***RMR:*** *Rock mass rating,* ***TC:*** *Tunnel convergence,* ***SS:*** *Subsidence,* ***EHT:*** *Equotip hardness Tester,* ***VIDS ///:*** *A high resolution semi-automatic image analysis system,* ***PCA:*** *Principal component analysis,* ***SA:*** *Sensitivity analysis,* ***RSE:*** *Relative strength of effects,* ***TSP230:*** *Tunnel seismic prediction,* ***FDM:*** *Finite difference method,* ***RA:*** *Simple and/or multiple regression analyses,* ***DOE:*** *Design of experiments technique*

3.2.4.2 ANN applications in blasting-related subjects

Drilling and blasting methods are acknowledged as the most cost-effective methods to excavate ore and are broadly employed in both surface and underground mining activities. In spite of the economic advantage, rock blasting is always accompanied by risk due to the inherent dynamic energy exposure behaviour. Thus, such methods should only be used after implementing safety measures and estimating the potential reactions of object materials and latent influences on the surrounding environment. The mechanism of rock blasting is very complex, and in fact, precise geological and geotechnical data are very difficult to obtain, meaning that rock blasting activities are generally planned on the basis of insufficient information. Furthermore, the rock blasting mechanism itself has yet to be clarified.

Many methods of statistical analysis have been used to predict potential hazards from rock blasting. Likewise, numerical analyses have often been used to simulate rock fracture behaviour. Now, because the aforementioned methods contain several engineering limitations; attempts have been made to adopt the artificial neural network (ANN) to this problem.

Traditionally, blasting-induced vibration, especially the peak particle velocity (PPV), has been predicted by regression analysis. To achieve better PPV predictability, Chakraborty et al. (2004) adopted an online feature selection net (FSMLP) (Pal & Chintalapudi, 1997) and a fusion ANN network. The structure of fusion networks is similar to that of a conventional multi-layer perceptron (MLP), but hidden neurons are substituted by MLP models. The designed fusion network showed consistently better PPV prediction performance than empirical statistical PPV prediction models and the conventional MLP.

Many other studies seeking to predict PPV by ANN have been conducted. Singh et al. (2004) applied two separate ANNs to predict the PPV and its corresponding frequencies. Moreover, attempts have been made to simultaneously predict PPV and frequencies in one ANN model by Lu (2005), Manoj and Singh (2009), Álvarez-Vigil et al. (2012), and Monjezi et al. (2012). ANN has been applied to numerous other blasting-related topics, and several representative studies are tabulated in Table 3-3.

Table 3-3 ANN applications in blasting-related subjects

Field of study	Author	Objects	SC methods			Auxiliary methods	
			ANN	FA	GA		
Blasting (Identifying blasting design parameters and hazards)	Chakraborty et al. (2004)	PPV	●			FSMLP	RA
	Singh (2004)	PPV	●			RA	
	Singh et al. (2004)	PPV, BFQ	●			RA	
	Manoj and Singh (2005)	BAO	●			RA	
	Lu (2005)	PPV, PPA, BFQ	●			NH-A	
	Monjezi et al. (2006)	BFR, MPL, TEX	●			RA	
	Remennikov and Rose (2007)	AF_p, AF_i	●				
	Monjezi and Dehghani (2008)	BBB	●				SA
	Manoj and Singh (2009)	PPV, BFQ	●			RA	SA
	Monjezi et al. (2010)	PPV	●			RA	SA
	Kulatilake et al. (2010)	BRF	●			RA	
	Monjezi et al. (2011a)	BP, BFQ, BBB	●		●	RA	
	Dehghani and Ataee-Pour (2011)	PPV	●				SA
	Bahrami et al. (2011)	BRF	●			RA	SA
	Monjezi et al. (2011b)	PPV	●			RA	SA
	Álvarez-Vigil et al. (2012)	PPV, BFQ	●			RA	
	Monjezi et al. (2012)	BFQ, BBB	●		●		SA
	Esmaeili et al. (2012)	BBB	●	●		RA	
	Ataei and Kamali (2012)	PPV	●	●		ANFIS	
	Verma and Singh (2013)	PWV	●	●		ANFIS	
	Sun et al. (2013)	BOB	●				
	Jang and Topal (2013)	BOB	●			RA	

SC: *Soft computing,* ***ANN:*** *Artificial neural network,* ***FA:*** *Fuzzy algorithm,* ***GA:*** *Genetic algorithm,* ***PPV:*** *Peak particle velocity,* ***BFQ:*** *Blasting-induced frequency,* ***BAO:*** *Blasting-induced air overpressure,* ***PPA:*** *Peak particle acceleration,* ***BFR:*** *Blasting-induced flyrock,* ***MPL:*** *Muck pile ratio,* ***TEX:*** *Total explosive required,* ***AF_p:*** *Air pressure pulse* ***AF_i:*** *Air pressure impulse,* ***BBB:*** *Blasting-induced backbreak,* ***BRF:*** *Blasting-induced rock fragmentation,* ***BP:*** *Blasting parameters,* ***PWV:*** *P-wave velocity,* ***BOB:*** *Blasting-induced overbreak,* ***FSMLP:*** *On-line feature selection net,* ***RA:*** *Simple and/or multiple regression analyses,* ***SA:*** *Sensitivity analysis,* ***NH-A:*** *Nonlinear hydrocodone – Autodyn,* ***ANFIS:*** *Adoptive network based fuzzy inference system (Jang, 1993)*

3.3 FUZZY ALGORITHMS

Unlike the classical two-valued Boolean logic that only accepts values of 0 (false) or 1 (true), fuzzy logic is a set of mathematical principles that is multi-valued and incorporates degrees of membership and degrees of truth. Multi-valued logic was originally introduced by Lukasiewicz (1920), who in this study extended the range of truth between zero and one. This work triggered the study of 'possibility theory'. In succession, Black (1937) defined the first fuzzy sets, and Zadeh (1965) extended the work into a formal system of mathematical logic and introduced fuzzy logic to calibrate the vagueness of natural linguistic terms. An example of crisp and fuzzy sets with a five membership function of rock mass ratings (RMR) (Bieniawski, 1974) is shown in Figure 3-4.

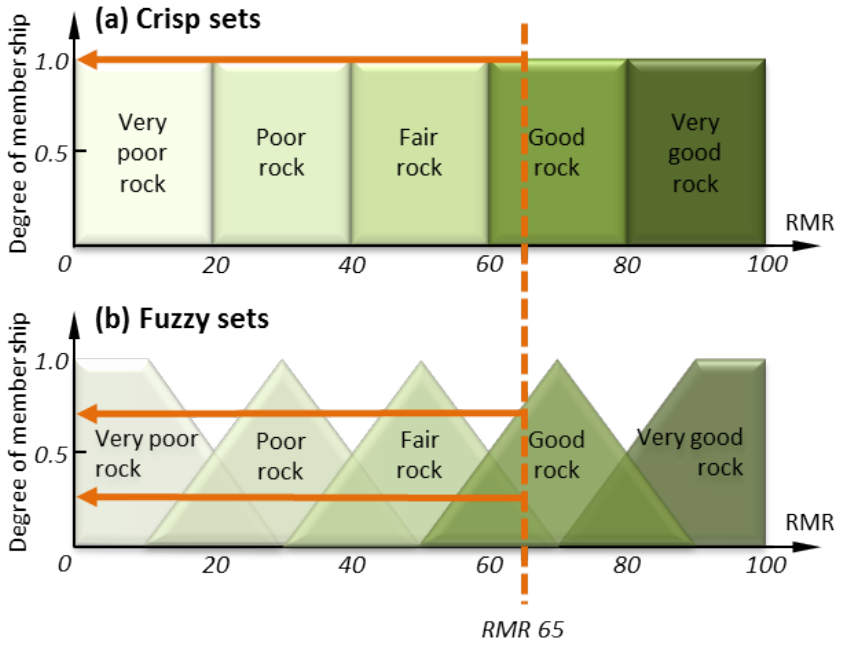

Figure 3-4 Example of crisp (a) and fuzzy (b) sets of a RMR system

As shown in Figure 3-4a, which displays classical Boolean logic, a rock with an RMR of 65 is only a member of the 'good rock' set with degree of membership of 1.0. In fuzzy logic (Figure 3-4b), however, a rock with an RMR of 65 is a member of the 'fair rock' set with a degree of membership of 0.25 and simultaneously a member of the 'good rock' set with a degree of 0.75. This mathematical feature of the fuzzy set theory (also called fuzzification) can incorporate expert knowledge into a mathematical model.

3.3.1 *Configurations of Fuzzy expert systems*

Determining membership functions and fuzzy 'IF-THEN' rules are the prerequisite conditions for developing a fuzzy expert system (FES). Fuzzy membership functions are the main component of FESs, and the formation and ranges of each membership function should be cautiously selected considering the idea of FES. Commonly, inputs and outputs of membership functions and rational fuzzy rules are left to subject experts.

3.3.2 *Fuzzy inference systems*

Fuzzy inference is a process of matching inputs to output space considering the predetermined fuzzy membership functions and fuzzy rules. The Mamdani and Assilian (1975) (referred to as Mamdani style) and Sugeno (1985a) styles are the most representative fuzzy inference systems. One large difference between these two fuzzy inference systems is that Sugeno model uses a bar-type singleton to represent the membership function, while Mamdani uses a two-dimensional membership function. In this study, a Mamdani-style fuzzy inference system was adopted to build the UB consultation system, which consists of four steps: fuzzification, rule evaluation, aggregation of the rule outputs, and defuzzification (Negnevitsky, 2005). The details of modelling fuzzy inference systems are described in detail in Chapter 6.

3.3.3 *Applications of fuzzy algorithms in mining conundrums*

Considering the complexities of various mining subjects, the ability to control vagueness and uncertainties offered by fuzzy algorithm has attracted mining engineers and scholars since the mid-1980s. Fuzzy algorithms have been employed in various difficult mining subjects, and many advanced theories have consequently been developed.

Among the numerous fuzzy algorithm applications in many mining conundrums, mining method selection (MMS), the equipment selection problem (ESP), several subjects related to rock mechanics, and certain subjects related to blasting are reviewed in the following sections.

3.3.3.1 Fuzzy algorithm applications in mining method selection

Mining Method Selection (MMS) is a vital process in the early stages of the mine planning process, the goal being to select the most appropriate mining method for a given mineral deposit. This process significantly influences the economics, safety, and productivity of a mine. However, MMS is a typical multiple-attribute decision-making (MADM) problem that encompasses numerous conditions and parameters, i.e., technical and industrial problems, financial concerns, mining-related policies, and environmental and social issues. A conceptual framework of MMS is illustrated in Figure 3-5.

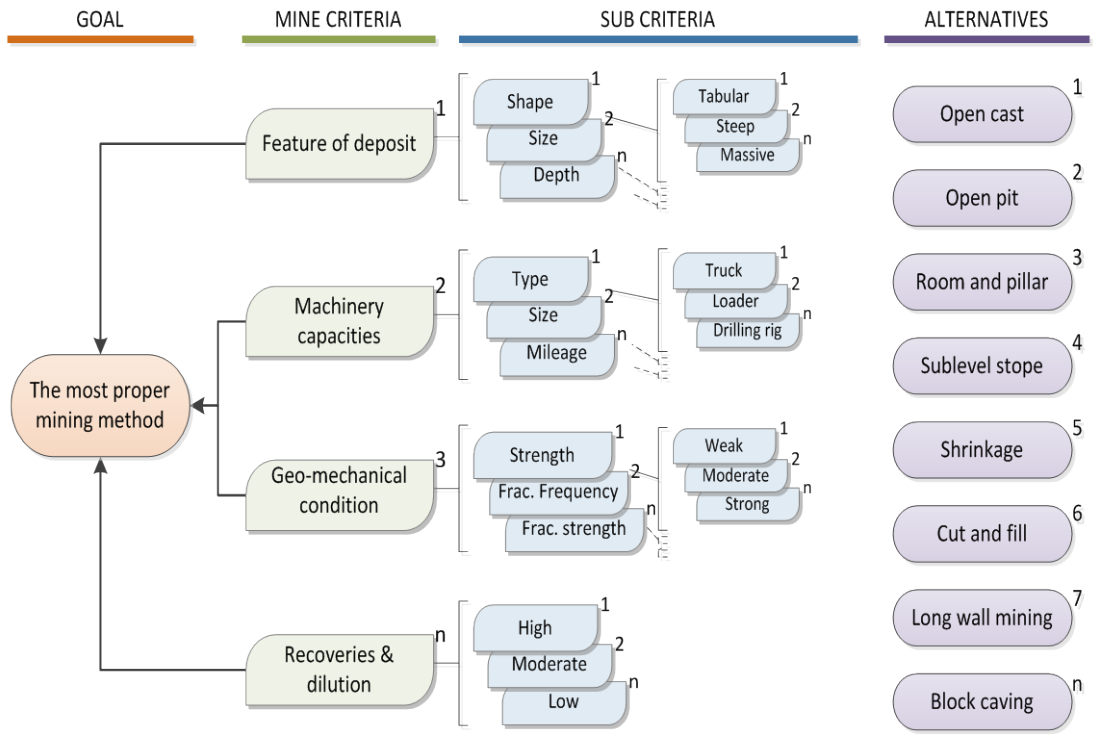

Figure 3-5 Conceptual frame work of MMS

As demonstrated in Figure 3-5, numerous criteria and their sub-criteria must be accounted for in order to select the optimal mining method among many alternatives. To aid the MMS, Nicholas (1992) introduced a quantitative ranking method that categorised vital factors in the MMS process. This method includes the 3D features of the deposit, geological and geotechnical surroundings, environmental and economic considerations, and other industrial factors. Moreover,

political and social limitations, machinery, and workforce supply conditions are also included as significant factors. In fact, the MMS was generally managed by artificially delimiting criteria, and its implementation was often left to mining experts. To achieve optimum MMS, many attempts have been made to employ fuzzy algorithms combined with certain MADM approaches.

Yun and Huang (1987) adopted a fuzzy algorithm for MMS, formulating a three stage system. In the first stage, fuzzy relation equations, which calculate the hamming distance from the geological requirements of candidate mining methods to the geological conditions where a mine can be planned, were formulated. The technical and economical values of each candidate mining method were evaluated in the second stage, and in the third stage, the decision was made based on the values from prior stages.

An expert system for underground MMS was developed by Guray et al. (2003) based on Nicholas's (1992) quantitative ranking method. The system developed 13 virtual experts for 13 different underground mining methods. One merit of the proposed system is its inclusion of an MMS tutorial that can be invaluable for inexperienced mining engineers. In addition, the system included criteria that were not listed in Nicholas's method, i.e., capital cost, operating cost, productivity, subsidence, spontaneous combustion, and the lake presence factor.

A method for assigning weights to MMS criteria was introduced by Bitarafan and Ataei (2004). The developed system was built based on Yagar's method (1978) and a fuzzy dominance method proposed by Hipel (1982). The proposed system modelled using exponential scalars to express the significance of given criteria. Therefore, the significance of a criterion was dramatically increased if its conditions were matched with the target deposit. Otherwise, the significance would be seriously decreased. The method was successfully applied to one of the anomalies at the Gol-e-Gohar iron mine in Iran, where the block caving method was chosen as the most appropriate mining method.

Azadeh et al. (2010) introduced an MMS system that modified Nicholas's (1992) quantitative ranking method using fuzzy logic and the Analytical Hierarchy Process (AHP) (Saaty, 1980). In the system, the imprecision of the decision maker's

judgements were expressed by trapezoidal fuzzy numbers; it was applied to the northern anomaly of the Choghart iron mine in Iran to validate the developed system.

Selected representative references to fuzzy algorithm applications in MMS problem are tabulated in Table 3-4.

Table 3-4 Representative applications of fuzzy algorithms in mining method selection

Field of study	*Author*	*SC methods*				*Auxiliary methods*	
		FA	*EXS*	*ANN*	*YAM*		
Mining method selection	*Yun and Huang (1987)*	●					
	Bandopadhyay and Venkatasubramanian (1988)		●				
	Gershon et al. (1993)		●				
	Yiming et al. (1995)		●	●			
	Guray et al. (2003)		●				
	Bitarafan and Ataei (2004)	●			●		
	Ataei et al. (2008)	●				*AHP*	
	Azadeh et al. (2010)	●				*AHP*	
	Namin et al. (2011)	●				*AHP*	*TOPSIS*

SC: *Soft computing,* ***FA:*** *Fuzzy algorithm,* ***EXS:*** *Expert system,* ***ANN:*** *Artificial neural network,* ***YAM:*** *Yagar's method,* ***AHP:*** *Analytic hierarchy process,* ***TOPSIS:*** *Technique for order performance by similarity to ideal solution (Hwang & Yoon, 1981)*

3.3.3.2 Fuzzy algorithm application in equipment selection problems

Excavation, loading and hauling are essential activities in mining. Because the cost of the necessary equipment easily exceeds several million dollars and its maintenance costs take up a large portion of a mine's budget, selecting the proper size, type, and number of machines has significant effects on mine profitability. According to a study by Blackwell (1999), haul trucks' operating costs may eat up one-third to one-half of total mining operation costs.

The goal of this problem is to optimise the material transfer system from a set of origins to certain destinations considering numerous factors, i.e., budget conditions, hauling distance, possible configuration of equipment, and alternative transfer systems. Due to its complexity, the equipment selection problem (ESP) is often left to equipment selection experts, although one practical solution that has been used is cutting back the dimensions of the problem by delimiting influential parameters and alternatives.

Because the ESP requires accounting for numerous factors with alternative transfer systems, attempts have been made to adopt soft computing technology, especially fuzzy algorithms, with MCDM methods, which have shown better solution than conventional ESP approaches. Figure 3-6 demonstrates concise processes of ESP through soft computing technologies with MCDM methods versus the conventional approach of using mining experts. Moreover, selected representative fuzzy algorithm applications concerning the ESP are reviewed.

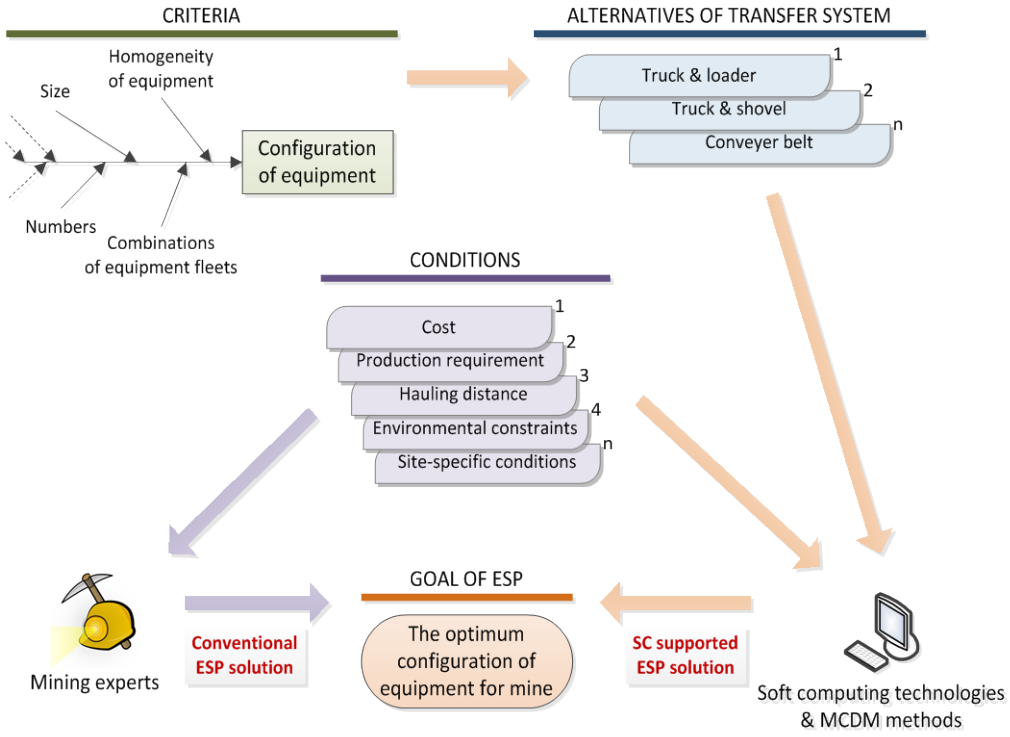

Figure 3-6 Demonstration of ESP solutions through mining experts and soft computing approach

Amirkhanian and Baker (1992) introduced VP-Expert, which is a rule-based ESP expert system. Several ESP experts' knowledge of and specifications for equipment were incorporated into the VP-Expert, which consists of 930 rules that cover ground conditions, operational performances, and the prerequisite operations of a given mining project. The VP-Expert was applied to three actual ESPs and demonstrated results that were fairly well matched to the selections made by companies.

Bascetin and Kesimal (1999) applied fuzzy algorithms to select optimum coal-hauling systems to transport coal from an open-cast coal mine to a power plant. The authors set twenty-one operational attributes as the criteria and suggested three alternative transfer systems. The membership values of each criterion were defined by the decision makers, and the reciprocal matrices of the criteria were formulated to present the significance of each criterion.

A fuzzy expert system was built for a surface mining ESP by Ganguli and Bandopadhyay (2002). The proposed system consists of seven tasks, where the relative significance of each factor on each tasks is specified by the user and the significance of the listed equipment is evaluated based on the conditions provided by user. To validate the proposed system, a case study was conducted at the Malanjkhand Copper Mine in India, and the expert system recommended equipment fleets that were similar to the actual equipment fleets used at the mine. The system does contain certain limitations, however, in that it does not account for production requirements; additionally, the criteria weights assignation process can be highly subjective, which may decrease the creditability of the system.

Fuzzy algorithms (FAs) have been successfully and practically applied to many actual ESPs in mining, and selected representative ESP studies adopting FAs are listed in Table 3-5.

Table 3-5 Representative studies of fuzzy algorithm applications in the mining equipment selection problem

Field of study	*Author*	*SC methods*				*Auxiliary methods*
		FA	*EXS*	*ANN*	*YAM*	
Mining equipment selection problem	*Bandopadhyay (1987)*	●				
	Bandopadhyay and Venkatasubramanian (1987)		●			
	Denby and Schofield (1990)	●	●			
	Clarke et al. (1990)		●			
	Amirkhanian and Baker (1992)		●			
	Bascetin and Kesimal (1999)	●			●	***AHP***
	Ganguli and Bandopadhyay (2002)		●			
	Bascetin (2004)	●				***AHP***
	Iphar and Goktan (2006)	●				
	Aghajani Bazzazi et al. (2011)	●	●			***AHP***

SC: *Soft computing,* ***FA:*** *Fuzzy algorithm,* ***EXS:*** *Expert system,* ***ANN:*** *Artificial neural network,* ***YAM:*** *Yagar's method,* ***AHP:*** *Analytic hierarchy process*

3.3.3.3 Fuzzy algorithm applications in rock mechanics and rock blasting

Natural rock is typically anisotropic and heterogeneous, and uncertainties, imprecision and data limitations are thus irremovable inherent obstacles in research related to rock mechanics and rock blasting. For this reason, beginning in the mid-1980s, many engineers and scholars have adopted FAs to manage the difficulties. Several representative studies concerning FA applications in rock mechanics and breakage are reviewed below.

Alvarez Grima and Babuška (1999) used the Takagi-Sugeno (TS)-type (Takagi & Sugeno, 1985) fuzzy inference system to predict the unconfined compressive strength (UCS) of rock samples. The proposed system was faster and more economical than the laboratory test and showed better predictability than multiple regression analysis.

A rule-based fuzzy system was employed to predict the deformation modulus by Kayabasi et al. (2003). The proposed system was evaluated by comparing the results with five empirical equations and actual laboratory test results. The proposed system showed superior a predictive performance to empirical approaches, although one limitation of the proposed system is that it can only apply to the rock types in the inputs database.

The fuzzy algorithm was applied to rock classification by Hamidi et al. (2010), whose proposed system was configured by the Mamdani fuzzy inference system (FIS) with seven inputs based on the rock mass excavability (RME) (Bieniawski & Grandori, 2007) system. The proposed system was applied to two water-transfer tunnels in Iran, which verified the applicability of fuzzy algorithm to rock mass classification.

Moreover, fuzzy algorithms were employed to establish a flyrock prediction system at the Gol-e-Gohar iron mine in Iran by Rezaei et al. (2011). The proposed model consisted of 390 fuzzy rules with eight inputs, i.e., burden, spacing, hole depth, specific drilling, stemming, charge per delay, rock density, and powder factor, and one output, the ranges of flyrock. The fuzzy model demonstrated better flyrock prediction performances than conventional statistical models.

As described, the fuzzy algorithm has also been effectively applied to numerous subjects related to rock mechanics and rock blasting, and selected representative studies are tabulated in Table 3-6.

Table 3-6 Representative studies of fuzzy algorithm applications in rock mechanics and breakage-related subjects

Field of study	Author	Objects	SC methods				Auxiliary methods	
			FA	EXS	ANN	YAM		
Rock mechanics (identifying the strengths & the deformation modulus)	Alvarez Grima and Babuška (1999)	E_d	●				EHT	RA
	Kayabasi et al. (2003)	E_d	●				RA	
	Sonmez et al. (2004)	UCS, E_{el}	●				RA	
Rock mechanics (predicting rock mass performance & stability study)	Li et al. (2007)	DG	●		●			
	Li et al. (2007)	DG	●				GA	GEP
	Li et al. (2013)	DG	●				MWC	RAC
Rock mechanics (rock mass classification)	Nguyen (1985)		●				RMR	
	ShengFeng et al. (1988)		●				-	
	Zhang et al. (1988)			●			GU	
	Juang and Lee (1989)		●	●			RMR	
	Butler and Franklin (1990)			●			RMR	Q
	Juang and Lee (1990)		●				FWA	RMR
	Habibagahi and Katebi (1996)		●				RMR	
	Aydin (2004)		●				RMR	
	Liu and Chen (2007)		●				FDAHP	LDA
	Hamidi et al. (2010)		●				RME	
Blasting (Identifying design parameters & hazards)	Azimi et al. (2010)	BD	●					
	Rezaei et al. (2011)	BFR	●				RA	SA
	Fişne et al. (2011)	PPV	●				RA	

SC: *Soft computing,* ***FA:*** *Fuzzy algorithm,* ***EXS:*** *Expert system,* ***ANN:*** *Artificial neural network,* ***YAM:*** *Yagar's method,* ***Ed:*** *Modulus of deformation,* ***UCS:*** *Unconfined compressive strength,* ***Eel:*** *Modulus of elasticity,* ***DG:*** *Displacements and/or ground settlement,* ***BD:*** *Blastability designation,* ***BFR:*** *Blasting-induced flyrock,* ***PPV:*** *Peak particle velocity,* ***EHT:*** *Equotip hardness Tester,* ***RA:*** *Simple and/or multiple regression analyses,* ***GA:*** *Genetic algorithm,* ***MWC:*** *Modified Wiebols-Cook criterion,* ***RMR:*** *Rock mass rating,* ***GU:*** *Gu's rock classification,* ***FWA:*** *Fuzzy weighted average,* ***FDAHP:*** *Fuzzy delphi analytic hierarchy process,* ***RME:*** *Rock mass excavability,* ***GEP:*** *Genetic programming,* ***RAC:*** *Rafiai criterion,* ***Q:*** *Q-system,* ***LDA:*** *Linear discriminant analysis,* ***SA:*** *Sensitivity analysis*

3.4 SUMMARY AND DISCUSSION

The fundamental ideas behind ANN and FA and their applications in several mining-related subjects are reviewed in this chapter. As mining is a melting pot of various engineering subjects and manages complex rock and rock masses, establishing reliable mining systems such as planning, scheduling, developing, producing, and conciliating is highly complex and cannot be efficiently modelled by conventional mathematical and statistical methods. For this reason, ANNs and FAs have been adopted in various mining-related subjects to positive results.

In fact, the rapid advancement of computer technology has created many synergy effects on soft computing (SC), and different types of advanced SC technologies have been employed in various industries. However, the history of the application of ANNs, FAs, and other soft computing technologies in mining engineering is somewhat shorter than in other industries. Furthermore, there is no proper system for controlling unplanned dilution and ore-loss in underground stoping. In fact, this study is a first attempt to establish an unplanned dilution and ore-loss management system through the use of ANN and FA.

CHAPTER 4. DATA COLLECTION AND MANAGEMENT

4.1 INTRODUCTION

Data collection and management are a herculean task but an essential stage for rational analysis. Moreover, the performance of the proposed model fully relies on the quantity and quality of the data. This chapter describes the data collection and management procedures used to obtain qualified datasets for establishing a UB-predicting ANN model. In addition, to build a dependable UB consultation model with a fuzzy expert system, 15 underground mining experts shared their knowledge via personal surveys. Data were collected from three underground mines in Western Australia. As unplanned dilution and ore loss are one of the major concerns in a mining company, the locations, specific geological information, and mine details cannot be noted in this thesis for security reasons. Thus, the three mines are labelled mines A, B, and C.

4.2 DATA COLLECTION FOR UB PREDICTING ANN SYSTEM

In this study, extensive ranges of historical stope design, blasting, geological, geotechnical data, and reconciliation documents were scrutinised to establish reliable uneven break (UB) prediction models without any bias.

As mentioned in Chapter 2, ten essential parameters which comprise blasting, geological, stope design, and human error categories, were collected via a thorough review of approximately over 30,000 historical documents from three underground long-hole and open stoping mines in Western Australia. Ultimately, 1,354 sets data points were collected and the details of ten uneven break (UB) causative factors were tabulated in Table 4-1.

Five parameters were collected as the representative blasting factors, i.e., average length of blasthole (Blen), powder factor (Pf), angle difference between the hole and wall (AHW), blasthole diameter (Bdia) and space and burden ratio (SbR). The adjusted Q rate (AQ) and average horizontal to vertical stress ratio (K) were considered as the representative geological factors. The planned tonnes of stope (Pt), aspect ratio (AsR), and stope either breakthrough to a nearby drift and/or stope or not (BTBL) were collected as the stope design factors. These ten uneven

break (UB) causative factors were allocated as independent variables. As a dependent variable, the percentage of uneven break (UB) was also collected.

Table 4-1 Details of the ten *UB* causative factors

Category			Abbr.	Unit	Range	Note
Input (independent variables)	Controllable	Blasting	*Blen*	m	0.70 ~ 25.80	Average length of blasthole
			Pf	Kg/t	0.15~ 3.00	Powder factor
			AHW	°	0.00 ~ 170.20	Angle difference between hole and wall
			Bdia	mm	76 ~ 89	Blasthole diameter
			SbR	(S/B)[1]	0.57 ~ 1.50	Space and burden ratio
		Stope design	*Pt*	T	130 ~ 51,450	Tonnes of stope planned
			AsR	(W/H)[3]	0.07 ~ 4.17	Aspect ratio
			BTBL	-	Breakthrough (0) ~ Blind (1)	Stope either breakthrough to a nearby drift and/or stope or not
	Uncontrollable	Geology	*AQ*	-	6.30 ~ 93.30	Adjusted Q rate
			K	(H/V)[2]	1.74 ~ 14.38	Average horizontal to vertical stress ratio
Output (dependent variable)			*UB*	%	-65.40 ~ 92.00	Percentage of uneven stope break (over and under breaks)

[1]***S/B:*** *ratio between toe space (S) and ring burden (B);* [2]***H/V:*** *ratio between average horizontal (H) and vertical (V) stress;* [3]***W/H:*** *ratio between width (W) and height (H) of stope*

4.2.1 *Blasting factors*

Uneven break (UB) is an inevitable phenomenon if a stope is excavated by drilling and blasting method. Even with a well-established blasting design, the massive dynamic explosion energy will break not only the planned stope but also waste rock in exterior of planned stope. Thus, the blasting factors have a vital importance to understand uneven break (UB) phenomenon. In this study, all data were collected from production ring blasting but not slotting processes. Figure 4-1 shows a schematic view of one example of blasting data collection.

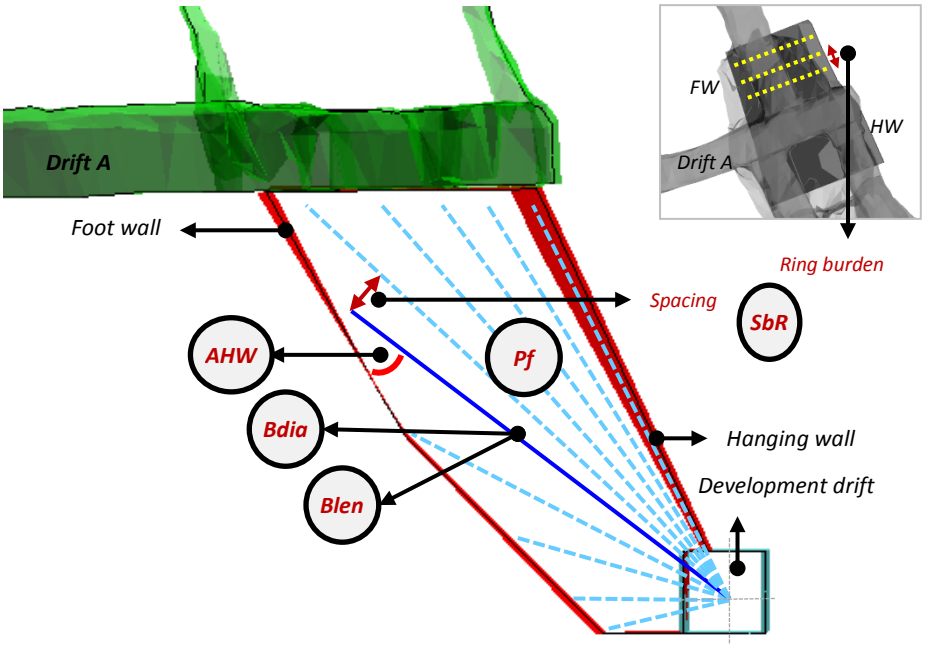

Figure 4-1 Schematic view of data collection for blasting factors; Blen: average length of blasthole, Pf: powder factor, AHW: angle difference between hole and wall, Bdia: blasthole diameter, SbR: space and burden ratio

Figure 4-1 shows a data collection in a foot wall of a stope and hanging wall also collected via the same strategy.

4.2.2 *Geological factors*

Geological factors are unalterable, and they have significance influences on uneven break (UB). Indeed, no blasting method can minimise unfavourable over and underbreaks, if the rock is not sustainable by itself. In this study, the modified Q rate (Q') (Mathews et al., 1981) and average horizontal to vertical stress ratio (K) were collected as representative geological factors.

The first geological factor in this study, the modified rock mass quality index (Q'), was introduced by Mathews et al. (1981). Q' has been applied for open stoping design and is defined as:

$$Q' = \frac{RQD}{J_n} \times \frac{J_r}{J_a} \qquad \text{Eq. 4-1}$$

where RQD is the rock quality designation (Deere, 1964), J_n is the number of joint set, J_r is the joint roughness number, and J_a is the joint alteration number from the rock mass rating system (Hoek & Brown, 1997).

The average horizontal to vertical stress ratio (K: $\boldsymbol{\sigma_v/\sigma_h}$) was also collected as a geological factor for this study. The in-site stress of mine-A was measured by the acoustic emission method (AE) (Villaescusa et al., 2002; Yoshikawa & Mogi, 1989) while the Hollow Inclusion cell over-coring method (HI) (Hooker & Bickel, 1974) was adopted in mine-B. These two methods (AE and HI) are both used in mine-C.

4.2.3 *Stope design factors*

Tonnes of stope planned (Pt), aspect ratio (AsR), and stope either breakthrough to a nearby drift and/or stope or not (BTBL) were collected as stope design factors. The BTBL value of a stope was 0 for a blind stope and 1 for a breakthrough stope. Figure 3-1 shows examples of blind and breakthrough stopes.

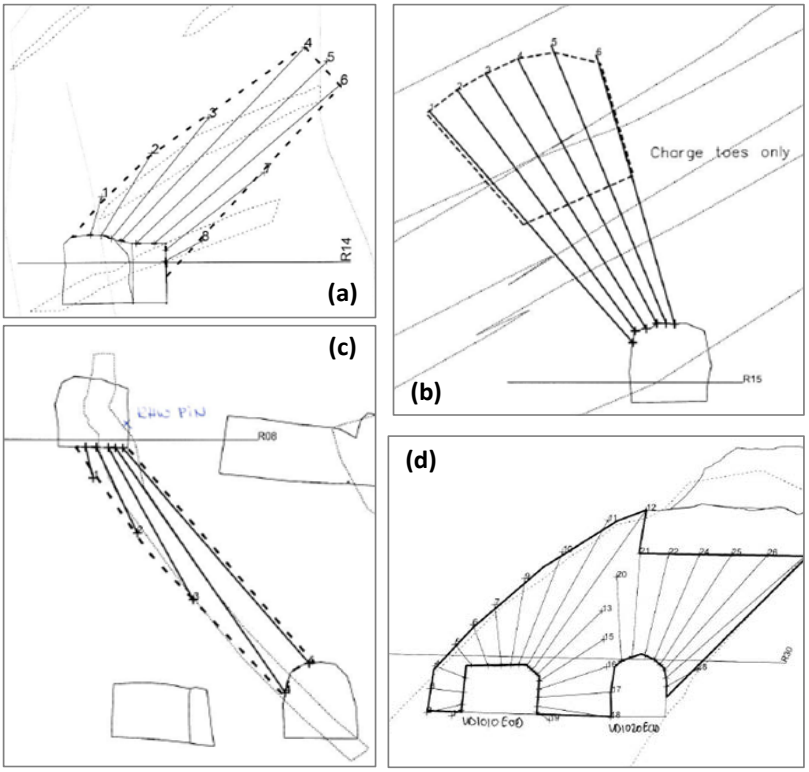

Figure 4-2 Schematic view of blind (a, b) and breakthrough (c, d) stope

The width (W) versus height (H) ratio was calculated as the AsR for each stope, and the planned tonnes (Pt) of each stope was collected to represent the influence of size effect on uneven break (UB) phenomenon.

4.2.4 *Uneven break*

The percentage of uneven break (UB; over- and underbreak) was collected as a dependent variable for UB prediction models. The three investigated mines used the CMS for stope reconciliation, and the overbreak and underbreak volumes were calculated not only from the hanging wall but also the foot wall of the stope. Ultimately, the percentage of uneven break (UB) was determined by calculating the percentage of over- and underbreak volume per the planned stope volume. For further rational computing, overbreak and underbreak values were multiplied by one and minus one, respectively. The collected data revealed that the UB range is between -65.40 and 92.00. Figure 4-3 demonstrates an example of typical stope reconciliation with CMS model.

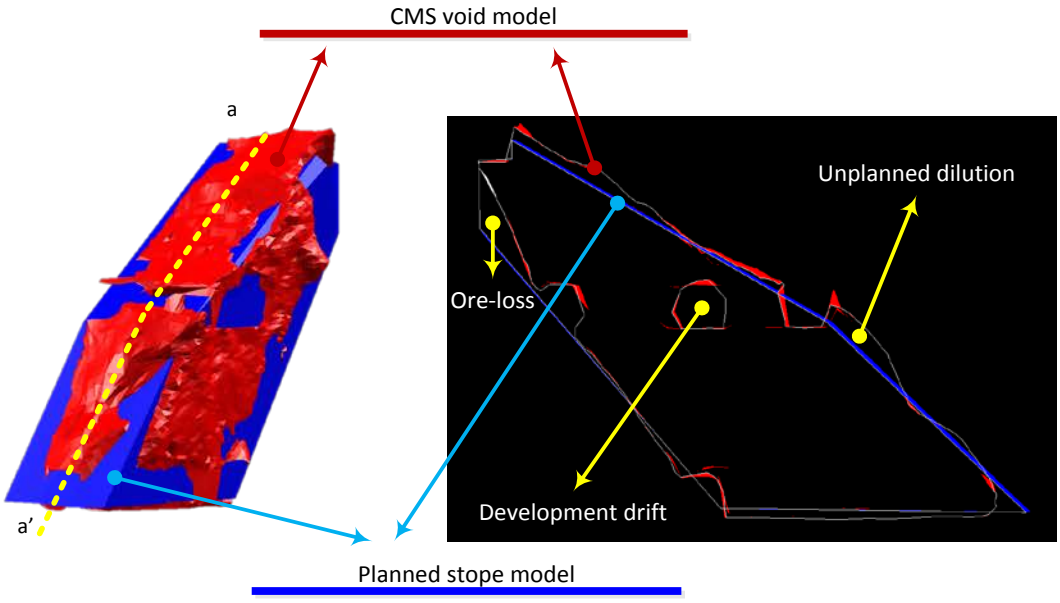

Figure 4-3 Typical stope reconciliation with the CMS model

As shown in Figure 4-3, the planned stope model was compared with the actual stope model obtained by CMS.

4.2.5 *Data filtering*

To conduct a coherent analysis, dirty data, mis-typed or mis-measured data, should be eliminated and outliers, abnormal data, are needed to be checked. Dirty and abnormal data influence an analysis in various respects. Because they can reduce

the reliability of proposed models, they should be checked and eliminated before proceeding further analysis. Their detection process should be carried out very carefully because it may also eliminate important data points. In this study, dirty data are referred as extreme outliers.

Outlier can be defined as data points that are far away from other data points, and their detection is a prerequisite to a coherent analysis. Univariate and bivariate outliers can be straightforwardly detected by monitoring the shape of the data distribution for flat and/or spatial spaces, e.g., the standard z-score test, box-plot, scatter-plot, and Euclidean distance. Contrastively, a multivariate outlier cannot be directly detected through visual inspection. For example, even if an observation point is a suspected outlier in one or two dimensional spaces, it could be an important observation point in other dimensions. These phenomena are called the *masking* and *swamping* effects (Hawkins, 1980; Iglewicz & Martinez, 1982).

In this study, one dependent and ten independent variables which compose ten dimensional matrixes, are employed. To rationally detect outliers from the ten dimensional matrixes, two separate data filtering stages were applied.

4.2.5.1 First filtering stage

In the first stage, potential outliers were identified by examining their z-score. As the number of datasets is 1,354, each parameter was assumed to follow normal distribution under the central limit theorem (Rosenblatt, 1956). The z-score results were crosschecked using the chi-square (χ^2) plot method (Garrett, 1989) to minimise errors in the outlier detection process.

The *z*-score signifies distance from a data point to the mean in units of the standard deviation, and it is defined as:

$$"z - score" = (x - \mu/\sigma) \qquad \text{Eq. 4-2}$$

where x is the raw data point, μ is the mean of the sample, and σ is the standard deviation of the sample. As in normal statistical heuristics, in this study, a data point is classified as an extreme value if the z-score is greater than four, and it is categorised as a possible outlier when the z-score is greater than three.

In succession, Garrett's χ^2 plot method was utilised to detect multivariate outliers. The basic convention of Garrett's method is a statistical axiom that normally distributed multivariate datasets approximately comply with a χ^2 distribution with p degree of freedom (χ^2_p). Garrett's method is recognised as a reliable multivariate outlier detection method, and it requires calculation of the Mahalanobis distance (MD), which is a distance measurement method for multivariate conditions. In contrast with Euclidean distance, MD considers the covariance matrix of a given dataset, and the distance between the centroid (multidimensional mean) and covariance (multidimensional variance) of a distribution is measured (Mahalanobis, 1936). For a p-dimensional multivariate sample x_i $(i = 1, 2, 3, \dots, n)$, the MD is defined as:

$$MD_i = \left((x_i - t)^T C^{-1} (x_i - t)\right)^{1/2} \qquad \text{Eq. 4-3}$$

where t and C are the estimated multivariate location (multivariate arithmetic mean) and estimated covariance matrix (sample covariance matrix), respectively. In this study, the MD was calculated using SPSS (Statistical Product and Service Solutions). Ultimately, the χ^2_{10} plot for the 1,354 datasets is depicted in Figure 4-4.

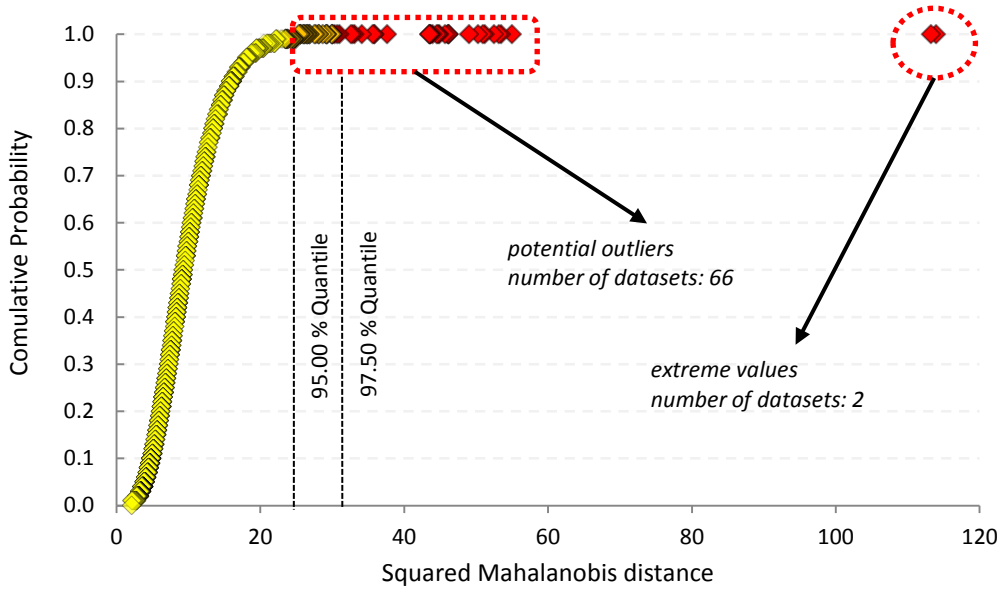

Figure 4-4 Plot of MD^2 against $\boldsymbol{\chi^2_{10}}$ for the 1,354 datasets

As shown in Figure 4-4, two extreme values were distinguished, and 66 datasets were considered as potential outliers falling within the 95% quantiles. A comparison

of the Garrett's χ^2 plot method result with the z-score result revealed that 83.33% of the candidate extreme values (z-score > 4) were in the $\chi^2_{10;\,0.950}$. Thus, 68 datasets were removed as outliers during the first filtering stage.

4.2.5.2 Second filtering stage

The majority of extreme outliers were eliminated by the thorough first filtering stage. However, a second filtering was carried out to increase the reliability of proposed models by removing certain abnormal data points. The second filtering stage was composed of two sub-stages. In the first sub-stage, abnormal data points were identified and scanned out using scatter plots of the dependent variables against each independent variable. Figure 4-5 shows examples of abnormal data points in a scatter plot matrix with 1,286 datasets after the first filtering.

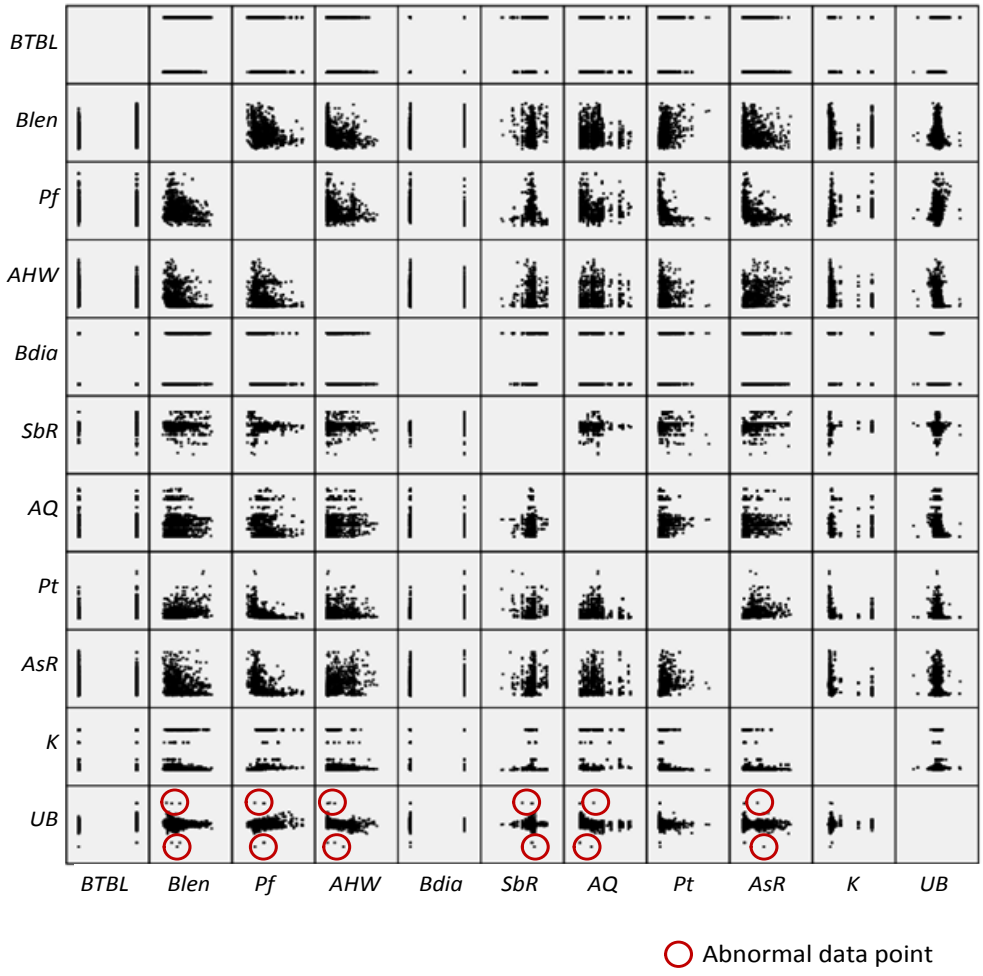

Figure 4-5 Scatter plot matrix of 1,286 datasets after the first filtering stage

As a result of the first sub-stage, four datasets were removed from each of the mine-B and mine-C datasets.

In the second sub-stage of the second filtering, 211 data points from mine-C were removed because they had improper K values. In 2004, mine-C conducted in-situ stress measurements by using the over-coring method at depths of 245 m and 577 m (BFP Consultants Pty Ltd, 2004). However, the in-situ stress from ground level to 245 m could not be correctly estimated with the method because stress was already distributed from earlier productions. Thus, 211 data points from above the 245 m level in mine-C were eliminated. The vertical stress and K values from mines A, B, and C are depicted in Figure 4-6 and Figure 4-7, respectively.

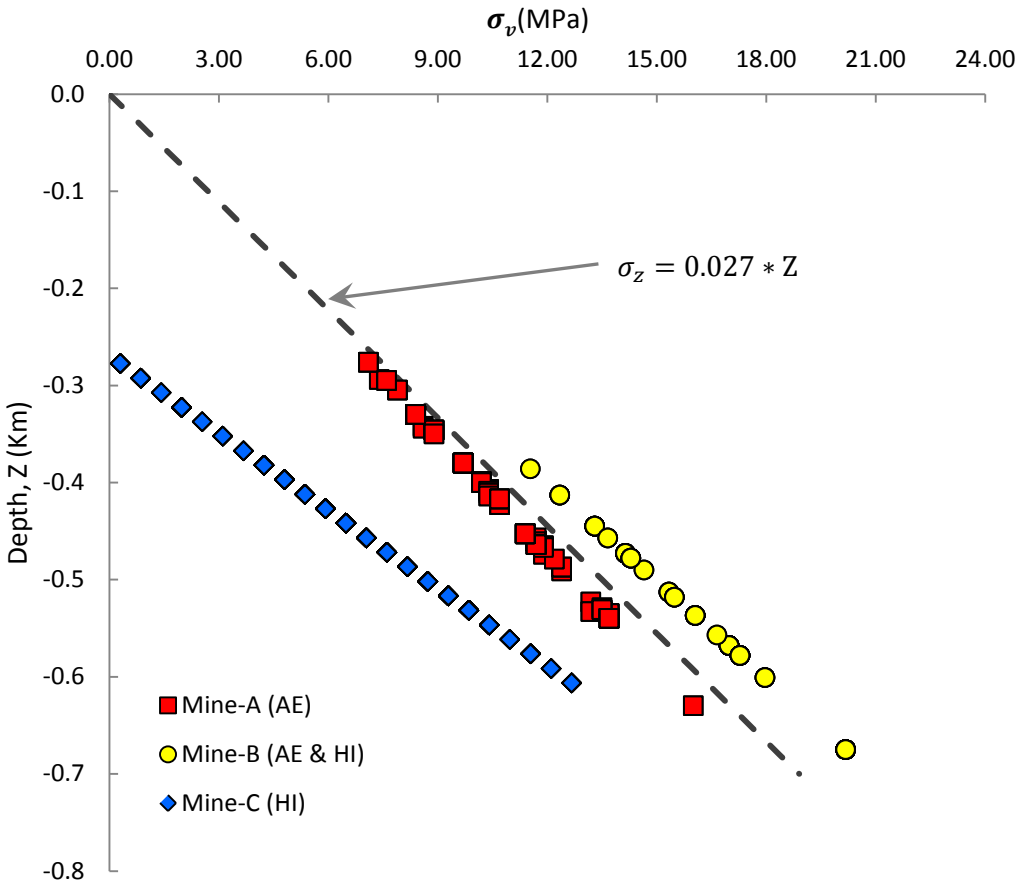

Figure 4-6 Vertical stress of mines A, B, and C. Modified after Brown and Hoek (1978). AE: acoustic emission method, HI: Hollow Inclusion cell over-coring method.

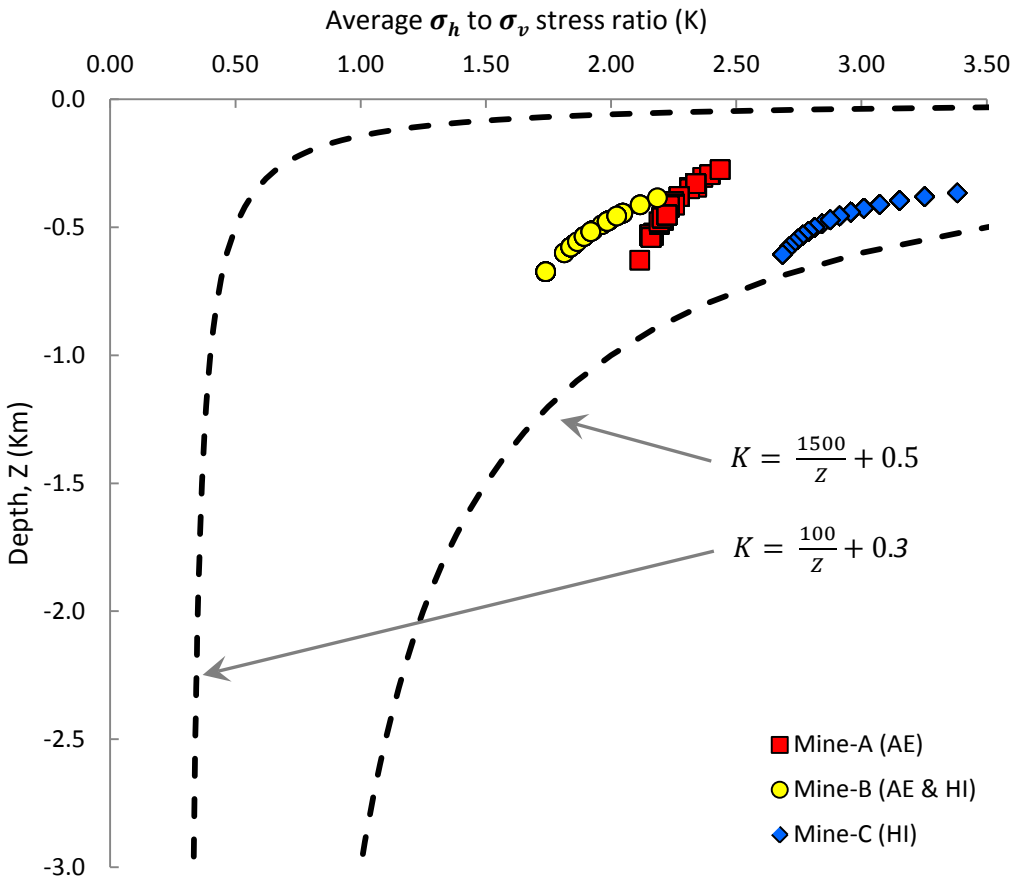

Figure 4-7 Average horizontal stress of mines A, B, and C. Modified after Brown and Hoek (1978).

As shown in Figure 4-6, the estimated vertical stress ($\boldsymbol{\sigma_v}$) of mine-C reaches zero at the depth of 245 m. Thus, the data collected above 245 m are not variable.

4.2.5.3 Result of data filtering

Through outlier filtering stages, 219 out of 1,354 datasets were removed to improve the quality of the datasets, and the results are summarised in Table 4-2.

Table 4-2 Summary of first and second filtering stages

DATA FILTERING	Mine-A	Mine -B	Mine -C	Overall datasets	Filtered datasets
Initial dataset	150	259	945	1,354	0
First filtering	126	235	925	1,286	68
Second filtering	126	231	710	1,067	219

As shown in Table 4-2, 68 and 219 datasets were removed from the first and second outlier filtering stages respectively. In the second filtering stage, 4 datasets from mine-B and mine-C were eliminated from the scatter plot scan and 211 invalid datasets were excluded. The quality improvements from each data filtering stage were monitored by multiple linear regression analysis (MLRA), and the results are demonstrated in Figure 4-8.

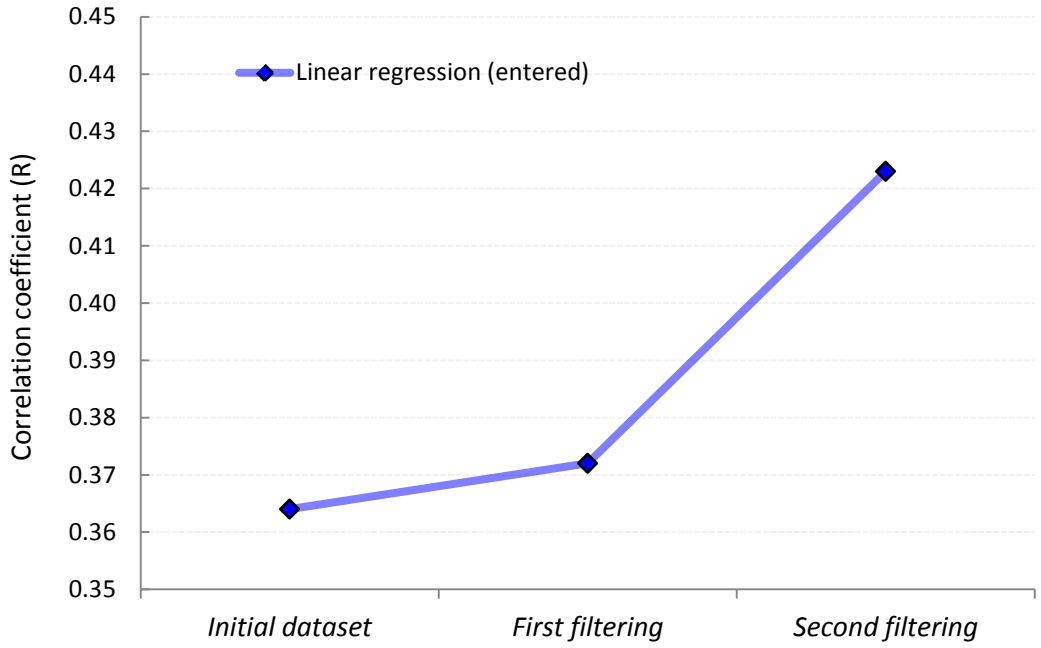

Figure 4-8 Multiple linear regression analysis results for each filtering stage

The MLRAs were conducted using an entered method that inputs ten independent variables simultaneously. The correlation coefficient (R) of the initial dataset was 0.364, and it increased modestly to 0.372 after the first filtering stage. Then, after the second filtering stage, R increased dramatically up to 0.423, which indicates the strong influence of invalid datasets on the reliability of the analysis. Scatter plots of the ten collected UB causative factors against the actual uneven break (UB) percentage are presented in Appendix A.

In addition, the Spearman's correlation between the dependent variable (UB) and each independent variable improved with each step. The independent variables are statistically significant (P-values < 0.05) except *Bdia*. The reason may be the low resolution of the data. A proper blasthole diameter for underground stoping is empirically adjusted to 76 and 89 mm, and the two values were the only options

during the data collection stage. However, Bdia was not rejected on further analysis because it functioned as a critical variable for predicting UB. Indeed, in statistics, insignificance (P-values > 0.05) is not synonymous with unimportance, and insignificance can be ignored when a variable with a poor P-value is indispensable for the meaningful interpretation of a study (Carver, 1978). The variations in Spearman's correlation due to each filtering stage are shown in Figure 4-9.

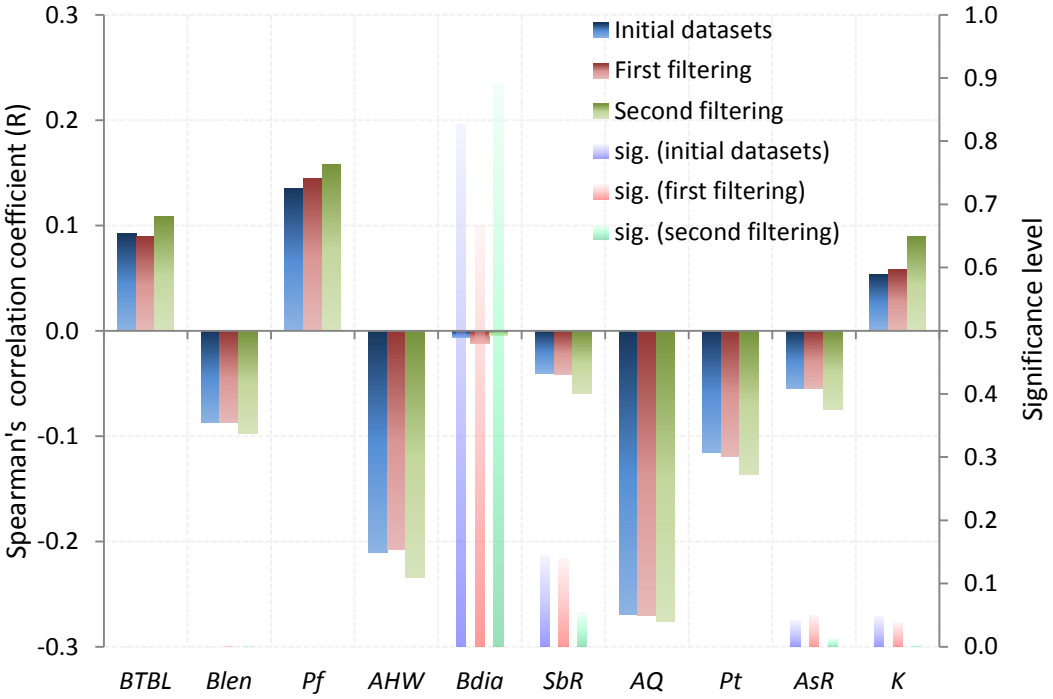

Figure 4-9 Variations of the Spearman's correlation due to data filtering stages

4.3 SURVEY FOR UB CONSULTATION FUZZY EXPERT SYSTEM

Membership functions and fuzzy 'IF-THEN' rules must be determined to develop a fuzzy expert system (FES). To develop an UB consultation FES, a survey was conducted that was intended for underground mining experts. Fifteen experts with 10 to 30 years of underground mining experience participated in this survey. Three experts were currently working in an underground stoping mine in Western Australia and twelve experts are members of the International Society of Explosive Engineers (ISEE) in the U.S. and Canada.

To prepare the survey, the overall feature of the FES was specified. The quality of the rock mass and the degree of uneven break were allocated as input factors, and the ratio of powder the factor and ground support were allocated as output values

of the proposed FES. The details of the fuzzy membership functions and the 'IF-THEN' rules were formulated based on the survey results, which are tabulated inTable 4-3.

Table 4-3 Summary of survey results from fifteen underground mining experts

Rock quality	Dilution type	Powder factor			Ground support		
		Dec	ReT	Inc	Dec	ReT	Inc
Poor Rock	*MovB*	90%	0%	10%	0%	40%	60%
	ovB	70%	20%	10%	0%	90%	10%
	Act	0%	100%	0%	0%	100%	0%
	unB	10%	60%	30%	30%	70%	0%
	MunB	10%	0%	90%	20%	70%	10%
Fair Rock	*MovB*	80%	10%	10%	0%	40%	60%
	ovB	50%	40%	10%	0%	90%	10%
	Act	0%	100%	0%	0%	100%	0%
	unB	10%	60%	30%	20%	80%	0%
	MunB	10%	0%	90%	40%	60%	0%
Good Rock	*MovB*	100%	0%	0%	10%	30%	60%
	ovB	50%	40%	10%	0%	90%	10%
	Act	0%	100%	0%	0%	100%	0%
	unB	10%	40%	50%	0%	100%	0%
	MunB	10%	0%	90%	50%	50%	0%

MunB: *massive-underbreak;* ***unB:*** *underbreak;* ***AcT:*** *acceptable;* ***ovB:*** *overbreak;* ***MovB:*** *massive-overbreak;* ***Dec:*** *decrease;* ***ReT:*** *retain;* ***Inc:*** *increase*

The modified rock mass quality (Q') values collected from the mines vary from 6.30 to 93.30, and the rock quality was classified as poor, fair, and good. The survey was conducted to discover the strength of the optimal dilution via verifying powder factor degree and the ground support. For example, as highlighted with blue in Table 4-3, if massive overbreak (MovB) is expected in poor rock, 90% of the experts decided to decrease the powder factor, 60% of the experts intended to increase ground support, while 40% decided to retain the ground support to optimise potential UB. The membership functions and the fuzzy rules of the proposed fuzzy expert system (FES) were determined based on the survey results, and detailed information will be provided in Chapter 6.

4.4 SUMMARY AND DISCUSSION

Data collection for an uneven break (UB) prediction model and a survey for a UB consultation model have been discussed in this chapter. As the reliability of the proposed models significantly relies on the quality and the quantity of the datasets, ten UB causative factors were cautiously selected to cover all three UB causative categories. Comprehensive field data were collected from three underground stoping mines in Western Australia. To improve the quality of the datasets, two separate data filtering stages were conducted and 219 out of 1,354 datasets were eliminated as possible outliers. As a result of the data filtering stages, the linear regression analysis correlation coefficient (R) improved from 0.364 to 0.432.

To build a reliable UB consultation fuzzy expert system (FES), a survey was conducted of fifteen underground mining experts. The collected experts' knowledge was used to formulate membership functions and fuzzy rules for a UB consultation system.

CHAPTER 5. UB PREDICTION SYSTEM MODELLING

5.1 INTRODUCTION

Uneven break (UB) is the most critical conundrum in underground mining. Certainly, the UB phenomenon is inevitable if an underground stope is excavated by the drilling and blasting method. Although the drilling and blasting method guarantees some financial flexibility through low production cost, the mine is always exposed to the unexpected danger of uneven break. Hence, UB management is an essential task not only for underground stoping but also for other mining methods employing drilling and blasting.

To effectively manage uneven break (UB), a UB prediction system must be established. By doing so, UB can be optimised. In this study, UB prediction systems were modelled using both the conventional statistical manner and an advanced soft computing approach. In the statistic manner, multiple linear and nonlinear regression analyses (MLRA and MNRA) were employed. Moreover, an artificial neural network (ANN) was utilised to establish a more reliable UB prediction model as a soft computing approach. This chapter initially reviews the current UB management results in the three investigated mines. Then, the UB prediction models established by MLRA, MNRA, and ANN are introduced.

5.2 CURRENT UB PREDICTION METHODS IN THE INVESTIGATED MINES

The three investigated mines employed the stability graph method to predict unplanned dilution and to assist in stope design. Because there is no method to predict ore loss, the prediction performance evaluation was limited to unplanned dilution. The actual unplanned dilution and ore loss were obtained by comparing a stereoscopic stope design model with the CMS model captured after production. The performance of the predictions was evaluated by computing the correlation coefficient (R) between the engineers' prediction and the actual stope uneven break (UB). Table 5-1 shows the prediction performance of the three mines, and the overall results were integrated into a general model (GM).

Table 5-1 Results of unplanned dilution and UB predictions in mines A, B, and C, and the GM

Correlation coefficient (*R*)	Mine-A	Mine-B	Mine-C	GM
Unplanned dilution and ore-loss (*uneven break*)	0.0734	-0.0518	0.0583	0.0884
Unplanned dilution (*overbreak only*)	0.0971	-0.2159	0.2557	0.3101

As shown in Table 5-1, the uneven break (UB) predictions were very unsatisfactory. None of the three mines had a competent correlation coefficient (R) for either uneven break (UB) or unplanned dilution solely. Figure 5-1 shows the low correlation results of the general model (GM), and it includes unplanned dilution only (a) and unplanned dilution with ore-loss (b).

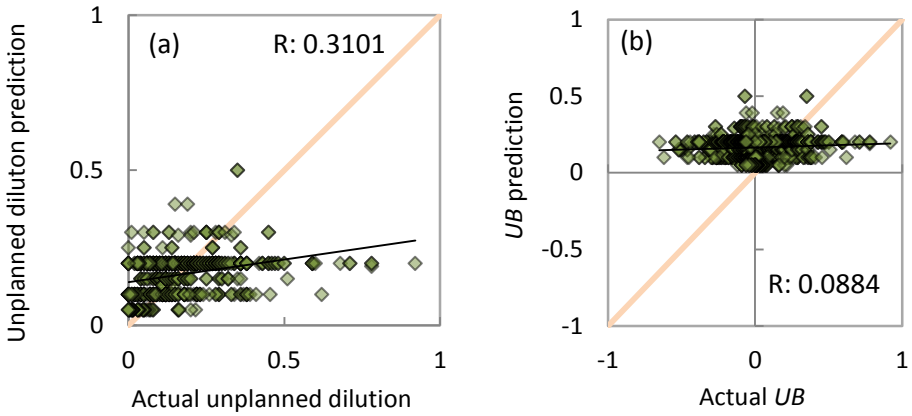

Figure 5-1 Correlation results of the general model (GM) (a) Unplanned dilution comparison (B) *UB* comparison

The results imply the difficulties of predicting uneven breaks. In other words, mines are severely suffering from unexcitable over and under breaks. Despite endeavours by many researchers, no uneven break (UB) prediction system yet provides a satisfactory solution.

5.3 MULTIPLE REGRESSION MODELS

As a conventional statistical method, multiple linear and nonlinear regression analyses (MLRA and MNRA) were employed to build an applicable uneven break (UB) estimation model by using a software package for statistical analysis: Statistical Product and Service Solutions (SPSS) (IBM, 2012). MLRA and MNRA were used to model each mine site and for a general model (GM) based on all of the datasets.

5.3.1 *Multiple linear regression analysis*

Primarily, an MLRA model was built for each dataset with all independent variables, and this is referred to as the MLRA-enter model. Subsequently, insignificant variables were removed in a stepwise manner to obtain the optimised MLRA-stepwise model using statistical significance levels for F and t. Details of Multiple regression models are provided in Appendix D and the MLRA-enter and stepwise models for mines A, B, and C and the General Model (GM) are tabulated inTable 5-2.

Table 5-2 Multiple linear regression analysis (MLRA) results for mine A, B, C, and GM

DATA SETS	MODEL	EQUATION	R	$R^2_{adj.}$
Mine-A	*En*[2]	$UB = .969 - .018BTBL - .009Blen + .375Pf - .067AHW + .024Hdia + .017SbR - .091AQ + .048Pt + .042AsR + .104K$	.581	.280
	St[3]	$UB = 1.088 + .377Pf - .048AHW - .093AQ + .039Pt + .044AsR$	.567	.293
		K, Blen, Hdia, BTBL, and SbR are removed in stepwise-MLRA		
Mine-B[1]	*En*	$UB = -.651 + .005BTBL - .162Blen + .123Pf - .137AHW - .052SbR - .756AQ + .018Pt - .037AsR + 3.229K$	.590	.322
	St	$UB = .114 - .158Blen - .144AHW - .156AQ + 2.528K$	.584	.330
		BTBL, SbR, Pt, Pf, and AsR are removed in stepwise-MLRA		
Mine-C	*En*	$UB = 1.129 + .034BTBL - .125Blen + .140Pf - .138AHW - .026Hdia + .123SbR - .133AQ + .135Pt + .203AsR + .021K$	.422	.166
	St	$UB = 1.489 + .033BTBL - .127Blen + .134Pf - .143AHW - .125AQ + .190AsR$	.412	.163
		K, Hdia, SbR, and Pt are removed in stepwise-MLRA		
GM	*En*	$UB = 1.521 + .029BTBL - .119Blen + .123Pf - .152AHW + .013Hdia + .015SbR - .113AQ + .023Pt + .069AsR + .039K$	.423	.171
	St	$UB = 1.595 + .031BTBL - .105Blen + .122Pf - .149AHW - .106AQ + .073AsR$	.419	.171
		K, Hdia, SbR, and Pt are removed in stepwise-MLRA		

[1]Hdia was removed from the MLRA and MNRA because the Mine-B dataset had only one value for this variable.
[2]En (enter model): All independent variables were considered in a single model.[3]St (stepwise model): A proposed model only includes independent variables that are satisfied with the criteria (F<=.050).

As observed from Table 5-2, the adjusted coefficients of the determinant (R^2_{adj}) for the MLRA-enter and stepwise models for the mine-A dataset were 0.280 and 0.293, respectively. In the optimised MLRA-stepwise model, the variables K, Blen, Hdia, BTBL, and SbR were removed because of their insufficient t-values. The mine-B dataset MLRA models yielded the highest R^2_{adj} values among the MLRA models with MLRA-enter and stepwise R^2_{adj} values of 0.322 and 0.330, respectively. Hdia was not included in the models because only one value for Hdia is in the mine-B dataset. In the MLRA-stepwise model, BTBL, SbR, Pt, Pf, and AsR were removed due to inadequate t-values. The mine-C model shows the lowest R^2_{adj} for both the MLRA-enter and stepwise models with 0.166 and 0.163, respectively. The F and t values for K, Hdia, SbR, and Pt were unacceptable and were removed from the MLRA stepwise model. All of the data from the three mines were integrated for the general model (GM), and the R^2_{adj} was calculated as 0.171 for both the MLRA-enter and stepwise models. The MLRA-stepwise model was established without K, Hdia, SbR, and Pt because of their improper F and t values.

5.3.2 *Multiple nonlinear regression analysis*

As shown by the previous MLRA modelling, the complexity of uneven break (UB) cannot be adequately interpreted using a linear model. Hence, multiple nonlinear regression analysis was conducted to build a proper UB prediction model. Among several nonlinear approaches, the twin-logarithmic model was adopted, assuming the following nonlinear relation:

$$Y = \beta_0 \left(X_1{}^{\beta_1}\right)\left(X_2{}^{\beta_2}\right)\cdots\left(X_n{}^{\beta_n}\right) \qquad \text{Eq. 5-1}$$

where Y represents the predicted value corresponding to the dependent variables $(X_1, X_2, \cdots, X_n)$ and β_0 to β_n are the parameters for the nonlinear relationship. The formula (Eq. 5-1) can be converted into a linear domain through log transformation, as shown in Eq. 5-2. Therefore, the β values can be determined based on a multiple linear regression of $log(Y)$ on $log(X_1), log(X_2) \cdots log(X_n)$ (Cankaya, 2009).

$$log(Y) = \log(\beta_0) + \beta_1 log(X_1) + \beta_2 log(X_2) + \cdots + \beta_n log(X_n) \qquad \text{Eq. 5-2}$$

Logarithmic functions cannot compute negative or zero values. Because the ore loss rate is expressed as a negative value of the dependent variable (UB) and two independent variables (BTBL and AHW) contain zero values, an additional transformation process was employed to transform the zero and negative values into positive real values in an unbiased manner. To do so, the value of one was added after the datasets were normalised to between zero and one. After this transformation process, the datasets yielded values between one and two.

The Levenberg-Marquardt iterative estimation algorithm (Marquardt, 1963) was used to generate the proposed MNRA models. Consequently, optimal MNRA models for mines A, B, and C and the GM were obtained after eight, twelve, six, and six iterations, respectively, when the residual sum of squares reached 1.0E-008. The MNRA model results are tabulated in Table 5-3.

Table 5-3 Multiple nonlinear regression analysis (MNRA) results for mines A, B, and C, and the GM

DATA SETS	EQUATION	R	$R^2_{adj.}$
Mine-A	$UB = 1.407(Pf^{.306})(AHW^{-.040})(AQ^{-.090})(Pt^{.035})(AsR^{.042})$	.563	.317
	K, Blen, Hdia, BTBL, and SbR was removed in MNRA		
Mine-B[1]	$UB = 1.669(Blen^{-.164})(AHW^{-.163})(AQ^{-.652})(K^{1.359})$	.607	.368
	BTBL, SbR, Pt, Pf, and AsR was removed in MNRA		
Mine-C	$UB = 1.455(BTBL^{.033})(Blen^{-.129})(Pf^{.129})(AHW^{-.126})(AQ^{-.127})(AsR^{.167})$	.425	.181
	K, Hdia, SbR, and Pt was removed in MNRA		
GM	$UB = 1.473(BTBL^{.031})(Blen^{-.116})(Pf^{.107})(AHW^{-.144})(AQ^{-.112})(AsR^{.079})$	.438	.192
	K, Hdia, SbR, and Pt was removed in MNRA		

The adjusted coefficients of determinant (R^2_{adj}) for mines-A, B, and C and the GM were 0.317, 0.368, 0.181, and 0.192, respectively, which are slightly higher than the MLRA-stepwise models. The contributions of the independent variables were similar to those in the MLRA models. Indeed, the MNRA models were also insufficient for expounding the relationship between UBs and the given independent variables.

When building the MLRA and MNRA models, heteroskedasticity, multicollinearity, and autocorrelation problems were checked through residual plots, the variance Inflation Factor (VIF), and the Durbin-Watson value (Durbin & Watson, 1950) because these phenomena may lead to an invalid conclusion. No suspicious circumstances were found in the proposed multiple regression models.

5.4 ARTIFICIAL NEURAL NETWORK MODEL

Unfortunately, the proposed multiple regression methods were not adequate to reveal the relationship between uneven break (UB) and the ten causative parameters. Thus, attempts were made with an artificial neural network (ANN), which is well recognised as an advanced nonlinear approximation approach.

Special caution must be taken when preparing ANN applications because the performance of ANN is prominently affected by the learning algorithm, the transfer function, and ANN architecture. As described in Chapter 3, the innovative conjugate gradient algorithm (CGA) (Hestenes & Stiefel, 1952) was adopted as the learning algorithm.

Among several transfer functions, the hyperbolic tangent (tansig) and log sigmoid (logsig) functions are extensively employed as nonlinear activation functions. In this study, tansig was chosen as the transfer function because it showed better performance than logsig in an earlier over and under breaks prediction study accomplished by Jang and Topal (2013). The tansig output varies from minus one to one. Thus, all datasets were scaled into the same range by using Eq. 5-3. After the trained ANN model estimates the output, which is also scaled into the minus one to one range, the scaled output is standardised using Eq. 5-4.

$$x_s = [2(x - x_{min})/(x_{max} - x_{min})] - 1 \qquad \text{Eq. 5-3}$$

$$x = [0.5(x_s + 1)(x_{max} - x_{min})] + x_{min} \qquad \text{Eq. 5-4}$$

The structure of the proposed UB prediction ANN is composed of three layers: input, hidden, and output. As the collected datasets are made up of one dependent and ten corresponding independent variables, the output and input layers are composed of one and ten nodes. The last key component of the appropriate ANN is

the optimum number of hidden neurons. Empirical suggestions have been reported, such as by Hecht-Nielsen (1987) and Kaastra and Boyd (1996). However, the optimal number of hidden neurons may differ in simulations even for the same problem. Hence, in this study, the appropriate number of hidden neurons for each model was determined by an iterative loop operation algorithm coded by MATLAB. Figure 5-2 shows a schematic view of the proposed ANN.

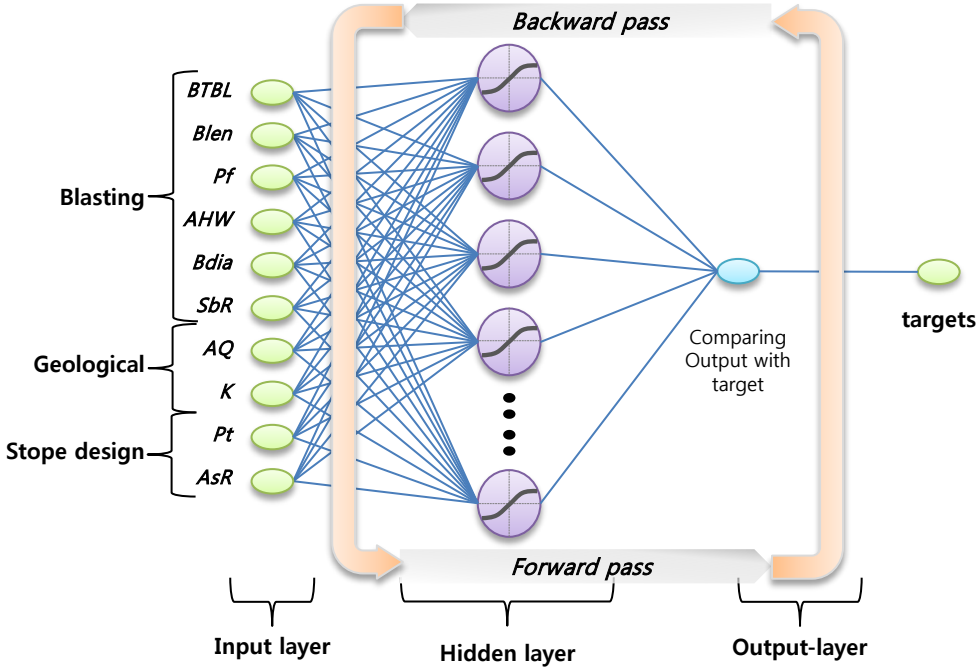

Figure 5-2 Architecture of the proposed ANN model

Another difficulty in programming ANNs is the over-fitting problem. The sign of an over-fitting problem is that the model demonstrates excellent fitting during the training stage, but it cannot correctly predict the output for an untrained sample. In other words, the model is not generalised. Over-fitting problems can happen if an ANN model contains too many parameters or has excessively complex architecture (Hawkins, 2004). Various algorithms have been introduced to remedy the over-fitting problem in ANN models, e.g., pruning (Karnin, 1990; Reed, 1993), early-stopping (Morgan & Bourlard, 1989), and cross-validation (Hansen & Salamon, 1990). In this study, the most prevalent cross-validation algorithm was adopted to prevent over-fitting. For the validation process, some portion of untrained datasets is assigned as validation datasets that are not involved in the training process.

During the training process, the generalisation for each training step is cross-checked using untrained validation datasets.

In this study, the datasets were randomly apportioned into three subsets: training, validation and test. A total of 70% of the datasets were used for training, 15% were assigned to the validation stage, and 15% were assigned to the test stage. The proposed artificial neural network (ANN) was programmed using MATLAB code (MathWorks, 2013), and ANN training and forward pass codes are given in Appendix B. Ultimately, optimum UB prediction models for mines A, B, and C and the GM were obtained. The details of the generated UB prediction models are tabulated in Table 5-4, and the test performance of each model is demonstrated in Figure 5-3.

Table 5-4 Details of the UB prediction models for mines A, B, and C and the GM

Model	Number of datasets				Structure of ANN	RMSE[4]		R[5]	
	TR[1]	VA[2]	TE[3]	Total	Input-Hidden-Output	TR[1]	VA[2]	TR[1]	TE[3]
Mine-A	88	19	19	126	10 – 7 – 1	1.04E-2	6.75E-2	0.92	0.94
Mine-B	161	35	35	231	10 – 16 – 1	2.15E-2	8.04E-2	0.86	0.80
Mine-C	496	107	107	710	10 – 16 – 1	2.36E-2	3.19E-2	0.74	0.70
GM	747	160	160	1,067	10 – 40 – 1	1.90E-2	2.80E-2	0.66	0.72

[1] ***TR:*** *Training;* [2] ***VA:*** *Validation;* [3] ***TE:*** *Test;* [4]***RMSE:*** *Root Mean Square Error;* [5]***R:*** *Correlation coefficient*

As demonstrated in Table 5-4, the ideal number of hidden neurons for mines A, B, and C and the GM were 7, 16, 16, and 40, respectively. In each iteration, the root mean square error (RMSE) was calculated to check the performance of the model. While training, the RMSEs of the training and validation stages were considerably lower after 30 iterations, and they decreased progressively through 100 iterations. As a result of the training stage, the RMSEs for mines A, B, and C and the GM reached 1.04E-2, 2.15E-2, 2.36E-2, and 1.90E-2, respectively. The four proposed ANN models were tested with the 15% untrained datasets, and the correlation coefficient (R) was calculated between the actual UB rate and the UB rate predicted by the ANN model. A graphical view of the test results for mines A, B and C and the GM model is shown in Figure 5-3.

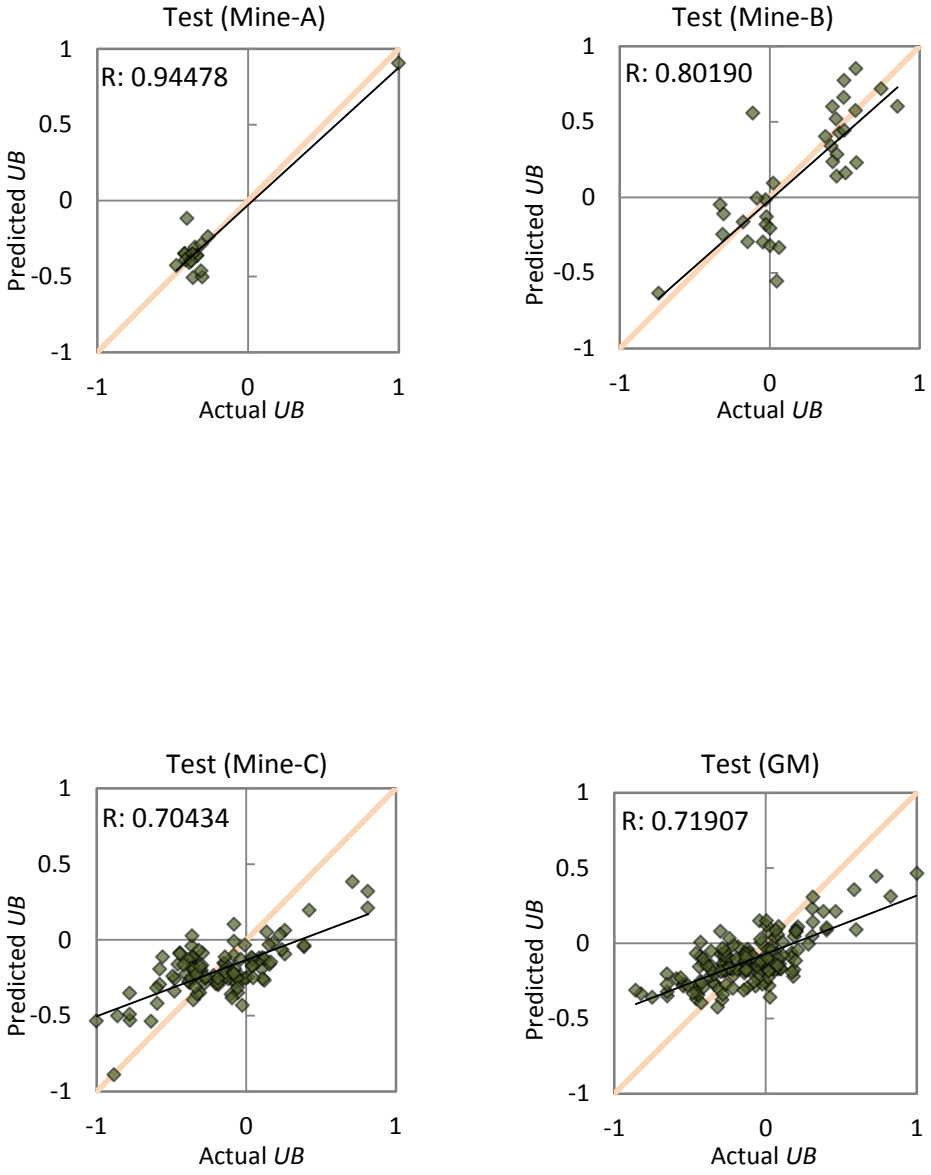

Figure 5-3 Test performance of *UB* prediction ANN models for mines A, B, and C and the GM

As shown in Figure 5-3, strong positive correlations (R > 0.7) were observed in all models. Because the GM model consisted of the mines A, B, and C investigations and yielded a correlation coefficient (R) of 0.72, the possibility exists of establishing a general uneven break prediction model.

5.5 SUMMARY AND DISCUSSION

In this chapter, multiple linear and nonlinear regression analyses (MLRA and MNRA) and a conjugate gradient artificial neural network (CG-ANN) were used to generate uneven break (UB) prediction models from 1,067 datasets with ten uneven break (UB) causative factors collected from three underground stoping mines in Western Australia. The performance of each established model is compared with actual uneven break (UB) predictions in the investigated mines in Figure 5-4.

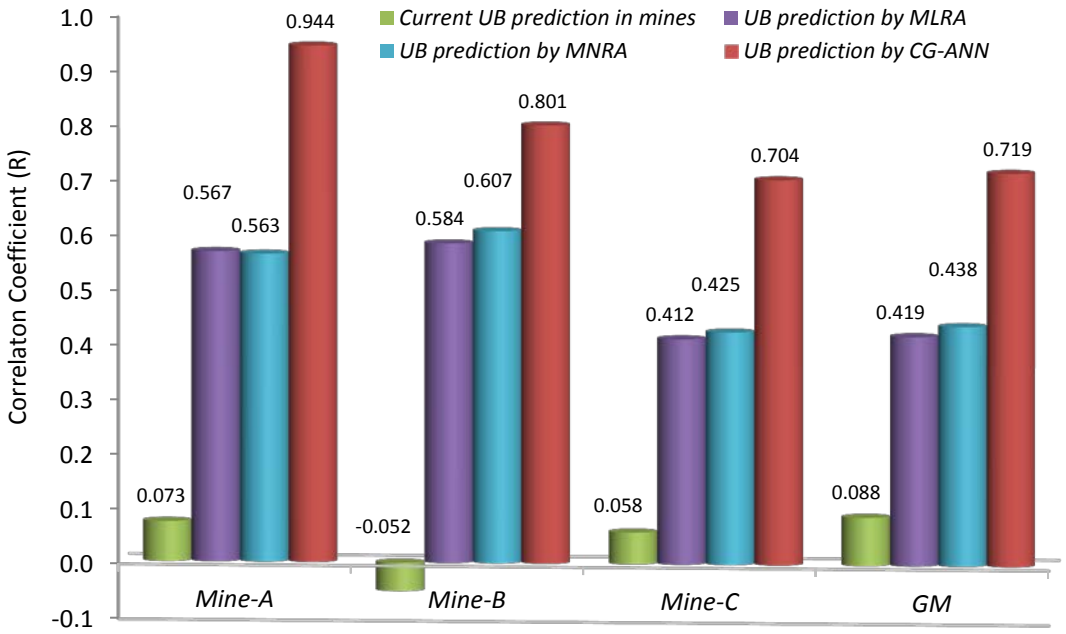

Figure 5-4 Comparison of uneven break (UB) predictions between the investigated mines and the MLRA, MNRA, and CG-ANN models for mines A, B, and C and the GM.

As shown in Figure 5-4, the MLRA and MNRA models show poor to moderate prediction performance, as the correlation coefficient (R) ranges between 0.412 and 0.607. In each dataset except mine-A, the R of the MNRA model was slightly higher than that of the MLRA model. These irregular phenomena imply the difficulties of uneven break (UB) prediction by such statistical methods.

In contrast with the MLRA and MNRA results, the CG-ANN models provided reliable UB prediction performance. As demonstrated in Figure 5-4, the highest correlation coefficient (R) of 0.944 occurred in the mine-A dataset, while those in the mine B, C, and GM models were 0.801, 0.704, and 0.719. The advanced uneven break (UB)

prediction performance of the CG-ANN model is highlighted by comparing it to the current UB prediction performance in the investigated mines, as shown in Figure 5-5.

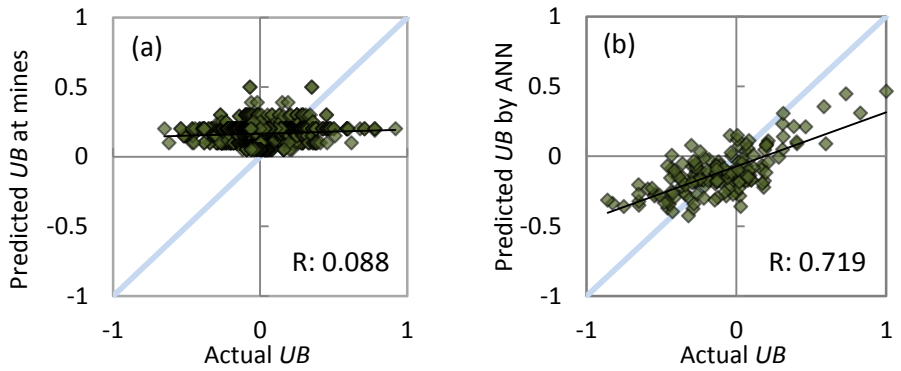

Figure 5-5 Comparison of current UB prediction in the mines with the test performance of the ANN model

As shown in Figure 5-5a, currently, uneven break (UB) prediction by the investigated mine sites is highly unsatisfactory and is limited to unplanned dilution without including ore-loss. In contrast to the poor performance of current UB prediction, the optimised CG-ANN (Figure 5-5b) provides reliable UB prediction performance.

Uneven break (UB) prediction has been recognised as one of the challenging tasks in underground stoping mines, and it has been neglected as an unpredictable phenomenon. However, the proposed CG-ANN model provides an optimistic perspective on uneven break (UB) prediction.

CHAPTER 6. PARAMETERS CONTRIBUTION TO UB PHENOMENON

6.1 INTRODUCTION

Despite numerous studies on unplanned dilution and ore-loss (uneven break: UB), the exact mechanisms occurring have yet to be investigated clearly. As demonstrated in Chapter 2, the UB phenomenon is affected by numerous known and unknown factors, and their mutual interactions exacerbate the complexity of UB. The basis of the complexity of UB mechanisms derives from both the object material, the rock mass, and the subject of explosion, the dynamic shock wave and gas pressure. The inherent features of the rock are anisotropic and inhomogeneous. Furthermore, the elastic-plastic behaviour of rock with randomly distributed discontinuities of different weights makes it difficult to estimate its fracture behaviour. The fracture behaviour of rock becomes more complex when the rockmass is forced by the dynamic power of an explosion, and it becomes even more complicated when considering the design of an underground stope.

The exact UB causative factors are yet to be clearly defined. Thus, surveying all potential UB causative parameters is impractical although it possibly guarantees more accurate determination of UB mechanism. As described in Section 2.4, after careful consideration, ten major UB causative factors were selected through a rigorous inspection of previous studies which can cover most of possible influences.

In this study, ten UB causative factors, i.e., average blasthole length (Blen), powder factor (Pf), angle difference between the hole and wall (AHW), blasthole diameter (Bdia), space and burden ratio (SbR), adjusted Q-value (AQ), average horizontal to vertical stress ratio (K), planned tonnes of stope (Pt), aspect ratio (AsR), and stope either breakthrough to a nearby drift and/or stope or not (BTBL), were collected as independent variables for the one dependent variable, uneven break (UB). Thus, the relationship between uneven break (UB) and the selected independent variables can be written as:

$$UB = f(Blen, Pf, AHW, Bdia, SbR, AQ, K, Pt, AsR, BTBL) \quad \text{Eq. 6-1}$$

In this chapter, attempts have been made to enlighten the parameter contributions to UB phenomenon. Parameter contribution analyses were conducted based on multiple linear and nonlinear regression analyses (MLRA and MNRA) and artificial neural network (ANN) UB prediction models of GM datasets.

6.2 PARAMETER CONTRIBUTION OF MULTIPLE REGRESSION ANALYSIS

Multiple regression analysis is an expanded bivariate regression that incorporates more than one independent variable into regression analyses. In this study, both multiple linear and multiple nonlinear regression analyses (MLRA and MNRA) were employed to examine the linear and nonlinear relationships between the one dependent variable, UB, and the ten independent variables. Thus, the basic format of the equation for multiple regression analysis can be defined as:

$$UB = \beta_0 + \beta_1 BTBL + \beta_2 Blen + \beta_3 Pf + \beta_4 AHW + \beta_5 Hdia + \beta_6 SbR + \beta_7 AQ + \beta_8 Pt + \beta_9 AsR + \beta_{10} K \quad \text{Eq. 6-2}$$

As stated in Chapter 5, the twin-logarithmic model was employed to build the multiple nonlinear regression models, and they were also converted into the linear domain (Eq. 5-2) through log transformation. In Eq. 6-2, the regression coefficients $(\beta_0, \beta_1, \beta_2 \dots, \beta_{10})$ represent the effects of the corresponding variables on the dependent variable while the effects of the other variables are held constant. The contribution of the ten independent variables to the dependent variable (UB) in the MLRA-enter & stepwise and MNRA are computed based on the general model (GM) in Table 5-2 and Table 5-3. Ultimately, the results are demonstrated in Figure 6-1.

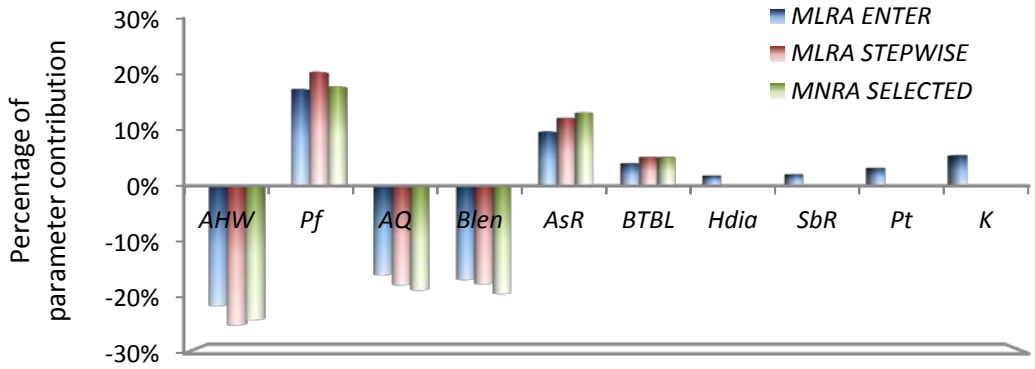

Figure 6-1 Contribution of the ten inputs to the output (UB) of multiple regression analyses of the general model (GM)

As shown in Figure 6-1, four variables, i.e., Hdia, SbR, Pt, and K, were excluded from the MLRA-stepwise and MLRA models because of insufficient t-values. As assessed in Chapter 5, the MLRA and MNRA models present poor and moderate relationships with the dependent variable, but certain essential engineering aspects can be clarified. In all three models, the AHW, AQ, and Blen variables displayed a negative relationship with uneven break (UB), while the others are positively related. Overall, AHW appeared to be the most influential parameter for UB, as it shows a percentage contribution of 21.87%, 25.43%, and 24.45% in the MLRA-enter, MLRA-stepwise, and MNRA-selected models, respectively. The variables Pf, AQ, Blen, AsR, and BTBL appeared as relevant contributors to UB in descending order.

6.3 PARAMETER CONTRIBUTIONS TO THE UB ON ANN MODEL

As the UB prediction ANN model has shown good performance with the GM dataset, the reliability of the parameter contribution analysis is higher for the ANN model than for the multiple regression analysis. However, ANN is often called a 'black box' due to its lack of descriptive insight into the prediction process (Olden & Jackson, 2002) even though it is recognised as an intelligent statistical modelling method. Various methods for elucidating the contribution of the input to the output of ANNs have been introduced, and these can be categorised into two groups as shown in Table 6-1.

Table 6-1 Representative methods for examining the contribution of input to output in ANN

Category	Representative methods
Weight based algorithm	o Garson's algorithm (Garson, 1991) o Connection weight approach (CWA) (Olden & Jackson, 2002)
Sensitivity based algorithm	o Partial derivatives (PaD) method (Dimopoulos et al., 1995) o Relative Strength of Effect (RSE) (Yang & Zhang, 1998) o Profile method (PM) (Lek et al., 1996) (referred to as the 'Profile method' by Gevrey et al. (2003))

Weight-based algorithms compute the input's contribution to the output based on the connection weights of the ANN model. The advantages of this algorithm are that the computation process is simpler than in sensitivity-based algorithms, and the direction of each variable's contribution can be easily monitored. Sensitivity-

based algorithms investigate the variance of the output subject to the entire range of inputs. Although the computation process is more burdensome for sensitivity-based algorithms than for weight-based algorithms, it can demonstrate the contribution of the entire range of each parameter. In this study, the connection weight approach (CWA) and the profile method (PM) were employed as representative weight- and sensitivity-based algorithms to scrutinise the parameter contributions of the GM dataset.

6.3.1 *Application of a weight-based algorithm*

The original weight-based algorithm was introduced by Garson (1991) to examine input parameters' contributions to output in ANN. Garson's algorithm calculates the sum of the product of input-hidden and hidden-output connection weights across all hidden neurons (Olden et al., 2004). Garson's algorithm was widely used in many fields of studies however, Olden and Jackson (2002) noted that the algorithm does not consider the counteracting connection weight, which could result in incorrect variable importance. Thus, by modifying Garson's algorithm, they introduced a new algorithm, the connection weight approach (CWA). The CWA computes the contribution of input i_1 to output k_1 as:

$$I_{i1,k1} = \sum_{j=1}^{m} w_{j,i1} w_{k1,j} \qquad \text{Eq. 6-3}$$

where i, j, k, and m represent input, hidden, output neuron, and the number of hidden neurons, respectively. In this study, the CWA was used to calculate the input parameters' contributions to the output in the GM datasets and the results are demonstrated in Figure 6-2.

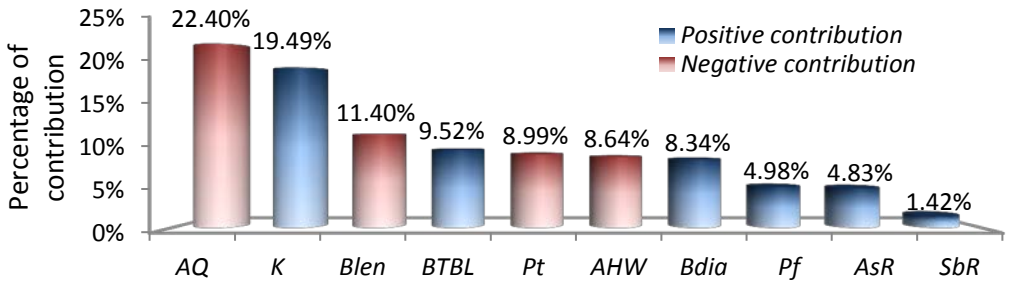

Figure 6-2 Contribution of the ten input parameters to UB for the general model (GM) dataset by the connection weight algorithm (CWA)

As shown in Figure 6-2, AQ is ascertained as the most influential contributor to UB with a 22.40% contribution. K and Blen also exposed relatively high contributions at 19.49% and 11.40%, while the other variables contributed less than 10%.

Through CWA application, the direction of the input parameters' influence was also identified. As shown in Figure 6-2, AQ, Blen, Pt, and AHW revealed to have a negative relationship with UB. These results correspond to the multiple regression analysis results with the exception of Pt. Pt had a positive influence in the MLRA-enter model, but it was removed from the MLRA-stepwise and MNRA models due to insufficient t-values. Thus, it is appropriate to consider Pt as a negative influence parameter.

6.3.2 *Application of a sensitivity-based algorithm*

Another group of parameter contribution investigation methods can be categorised as 'sensitivity-based algorithms', which include PaD, RSE, and the profile method (PM). The primary idea of the three methods is that they examine the sensitivity of output variances for given inputs. The fundamentals of PaD and RSE are similar because they compute the output's derivative with respect to inputs to investigate the variances. The PaD and RSE processes are faster and simpler than the profile method (PM). Thus, they have been employed by many researchers and modified. Details and practical applications of the Pad and RSE methods can be found in the cited references (Beiki et al., 2010; Dimopoulos et al., 1999; Dimopoulos et al., 1995; Kim et al., 2001b; Nourani & Sayyah Fard, 2012; Yang & Zhang, 1998). The profile method (PM) (Lek et al., 1995) is relatively cumbersome compared with PaD and RSE; however, it was applied in this study because it can thoroughly investigate the entire range of input sensitivity with respect to the output. The parameter sensitivity assessment process of AQ by the profile method (PM) can be described as:

$$UB_{(AQ,p)} = ANN(AQ_n, K_p, AsR_p, SbR_p, Pt_p, Pf_p, Bdia_p, Blen_p, BTBL_p, AHW_p) \quad \text{Eq. 6-4}$$

where n represent the overall range of the investigated input parameter, and p is the 20th, 40th, 60th, and 80th of the other input variables. The minimum and

maximum values were not considered in this application because the extreme values seldom occur in actual mining activities.

6.3.2.1 Contribution of AQ to the uneven break phenomenon

An example of profile method (PM) application to the input parameter AQ, which is the most effective contributor to UB is demonstrated in Figure 6-3.

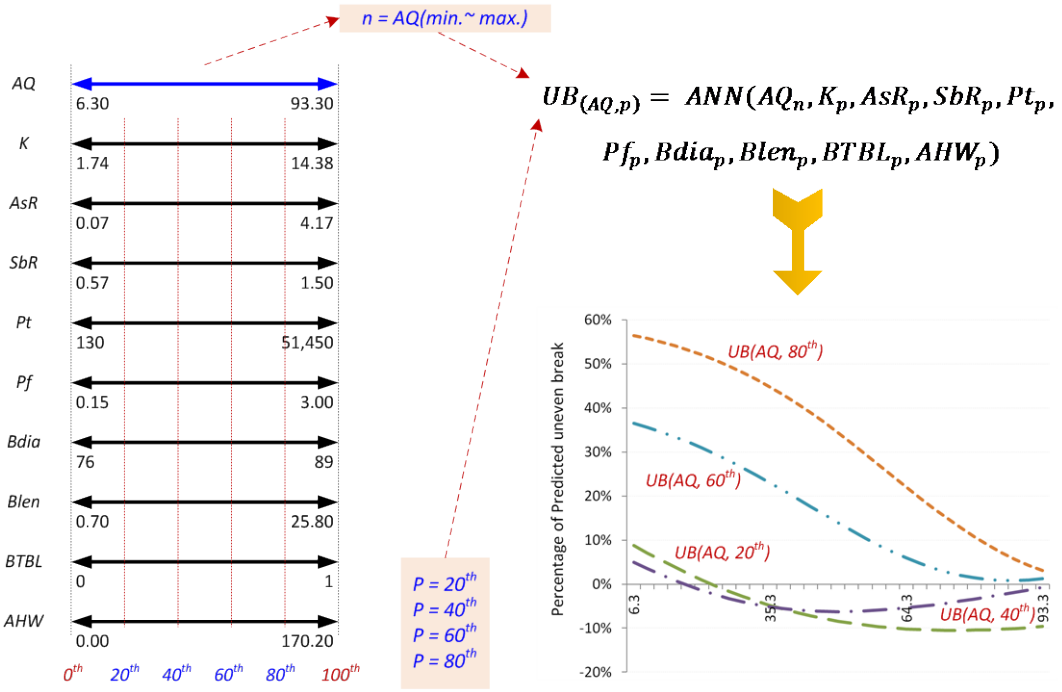

Figure 6-3 Representative application of the profile method (PM) to the input parameter AQ

In Figure 6-3, the output, i.e., uneven break (UB), of the ANN was computed for the full range of AQ while the other parameters were set as the 20th, 40th, 60th, and 80th. Then, the UB variance was graphically displayed, which can facilitate examination of the sensitivity of uneven break (UB) to AQ.

As graphically demonstrated in the right-hand side of Figure 6-3, UB generally decreases when the quality of the rock gets better. This trend is clear when the remaining parameters are delimited to the 60th and 80th of their ranges. In this example, the contribution of each of the delimited ranges of the parameter AQ to the output were obtained by comparing the output variable breadths. Ultimately, the contribution percentage of each delimited AQ range was determined by

comparing the output sensitivity magnitude of each parameter in each corresponding delimited range, which is graphically shown in Figure 6-4.

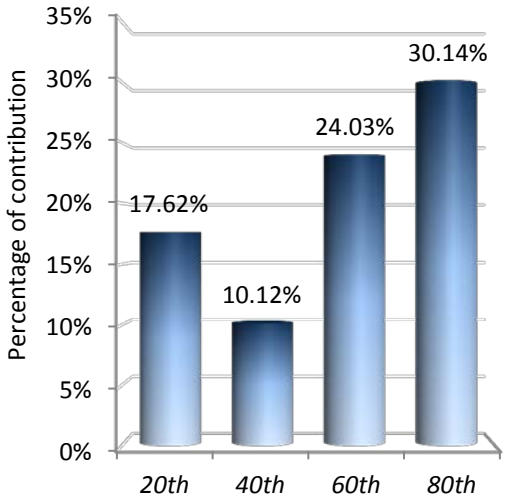

Figure 6-4 AQ Percentage contribution of AQ to output (UB) in each delimited range

As shown in Figure 6-4, the AQ shows a 17.62% contribution to uneven break (UB) when the other nine parameters are held at 20th of their value. Then, AQ shows a relatively low contribution to UB at 40th, and it increases to 23.03% and 30.14% at 60th and 80th, respectively. These results clearly indicate that rock quality is a dominant parameter for uneven break (UB) when other parameters are delimited at relatively high values. Finally, the sensitivity and contribution plots of the remaining nine input parameters on the output were investigated using the identical approach, as demonstrated from Figure 6-5 to Figure 6-13.

6.3.2.2 Contribution of K to uneven break phenomenon

The overall contribution of input K was achieved and demonstrated in Figure 6-5 based on the sensitivity magnitude with respect to each delimited remaining parameter range. K appears as the second highest contributor to UB phenomenon among the ten parameters. The relatively high contribution of K was observed overall ranges. Especially, K shows a proportional relationship to UB overall ranges, which indicates that dynamic overbreak will likely decrease with stope depth. This trend conspicuously appears when the remaining parameters are delimited in 40th of their ranges. As the percentage contribution gradually decreases at 60th and 80th,

the influence of K to uneven break (UB) becomes less when the rock quality is better.

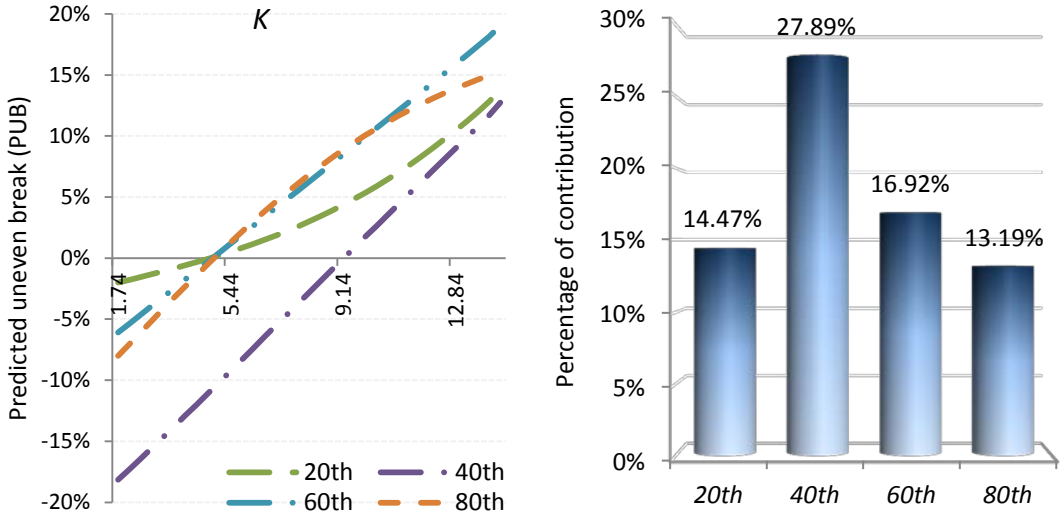

(a) sensitivity plot *(b) contribution plot*

Figure 6-5 Sensitivity and contribution plots of average horizontal to vertical stress ratio (K)

6.3.2.3 Contribution of AsR to uneven break phenomenon

The stope aspect ratio (AsR) was the third highest contributor to UB (uneven break) phenomenon. The result of the profile method (PM) approach to AsR is demonstrated in Figure 6-6.

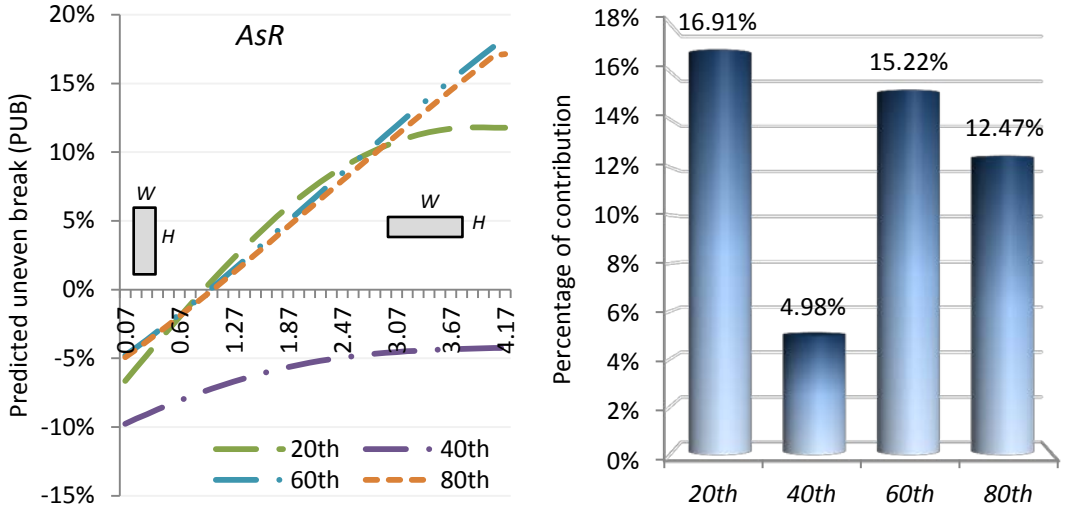

(a) sensitivity plot *(b) contribution plot*

Figure 6-6 Sensitivity and contribution plots of aspect ratio (AsR)

As shown in Figure 6-6a, AsR also shows a proportional relationship to UB overall ranges, which indicates that the overbreak occurrence is somewhat proportional to the stope width. As presented in Figure 6-6b, a relatively high contribution of aspect ratio (AsR) was observed over all ranges except the 40th delimiting range of the other parameters. These results show that the influence of aspect ratio on uneven break (UB) is higher when the surrounding rock is either poor or good. In other words, if the rock is either poor or good enough to support by itself, the occurrence of over and under breaks is dominated by the aspect ratio. However, if the rock is moderate, the influence of aspect ratio of uneven break (UB) is less and the occurrence of over and under breaks is more affected by factors other than the aspect ratio of the stope.

6.3.2.4 Contribution of SbR to uneven break phenomenon

The fourth contributor to UB is the space and burden ratio (SbR). As demonstrated in Figure 6-7, the contribution of SbR was achieved by the profile method (PM) based on sensitivity magnitudes with respect to each delimited remaining parameter range.

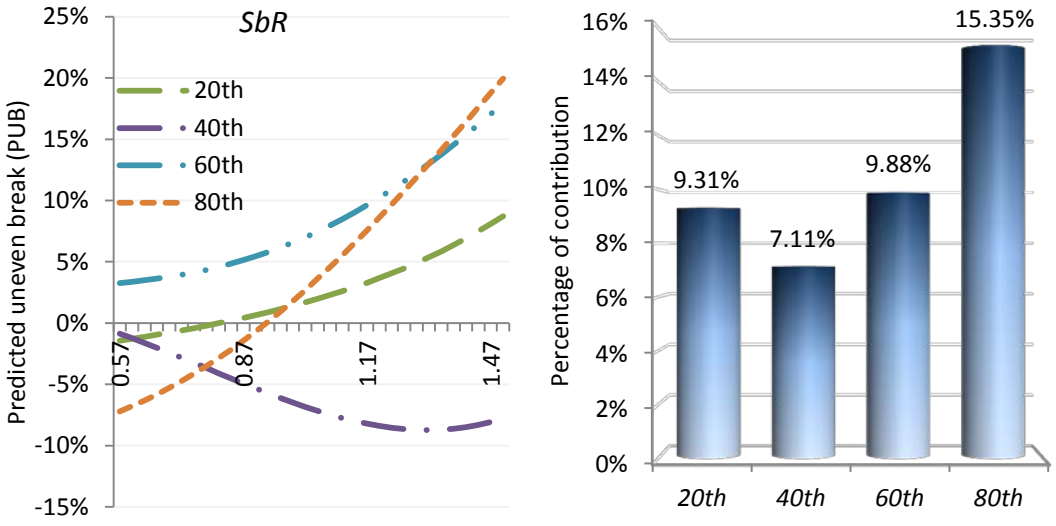

(a) sensitivity plot *(b) contribution plot*

Figure 6-7 Sensitivity and contribution plots of space and burden ratio (SbR)

As shown in the sensitivity plot of SbR (Figure 6-7a), the magnitude of overbreak increases when the SbR ratio increases except when the remaining parameters are delimited at the 40th. In other words, the more the ring burden increases, the more

the magnitude of overbreak increases. The SbR shows moderate contributions of 9.31% and 9.88% in the 20th and 40th delimited range of the remaining factors, respectively. Moreover, a relatively high contribution was observed in the 80th, which implies that the SbR ratio is a comparatively major contributor when the quality of the rock is good.

6.3.2.5 Contribution of Pt to uneven break phenomenon

The fifth influential contributor to uneven break (UB) is tonnes of planned stope (Pt), and the sensitivity and contribution plots are schematically demonstrated in Figure 6-8.

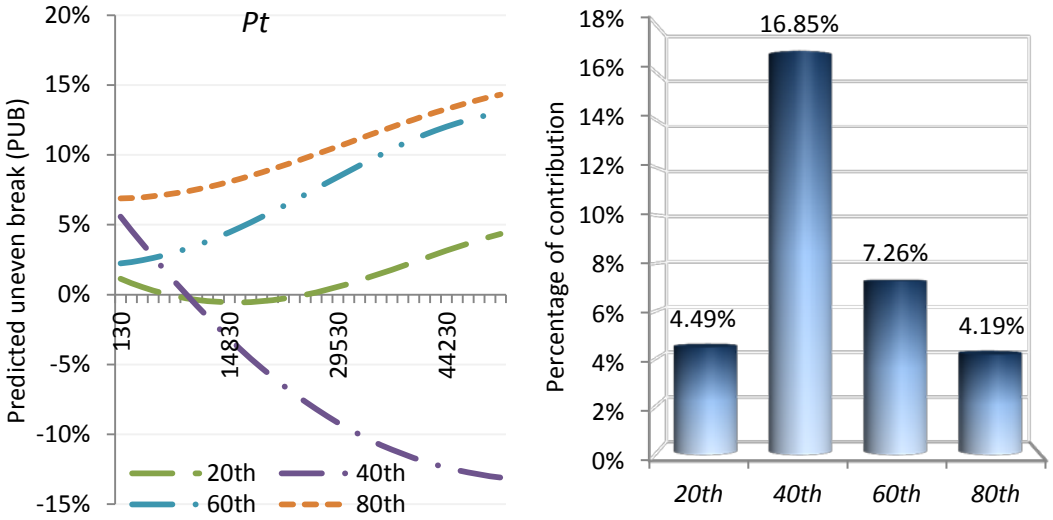

(a) sensitivity plot *(b) contribution plot*

Figure 6-8 Sensitivity and contribution plots of tonnes of stope planned (Pt)

The results of the sensitivity plot of Pt (Figure 6-8a) are somewhat analogous to the sensitivity plot of SbR (Figure 6-7a), but contrasting results were observed in the contribution plots. As observed in Figure 6-8b, Pt can be regarded as a minor contributor among the ten investigated parameters in the 20th, 60th, and 80th parameter delimiting ranges due to the low contribution percentage. Thus, these three delimiting ranges are negligible in the sensitivity plots of Pt (Figure 6-8a). In this view, the overbreak percentage shows an inverse relationship with stope size, i.e., Pt. In other words, increasing the size of the stope is one alternative for decreasing the overbreak percentage.

6.3.2.6 Contribution of Pf to uneven break phenomenon

The profile method computed the powder factor (Pf) as the sixth most influential contributor to uneven break (UB). Figure 6-9 demonstrates the sensitivity and contribution plots of the powder factor (Pf) on uneven break (UB).

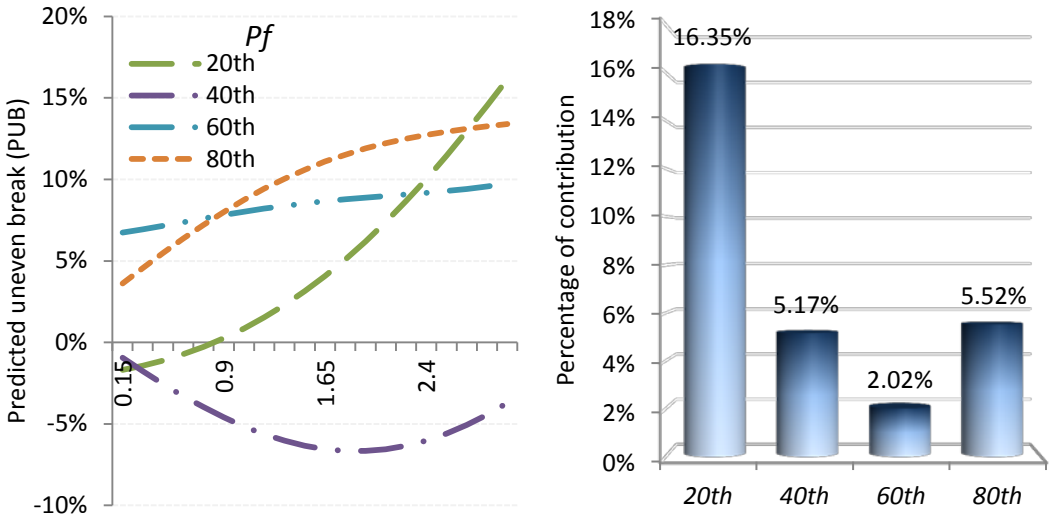

(a) sensitivity plot *(b) contribution plot*

Figure 6-9 Sensitivity and contribution plots of powder factor (Pt)

The contribution of Pf to UB is relatively high in the lower delimited range of the remaining parameters, i.e., the 20th, but negligibly low contributions were found at the other ranges. Considering the 20th delimited range in the powder factor sensitivity plot (Figure 6-9a), the overbreak magnitude is exponentially higher. Furthermore, this tendency governs in poor rock as shown in the contribution plots (Figure 6-9b). Considering that the highest contributor is AQ, uneven break (UB) is sensitive to Pf when the rock quality is 'poor' but is less sensitive when the rock quality is 'moderate' or 'good'. In other words, in 'moderate' and 'good' rock, UB is likely affected by a combination of factors other than Pf itself.

6.3.2.7 Contribution of Bdia to uneven break phenomenon

The blasthole diameter (Bdia) was found to be the seventh most influential contributor to uneven break (UB), and the sensitivity and contribution plots are demonstrated in Figure 6-10.

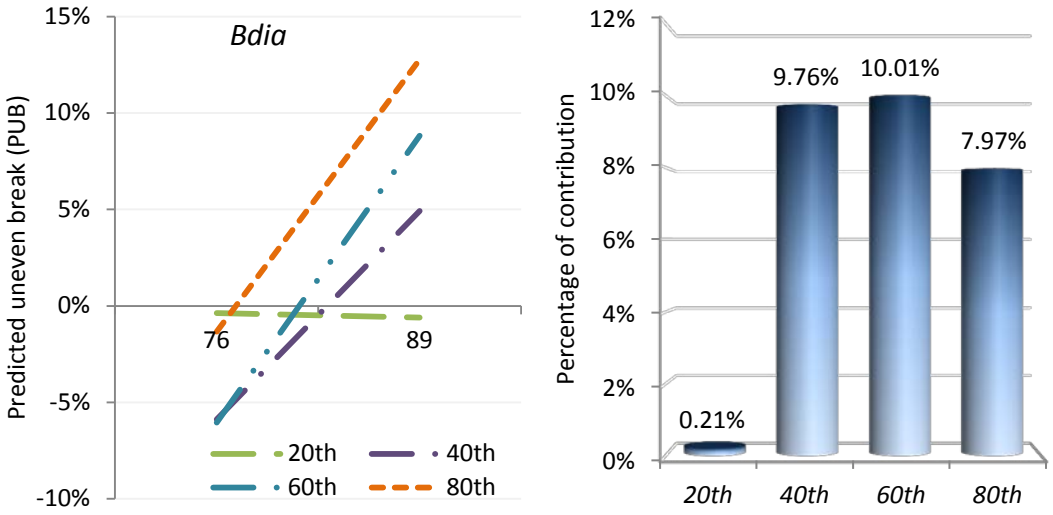

(a) sensitivity plot *(b) contribution plot*

Figure 6-10 Sensitivity and contribution plots of blasthole diameter (Bdia)

As shown in Figure 6-10b, Bdia shows a negligibly low contribution at the 20th remaining parameter range, but moderate contributions were observed at the 40th, 60th, and 80th. After excluding the 20th of the sensitivity plot on discussion, the overbreak magnitude shows a proportional relationship with blasthole diameter.

6.3.2.8 Contribution of Blen to uneven break phenomenon

The average length of blasthole (Blen) was found to be the eighth most influential contributor to uneven break (UB) and the results of PM are shown in Figure 6-11.

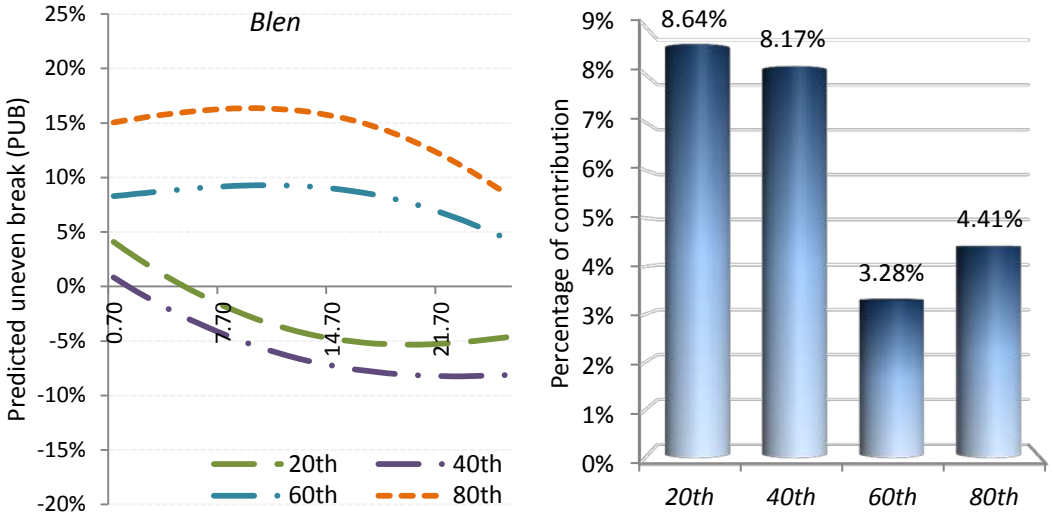

(a) sensitivity plot (b) contribution plot

Figure 6-11 Sensitivity and contribution plots of average length of blasthole (Blen)

Relatively low contributions were observed over all delimited ranges of the remaining parameters. In particular, the 60th (3.28%) and 80th (4.41%) showed highly insignificant values; thus, these ranges can be neglected on further consideration. Considering only the 20th and 40th on the sensitivity plot (Figure 6-11a), the scale of overbreak gradually decreases while the length of the blasthole increases. However, it is not a primary tendency in UB phenomenon considering the low contribution percentage.

6.3.2.9 Contribution of BTBL to uneven break phenomenon

The stope either breakthrough to a nearby drift and/or stope or not (BTBL) was found to be the ninth most influential contribution to uneven break (UB). The results of profile method (PM) application to BTBL are demonstrated in Figure 6-12.

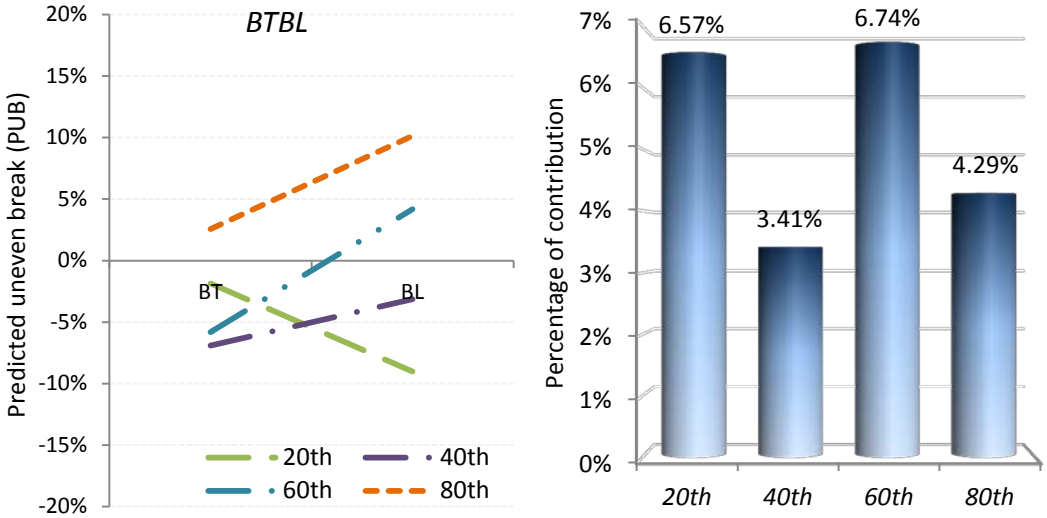

(a) sensitivity plot (b) contribution plot

Figure 6-12 Sensitivity and contribution plots of stope either breakthrough to a nearby drift and/or stope or not (BTBL)

Generally, low contributions were observed over all ranges without typical trends. As observed in Figure 6-12a, the overbreak magnitude is generally higher when the stope is blind, except in the 20th remaining parameter range. This tendency was obtained in low contribution ranges; thus, it could not be exploited in actual mining production.

6.3.2.10 Contribution of AHW to uneven break phenomenon

The angle difference between hole and wall (AHW) was computed as the least influential contributor to uneven break (UB) phenomenon. The contribution and sensitivity plots of AHW were generated using the profile method (PM) and are demonstrated in Figure 6-13 based on sensitivity magnitudes with respect to each delimited remaining parameter range.

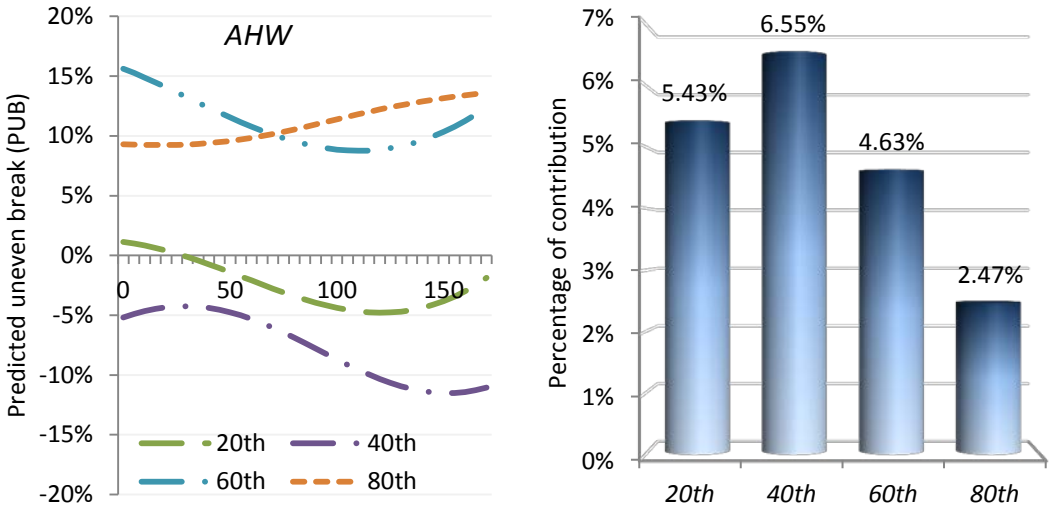

(a) sensitivity plot *(b) contribution plot*

Figure 6-13 Sensitivity plots of angle difference between hole and wall (AHW)

Even though the AHW was found to be the weakest contributor to UB, the contribution displays a tendency. As shown in Figure 6-13b, the percentage contribution of AHW is 5.43% in the 20th remaining parameter range. It increases to 6.55% at the 40th but gradually decreases to 4.63% and 2.47% at the 60th and 80th, respectively. Concerning the most influential contributor, i.e., AQ, the tendency of the AHW contribution implies that the influence of the angle between the blasthole and stope wall (AHW) on uneven break (UB) phenomenon becomes minor when the quality of the rock is better. The 80th delimitation on the sensitivity plot (Figure 6-13a) can be neglected due to its low contribution percentage. Considering the 20th, 40th, and 60th sensitivity plots, overbreak is likely higher with a parallel blasthole pattern than a fanned pattern.

6.3.2.11 Overall contribution of the ten inputs

Ultimately, the overall contribution of the ten inputs based on the sensitivity magnitude of each input with respect to each delimited remaining parameter range was calculated and are presented in Figure 6-14.

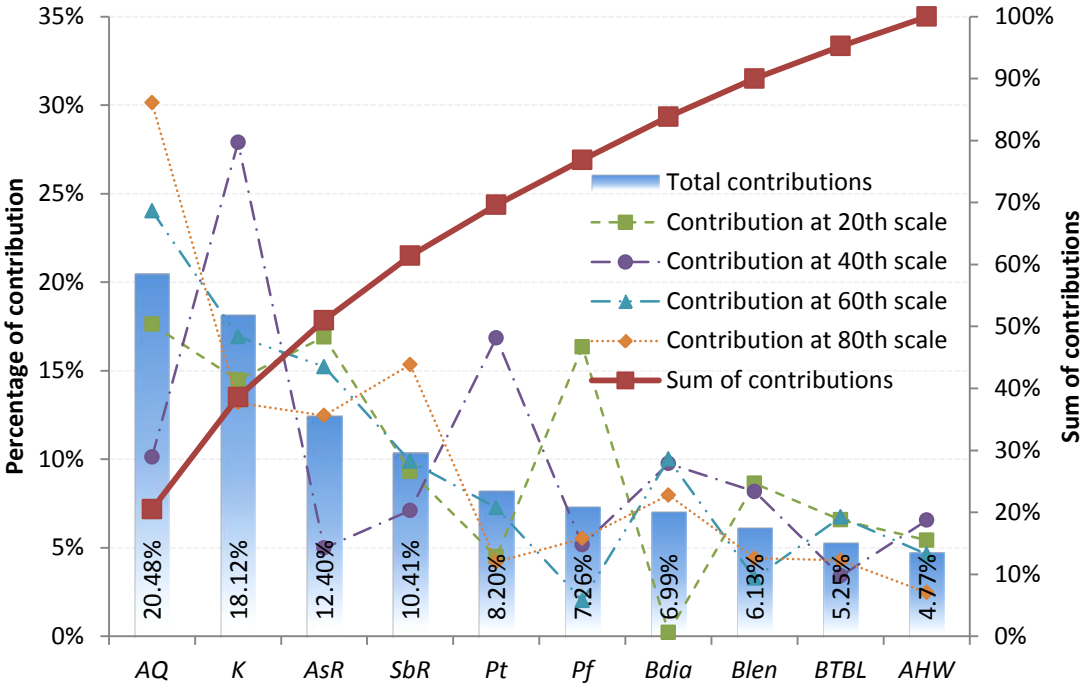

Figure 6-14 Overall contribution of the ten inputs to output in the UB predicting ANN model of the GM dataset by the profile method (PM)

As shown in Figure 6-14, AQ was the most relevant parameter for uneven break (UB) phenomena with a contribution of 20.48%. K was the second most relevant contributor to UB with an 18.12% contribution. AsR and SbR show moderately high contributions at 12.40% and 10.41%. The remaining parameters Pt, Pf, Bdia, Blen, BTBL, and AHW yielded low contributions of 8.20%, 7.26%, 6.99%, 6.13%, 5.25%, and 4.77%, respectively.

To sum up the parameter contribution analysis using the profile method (PM), the strength and the direction of contributions change not only with the parameter values but also with the value of the remaining parameters. These sensitivity and contribution plots are useful not only for stope design and management but also for elucidating uneven break (UB) mechanisms.

6.3.3 *Parameter contribution based on overall causative categories*

The contribution analyses for this study rely on the ten given parameters, but general trends for the UB mechanism were clarified in the previous section. In this section, the contributions of each causative category are calculated.

The overall contribution percentages of Blen, Pf, AHW, Bida, and SbR are aggregated as the blasting parameter contribution to the uneven break (UB) phenomenon. Along the same line, the contribution of geology is obtained by aggregating the overall contribution percentages of AQ and K. Moreover, the overall contribution percentages of Pt, AsR, and BTBL are aggregated as the contribution of stope design to the uneven break (UB) phenomenon. The outer circle of Figure 6-15 shows the geology, blasting, and stope design categories with their contributions to UB of 38.79%, 37.17%, and 24.04%, respectively.

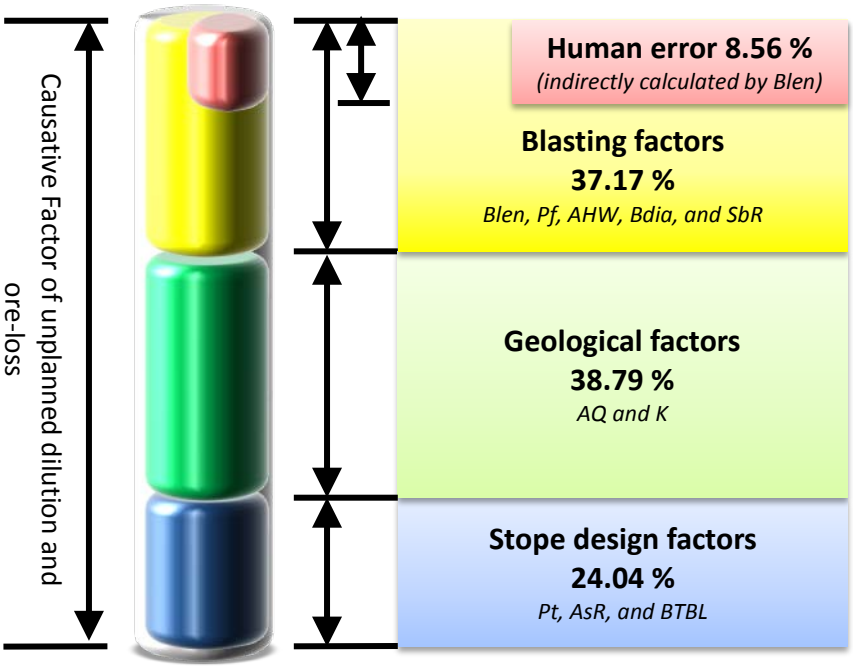

Figure 6-15 UB contribution of the three core categories

Even though the geology category is formulated with only two parameters, it has the greatest influence at 38.79%. This result highlights the significant influence of geological conditions on uneven break (UB) phenomenon. The blasting category consists of five parameters, and its overall contribution was computed at 37.17%, making it the second most influential UB category. In this category, if the average

length of the blasthole (Blen), with a contribution of 8.56%, is respected as the human error category, the contribution of blasting is reduced to 28.61%, as shown in the inner circle in Figure 6-15. Finally, the stope design category makes a 24.04% contribution to UB.

6.4 SUMMARY AND DISCUSSION

In this chapter, the contributions of the ten selected uneven break (UB) causative factors were investigated to illuminate the complex UB accrual mechanism. Parameter contribution analyses were performed based on the general dataset (GM) UB prediction models, i.e., the multiple regression analysis (MLRA and MNRA) and artificial neural network (ANN) models. The investigation of the parameters' contributions in the multiple regression analysis was performed in reference to the regression coefficients of the UB prediction models. As a result, AHW was found to be the most influential parameter for uneven break phenomenon with a contribution of 21.87%. In addition, AHW, AQ, and Blen all have a negative relationship with uneven break (UB), while K, AsR, SbR, Pt, Pf, Bdia, and BTBL all have a positive relationship.

For the ANN UB prediction model, the connection weight approach (CWA) and profile method (PM) were utilised to examine the parameter contributions in the GM dataset. As a result of CWA application, AQ was determined to be the most influential contributor to UB with 22.40%, while K and Blen show relatively high contributions at 19.49% and 11.40%. Furthermore, AQ, Blen, Pt, and AHW were found to have a negative relationship with uneven break (UB) phenomenon, which is similar to the parameter contribution investigation of the MNRA model.

The profile method (PM) is a sensitivity-based algorithm for analysing the contribution of inputs to outputs in an ANN model. This method is more cumbersome than other methods because it requires running the ANN model over the full ranges of all of the inputs. However, one of the merits of this method is that it can thoroughly investigate the entire range of input sensitivities with respect to the output. Through application of the profile method (PM), sensitivity and contribution plots of the ten contributors were generated. As a result, AQ was

verified as the most influential contributor to uneven break (UB) phenomenon with a contribution of 20.48%, followed by K (18.12%), AsR (12.40%), and SbR (10.41%). The remaining parameters, i.e., Pt, Pf, Bdia, Blen, BTBL, and AHW, all make less than a 10% contribution. Some of the key findings from the parameter contribution analysis by the profile method are tabulated in Table 6-2.

Table 6-2 Several key findings from the parameter contribution analysis by the profile method

Parameter / Per. contribution per. contribution/AQ	Essential notes
AQ 20.48%	• The better the rock quality, the less the overbreak
K 18.12%	• The deeper the stope, the less the overbreak.
AsR 12.40%	• The wider the stope, the more the overbreak.
SbR 10.41%	• The longer the ring burden, the more the overbreak.
Pt 8.20%	• The bigger the stope, the less the overbreak.
Pf 7.26%	• The overbreak magnitude increases exponentially when the powder factor is increased.
Bdia 6.99%	• The bigger the blasthole diameter, the more the magnitude of overbreak.
Blen 6.13%	• The longer the length of blasthole, the less the percentage of overbreak.
BTBL 5.25%	• The magnitude of overbreak is generally increased when the stope is blinded.
AHW 4.77%	• The overbreak is more likely increased on the parallel blasthole pattern than the fanned pattern.

Furthermore, the contribution of the three core categories, i.e., geology, blasting, stope design, on the uneven break (UB) was calculated based on the profile method (PM). As a result, the geological parameter turned out to be the most influential contributor category as it showed 38.79% contribution, while blasting and stope design category calculated as 37.17% and 24.04%, respectively.

CHAPTER 7. UB CONSULTATION SYSTEM

7.1 INTRODUCTION

In Chapter 5, a reliable prediction system for an uneven break (UB) was developed using a conjugate gradient artificial neural network (CG-ANN). Thus, a potential UB can be predicted quantitatively prior to stope production. However, there is another difficult decision-making problem that engineers will encounter. For instance, if the UB prediction system predicts +25% of an uneven break (UB; i.e., 25% of an overbreak) on a hanging wall, how can the predicted potential overbreak be reduced? In practice, the senior engineer may have to make a decision without any engineering guarantees.

In this chapter, a fuzzy expert system (FES) is developed to minimise a potential UB in a stope wall as a countermeasure for mining experts. To achieve the aim of the developed FES, new engineering recommendation criteria, a powder factor control rate (PFCR) and a ground support control rate (GSCR) are introduced and allocated to the FES outputs. The powder factor and the ground support are critical parameters in stope production planning that can be managed by mining engineers. Those two recommendation criteria provide an intuitive means of minimising the unwanted UB phenomenon by changing the powder factor and the ground support plan for the stope.

Ultimately, the developed UB consultation FES will be combined with an UB prediction ANN to serve as an integrated UB management cooperative neuro-fuzzy system that is entitled as an ‘uneven break optimiser’. Figure 7-1 demonstrates the stope optimisation process using the developed ‘uneven break optimiser’. The figure shows that a potential UB for an initial stope design and the remedies for the predicted UB that can be quantitatively achieved using the uneven break optimiser. Mining engineers can modify the initial stope design until the predicted potential UB reaches a certain recognition range by checking the output of the uneven break optimiser, i.e., the PFCR and the GSCR.

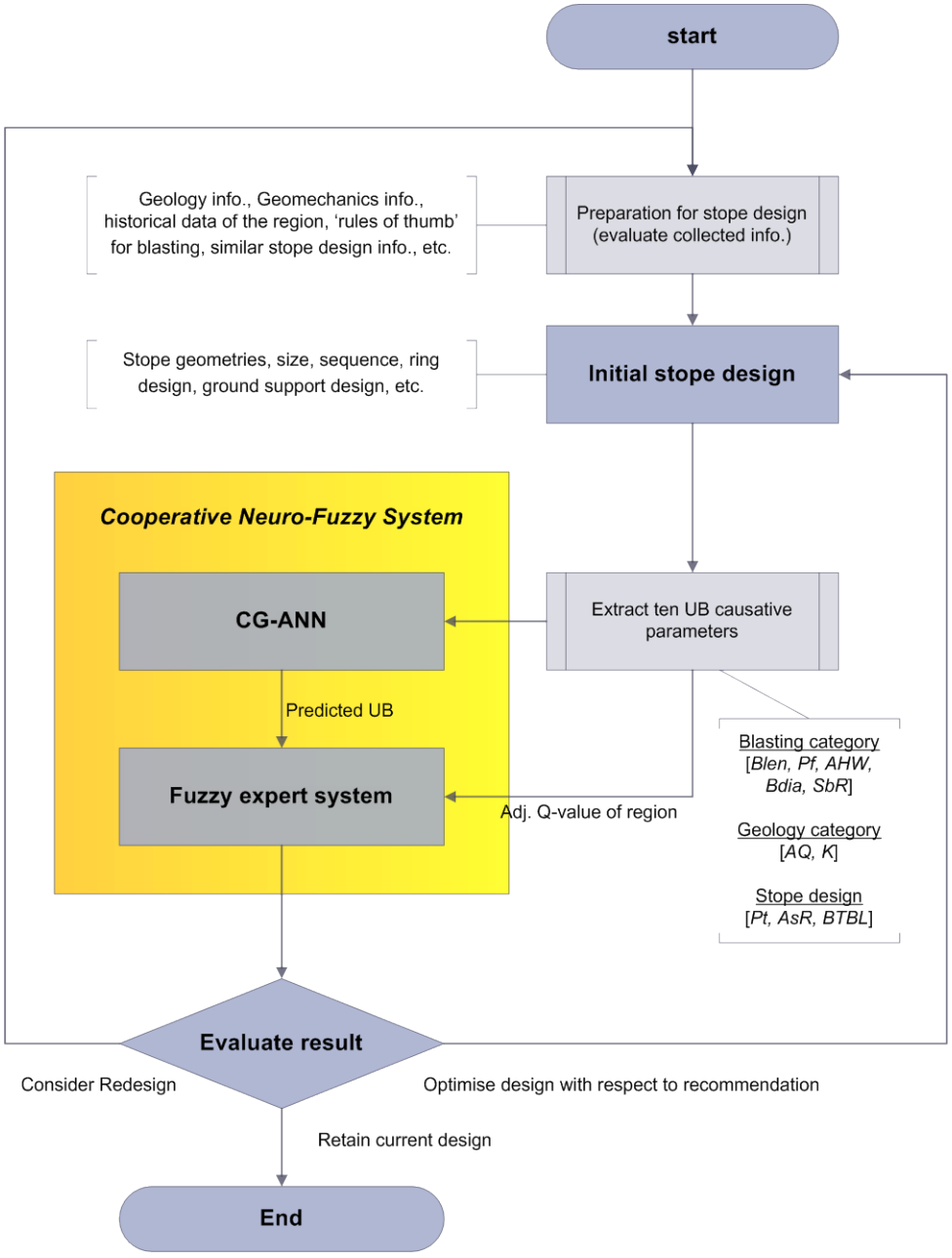

Figure 7-1 Demonstration of stope planning optimisation with 'uneven break optimiser'

7.2 FUZZY EXPERT SYSTEM

To construct an uneven break (UB) consultation fuzzy expert system (FES), an appropriate FES configuration must be selected. Figure 7-2 is a schematic of the developed UB consultation FES.

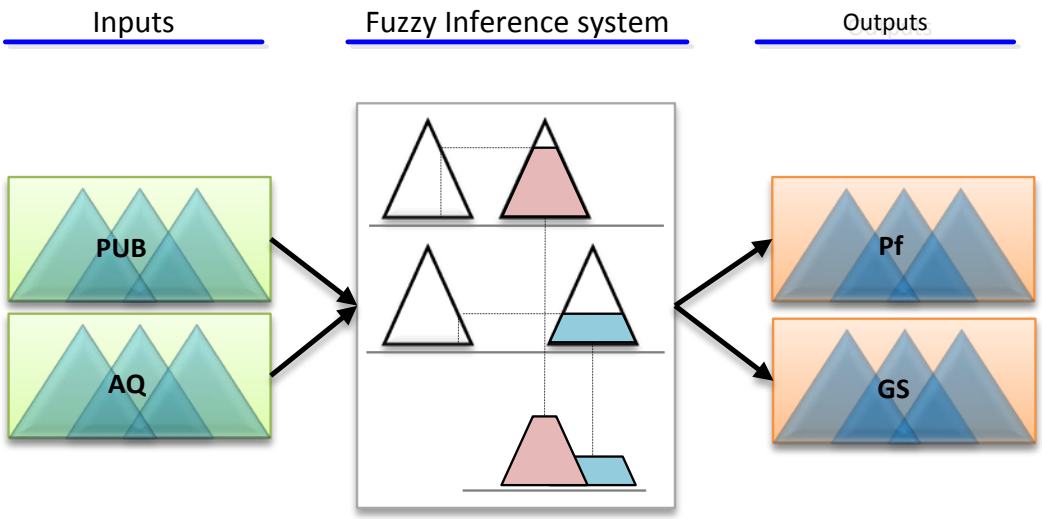

Figure 7-2 Configuration of developed fuzzy expert system

In constructing a configuration for a fuzzy expert system, the antecedents (inputs) and consequents (outputs) must be very carefully chosen. In this study, the objective of the FES is to minimise the potential UB by providing an appropriate UB consultation criteria; thus, the predicted uneven break (PUB) and the adjusted Q value (AQ) are chosen as input variables. The aim of the developed FES is to minimise the predicted uneven break (PUB), where the PUB is a standard input parameter of the FES. Moreover, by adopting the predicted uneven break (PUB) as one of the antecedents, the developed FES spontaneously connects to the UB prediction ANN model. Another important parameter that must be considered in the UB consultation system is the geological condition of the region, which is represented by adopting an AQ as one of the antecedents.

The consequents of the developed FES should be subjected to variables that significantly affect the UB phenomenon and are controllable. Thus, two new parameters, the powder factor and the ground support control rate (PFCR and GSCR), are introduced and allocated to the outputs of the developed FES. The computed PFCR and GSCR enable engineers to intuitively understand how to modify the blasting geometry and the ground support system of the initial stope design to minimise the predicted potential UB.

7.2.1 *Configuration of fuzzy expert system*

The membership functions and the fuzzy 'IF-THEN' rules are essential components of a FES upon which all of the calculation processes in the fuzzy inference system are based. As mentioned in Chapter 4.3, the membership functions of the inputs and outputs and the fuzzy rules are obtained from surveying fifteen underground mining experts. The detailed survey results are presented in Appendix C.

7.2.1.1 Fuzzy membership functions

To effectively represent the experts' knowledge, triangular and trapezoidal shapes are employed to develop the membership functions of the inputs and outputs. Figure 7-3 shows the developed membership functions for the inputs and outputs.

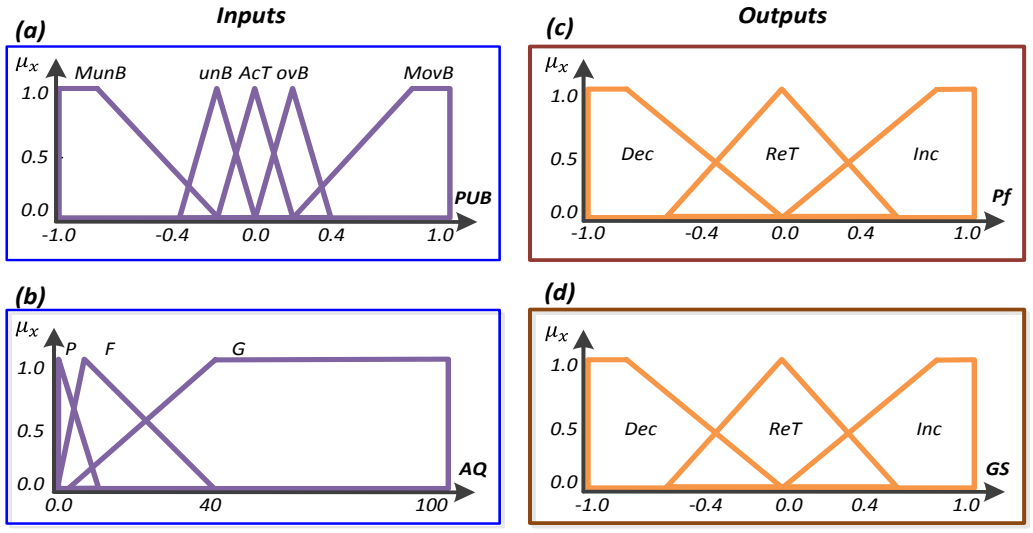

(a) input-PUB; (b) input-AQ; (c) output – PFCR; (d) output – GSCR. P: poor; F: fair; G: good; MunB: massive-underbreak; unB: underbreak; AcT: acceptable; ovB: overbreak; MovB: massive-overbreak; Dec: decrease; ReT: retain; Inc: increase; μ_x: degree of membership function

Figure 7-3 Schematic showing membership functions of input and output of an uneven break (UB) consultation fuzzy expert system (FES)

Figure 7-3a shows that the first input, the predicted uneven break (PUB), is composed of five sub-membership functions: massive-underbreak (MunB), underbreak (unB), acceptable (AcT), overbreak (ovB), and massive-overbreak (MovB). The PUB is obtained using the UB prediction ANN model and ranges from -1.0 (100% of the underbreak) to 1 (100% of the overbreak).

The second input AQ is shown in Figure 7-3a. The AQ is composed of three sub-membership functions: poor (P), fair (F), and good (G) because the collected AQ varies from 6.30 to 93.30. Figures 7-3c and d show the powder factor (Pf) and the ground support (GS) control rates (PFCR and GSCR) as outputs. The PFCR and GSCR vary from -1 to 1 and are composed of three sub-membership functions: decrease (Dec), retain (ReT), and increase (Inc). The linguistic values and the numerical ranges of the input and output fuzzy membership functions are tabulated in Table 7-1.

Table 7-1 Details of fuzzy input and output membership functions

category	Linguistic value	Notation	Numerical range
Input: Adjusted *Q*-value (*AQ*) fuzzy sets	Poor	*P*	[1, 1, 10]
	Fair	*F*	[1, 7, 40]
	Good	*G*	[4, 40, 100, 100]
Input: Predicted uneven break (*PUB*) fuzzy sets	Massive-underbreak	*MunB*	[-1, -1, -0.8, -0.2]
	Underbreak	*unB*	[-0.4, -0.2, 0]
	Acceptable	*Act*	[-0.2, 0, 0.2]
	Overbreak	*ovB*	[0, 0.2, 0.4]
	Massive-overbreak	*MovB*	[0.2, 0.8, 1, 1]
Outputs: Powder factor (*Pf*) & Ground support (*GS*) fuzzy sets	Decrease	*Dec*	[-1, -1, -0.8, 0]
	Retain	*ReT*	[-0.6, 0, 0.6]
	Increase	*Inc*	[0, 0.8, 1, 1]

7.2.1.2 Development of fuzzy rules for UB consultation fuzzy expert system

Fuzzy rules (IF-THEN rules) are the implication function of the fuzzy inference system that is based on the linguistic variables specified in the fuzzy membership functions. Arithmetically, one hundred and thirty-five fuzzy rules can be produced because the developed UB consultation fuzzy expert system consists of dual non-interactive antecedents (inputs) with three and five subclasses and dual non-interactive consequents (outputs) with three subclasses each. Among the 135 fuzzy rules, only 37 essential rules are employed to increase the reliability of the fuzzy

system. The rest of the 98 rules are eliminated based on expert knowledge that is obtained from the questionnaire survey and fundamental engineering considerations. The selected thirty-seven linguistic IF-THEN propositions are described as

$$IF\ AQ\ is\ A_1^k\ and\ PUB\ is\ A_2^k\ THEN\ Pf\ is\ C_1^k\ and\ GS\ is\ C_2^k,\quad for\ k = 1, 2, 3, \dots, 37 \qquad \text{Eq. 7-1,}$$

where A_1^k and A_2^k are the fuzzy sets of the k^{th} antecedent pairs, and C_1^k and C_2^k are the fuzzy sets of the k^{th} consequent pairs. The 37 fuzzy rules are tabulated in Table 7-2.

Table 7-2 Thirty-seven derived fuzzy rules

No.	IF AQ	IF PUB	THEN Pf	THEN GS	No.	IF AQ	IF PUB	THEN Pf	THEN GS	No.	IF AQ	IF PUB	THEN Pf	THEN GS	No.	IF AQ	IF PUB	THEN Pf	THEN GS
1	*P*	*MovB*	*Dec*	*Inc*	11	*F*	*MovB*	*Dec*	*ReT*	21	*F*	*MunB*	*Inc*	*ReT*	31	*G*	*Act*	*ReT*	*ReT*
2	*P*	*MovB*	*Dec*	*ReT*	12	*F*	*MovB*	*Dec*	*ReT*	22	*F*	*MunB*	*Inc*	*ReT*	32	*G*	*unB*	*Inc*	*ReT*
3	*P*	*MovB*	*Dec*	*ReT*	13	*F*	*MovB*	*Dec*	*Inc*	23	*F*	*MunB*	*Inc*	*Dec*	33	*G*	*unB*	*ReT*	*ReT*
4	*P*	*MovB*	*Dec*	*Inc*	14	*F*	*ovB*	*Dec*	*ReT*	24	*F*	*MunB*	*Inc*	*Dec*	34	*G*	*MunB*	*Inc*	*ReT*
5	*P*	*ovB*	*Dec*	*ReT*	15	*F*	*ovB*	*ReT*	*ReT*	25	*G*	*MovB*	*Dec*	*Inc*	35	*G*	*MunB*	*Inc*	*Dec*
6	*P*	*Act*	*ReT*	*ReT*	16	*F*	*Act*	*ReT*	*ReT*	26	*G*	*MovB*	*Dec*	*ReT*	36	*G*	*MunB*	*Inc*	*ReT*
7	*P*	*unB*	*ReT*	*ReT*	17	*F*	*unB*	*ReT*	*ReT*	27	*G*	*MovB*	*Dec*	*ReT*	37	*G*	*MunB*	*Inc*	*Dec*
8	*P*	*unB*	*Inc*	*ReT*	18	*F*	*unB*	*ReT*	*ReT*	28	*G*	*MovB*	*Dec*	*Inc*					
9	*P*	*MunB*	*Inc*	*ReT*	19	*F*	*unB*	*Inc*	*ReT*	29	*G*	*ovB*	*Dec*	*ReT*					
10	*F*	*MovB*	*Dec*	*Inc*	20	*F*	*unB*	*Inc*	*ReT*	30	*G*	*ovB*	*ReT*	*ReT*					

UB: *uneven break;* ***MunB:*** *massive-underbreak;* ***unB:*** *underbreak;* ***AcT:*** *acceptable;* ***ovB:*** *overbreak;* ***MovB:*** *massive-overbreak;* ***PF:*** *powder factor;* ***GS:*** *ground support;* ***Dec:*** *decrease;* ***ReT:*** *retain;* ***Inc:*** *increase*

7.2.2 *Fuzzy inference system*

The fuzzy inference system (FIS) is a process of mapping the inputs to the output space. In this study, the Mamdani-style fuzzy inference system (Mamdani & Assilian, 1975) was used to formulate the UB consultation fuzzy expert system. Figure 7-4

shows an example of four sequential steps of the UB-consultation Mamdani-type fuzzy inference system.

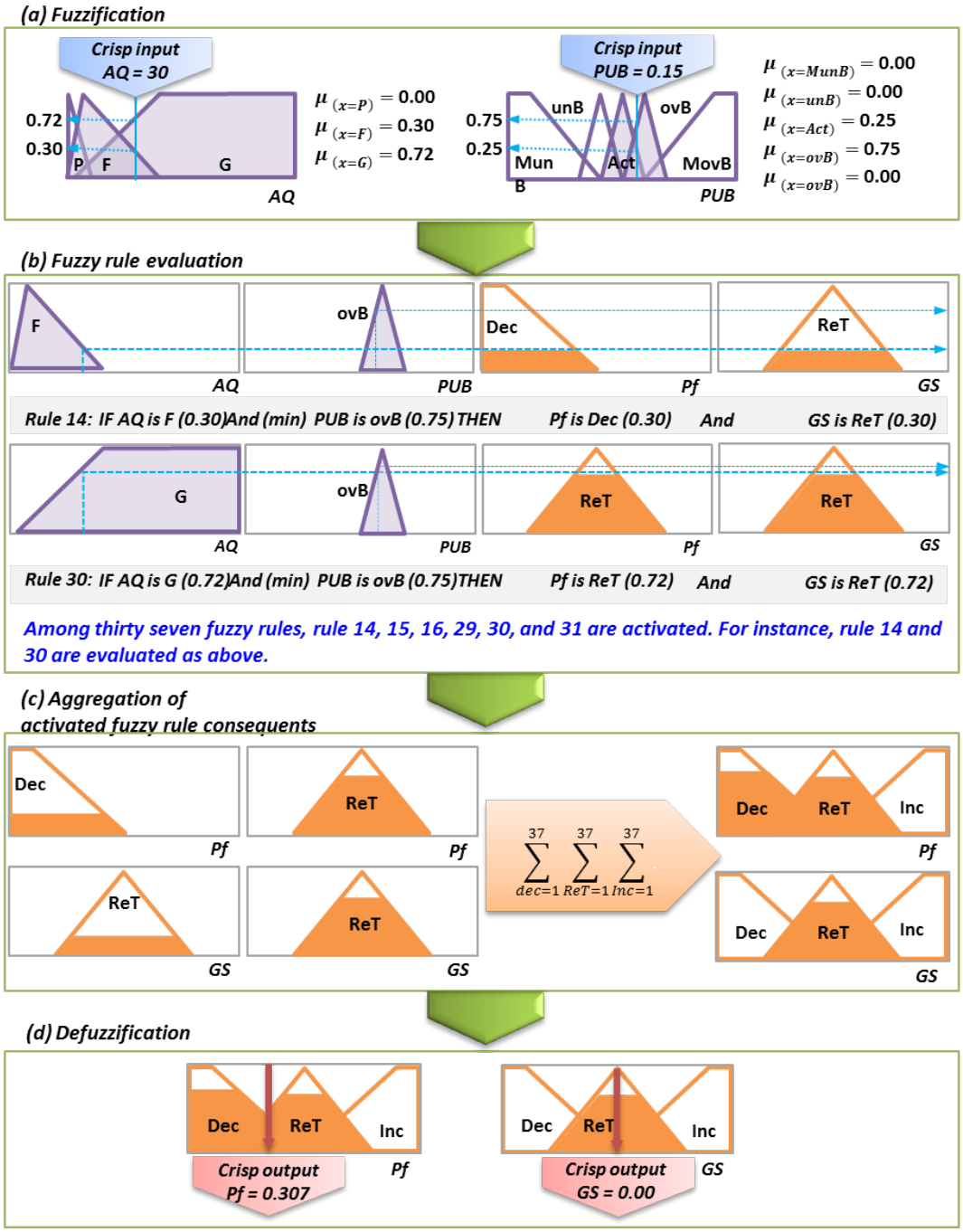

Figure 7-4 Sample of an UB-consultation Mamdani-style fuzzy inference system (taken from Negnevitsky (2005))

The first step in *FIS* is fuzzification (Figure 7-4a). The crisp inputs, the predicted uneven break (PUB) and the adjusted Q value (AQ) are converted to the corresponding degree of fuzzy membership functions, which is the truth value (T) of the fuzzy input propositions. In this example, the crisp inputs of 30 and 0.15 are

inserted into the AQ and PUB fuzzy membership functions, respectively, and the truth value (T) of the corresponding sub-membership functions is tabulated in Table 7-3.

Table 7-3 Truth value of sub-membership functions after fuzzification

AQ = 30		**PUB = 0.15**	
Sub-membership function	value	Sub-membership function	value
$\mu_{x=poor}$	0.00	$\mu_{x=MunB}$	0.00
$\mu_{x=fair}$	0.30	$\mu_{x=unB}$	0.00
$\mu_{x=good}$	0.72	$\mu_{x=AcT}$	0.25
		$\mu_{x=ovB}$	0.75
		$\mu_{x=MovB}$	0.00

Then, the fuzzified membership functions are evaluated according to the fuzzy rules in the antecedent and directed according to the evaluation results to the consequent membership function. This process is called fuzzy rule evaluation and is shown in Figure 7-4b. Similar to classical logic, the logical connectives such as negative, disjunction, conjunction, and implication are also defined in fuzzy logic. For example, the conjunction (the logical product AND) and disjunction (the logical sum OR) are determined as follows (Ross, 2009):

Disjunction
$$AQ \vee PUB: x \text{ is } F \text{ or } y \text{ is } AcT, T(AQ \vee PUB) = \max\big(T(AQ), T(PUB)\big). \quad \text{Eq. 7-2}$$

Conjunction
$$AQ \wedge PUB: x \text{ is } F \text{ and } y \text{ is } AcT, T(AQ \wedge PUB) = \min\big(T(AQ), T(PUB)\big). \quad \text{Eq. 7-3}$$

In this example, rules 14, 15, 16, 29, 30, and 31 are activated subject to the fuzzified sub-membership functions. Moreover, the activated sub-membership functions are evaluated by conjunction fuzzy logic because, as shown in 7.2.1.2, the fuzzy rules of the developed UB consultation FES are only formulated by conjunction. The third step is the aggregation of the fuzzy rule consequents (Figure 7-4c). The results of all of the fuzzy subsets are unified in a new single fuzzy set for each consequent.

The final stage of the Mamdani fuzzy inference system is defuzzification, which is a process of converting each aggregated fuzzy set of consequents into crisp values

(Figure 7-4d). Several defuzzification methods have been introduced, e.g., the centre of gravity (COG, which is also called the centre of area (COA) or centroid method), the max membership principle, the weight average method, the mean max membership, and the centre of sum. Among the defuzzification methods, the centre of gravity (COG) is used in this study because it has been is recognised as the most common and logical method (Grima, 2000; Sugeno, 1985b). In the COG method, the centre of gravity of the accumulated fuzzy consequent subsets is computed. For instance, a consequent α can be defuzzified as shown below:

$$Z^*_{\alpha:\,COG} = \left(\int \mu_\alpha(Z) Z\, dz\right) \Big/ \left(\int \mu_\alpha(Z)\, dz\right) \qquad \text{Eq. 7-4,}$$

where $Z^*_{\alpha:\,COG}$ is the defuzzified value of α, Z is the interval of α, and μ_α is the aggregated fuzzy subset α. The fuzzy expert system (FES) will be finalised after retrieving the crisp outputs of α (PFCR and GSCR). In this example, the Pf and GS control rate (PFCR and GSCR) are calculated as 0.307 and 0.000, respectively. Figure 7-5 shows the 3D map of the outputs versus the input sets of the developed UB consultation fuzzy expert system.

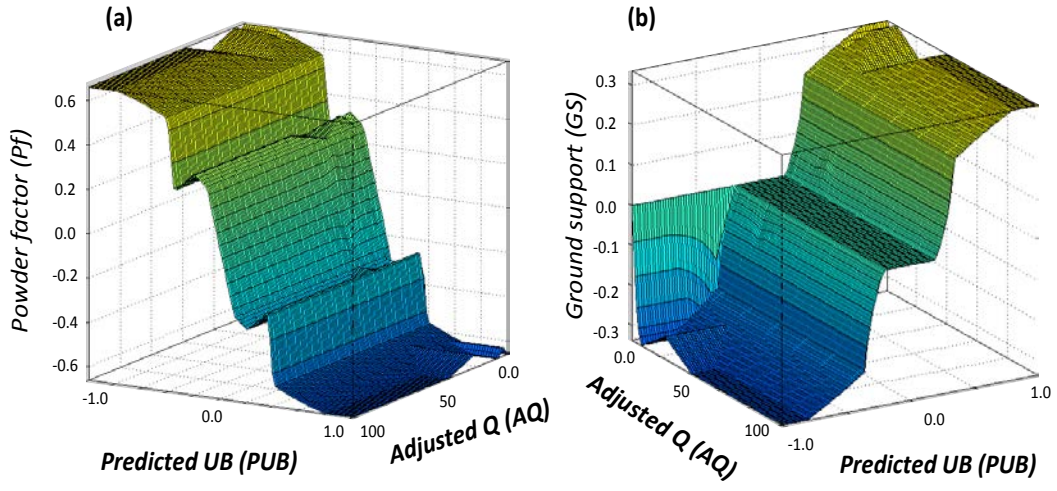

Figure 7-5 3D-mapping of predicted uneven break (PUB) and adjusted Q-value (AQ) to powder factor (Pf) and ground support (GS)

Figure 7-5 shows that the outputs of fuzzy expert system, the PFCR and GSCR, are more affected by PUB than AQ. The 3D-mapping of the Pf control rate (PFCR) is

shown in Figure 7-5a. For a PUB domain range from -1 to 1, the PFCR varies between -0.6 and 0.6. The PFCR increases or decreases significantly over the PUB range of -0.4 to 0.4, and the PFCR promptly converges to either -0.6 or 0.6 when the PUB is over -0.4 and 0.4. The results shows that if the predicted uneven break (PUB) is over 40% of the underbreak (PFCR < -0.4) or the overbreak (PFCR > 0.4), the uneven break (UB) cannot be effectively controlled by the Pf itself, but a redesign should be considered by reviewing the overall design parameters for the stope.

The 3D map of the GS control rate (GSCR) is shown in Figure 7-5b and exhibits quite similar trends to the PFCR. However, the GSCR shows a rather short range of variances compared to that of the PFCR. The GSCR only varies from -0.3 to 0.3 over the full PUB range (from -1 to 1). Furthermore, the GSCR remains at 0.00 over the PUB range of -0.2 to 0.2. The GSCR then precipitously increases and decreases over the PUB range of 0.2 to 0.4 and -0.2 to -0.4, respectively. The GSCR then converges at approximately -0.35 and 0.35. These short ranges converge, and the initial flat level of the GSCR values indicates that mining experts are more cautious in altering the ground support than the powder factor when a potential uneven break (UB) is expected in a planned stope. That is, mining experts believe that the powder factor is a more effective way to control the uneven break in stope wall than altering the ground support system.

7.3 UB CONSULTATION MAP

The developed UB consultation fuzzy expert system (FES) facilitates control of the potential uneven break (UB) by retrieving the *Pf* and *GS* control rate (PFCR and GSCR). However, it is less clear how the numerical values of PFCR and GSCR can be used to determine the implications of the potential UB. Thus, uneven break (UB) consultation maps are recommended to provide an intuitive understanding of the PFCR and GSCR results.

As the PFCR and GSCR are governed by the predicted uneven break (PUB), the UB consultation maps are modelled using the relationship among the PUB and the PFCR and GSCR. Figure 7-6 is a schematic of the UB consultation map.

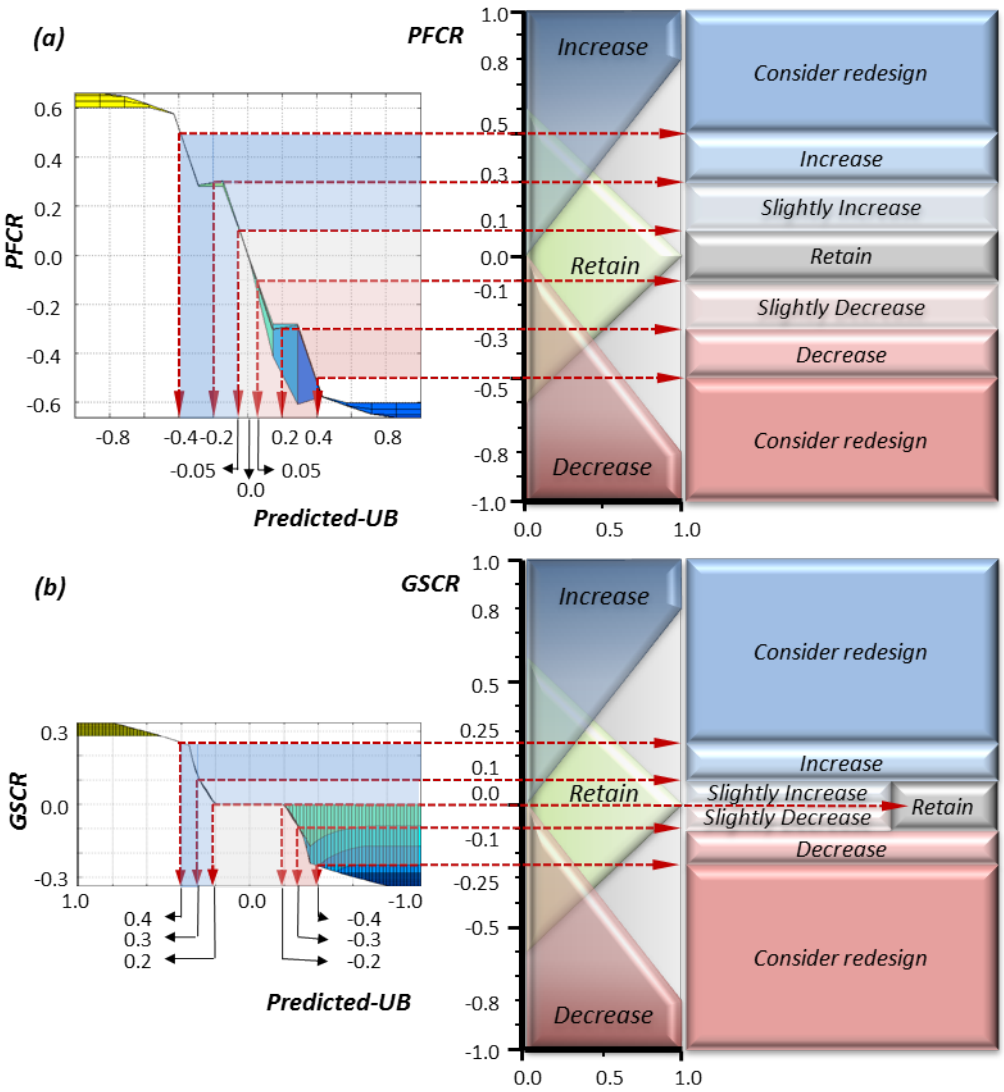

Figure 7-6 Derived UB consultation map for (a) powder factor control rate and (b) ground support control rate

The recommended UB consultation maps for the PFCR and the GSCR are composed of six control categories: 'retain', 'slightly increase', 'slightly decrease', 'increase, 'decrease', and 'consider redesign', which are shown in the right hand side of Figures 7-6a and b. These control categories are determined by the predicted uneven break (PUB) map that is derived from the UB consultation fuzzy expert system.

Figure 7-6a shows that the PFCR range of -0.1 to 0.1 is considered to be in the 'retain' category because the corresponding PUB ranges from -0.05 to 0.05 (i.e., 5% of an underbreak or an overbreak). Thus, the PFCR ranges of 0.1 to 0.3 and -0.1 to -0.3 are categorised as 'slightly decrease' and 'slightly increase', respectively,

because the PUB ranges from -0.05 to -0.20 and 0.05 to 0.20 (i.e., from 5% to 20% of the overbreak (positive) and the underbreak (negative)). Similarly, the PFCR is categorised as 'increase' and 'decrease' when it ranges from 0.3 to 0.5 and -0.3 to -0.5 because the corresponding potential overbreak and underbreak percentages vary from 20% to 40%. Finally, when the PUB is exceeded by under -0.4 or over 0.4 (i.e., 40% of an underbreak or an overbreak), the PFCR is categorised as 'consider redesign'.

The GSCR can similarly also be categorised into six categories, as shown in Figure 7-6b. The detailed UB consultation map for the PFCR and the GSCR are tabulated in Tables 7-4 and 7-5, respectively.

Table 7-4 Uneven break (UB) consultation map for powder factor control rate (PFCR)

Condition		PUB	PFCR	UB consultation category
Under break	Over 40%	< -0.40	> 0.50	Consider redesign
	20% ~ 40%	-0.40 ~ -0.20	0.30 ~ 0.50	Increase
	5% ~ 20%	-0.20 ~-0.05	0.30 ~ 0.10	Slightly increase
5% over & underbreak		-0.05 ~ 0.05	-0.10 ~ 0.10	Retain
Over break	5% ~ 20%	0.05 ~ 0.20	-0.30 ~ -0.10	Slightly decrease
	20% ~ 40%	0.20 ~ 0.40	-0.50 ~ -0.30	Decrease
	Over 40%	> 0.40	< -0.50	Consider redesign

Table 7-5 Uneven break (UB) consultation map for ground support control rate (GSCR)

Condition		PUB	GSCR	UB consultation category
Under break	Over 40%	> 0.40	> 0.25	Consider redesign
	20% ~ 40%	0.30 ~ 0.40	0.10 ~ 0.25	Increase
	5% ~ 20%	0.20 ~ 0.30	0.00 ~ 0.10	Slightly increase
20% over & underbreak		-0.20 ~ 0.20	0.00	Retain
Over break	20% ~ 30%	-0.20 ~ -0.30	0.00 ~ -0.10	Slightly decrease
	30% ~ 40%	-0.30 ~ -0.40	-0.10 ~ -0.25	Decrease
	Over 40%	< -0.40	< -0.25	Consider redesign

7.4 INTEGRATED UB MANAGEMENT NEURO-FUZZY SYSTEM

To build an integrated UB management system, the developed uneven break (UB) prediction ANN and the UB consultation FES were combined into a single concurrent neuro-fuzzy system (CNFS) using a graphic user interface (GUI) building software GUIDE in MATLAB. A standalone application was also created using the MATLAB compiler. Hence, the developed UB management neuro-fuzzy system can be run on any computer system without installing MATLAB. Figure 7-7 demonstrates the GUI of the UB management neuro-fuzzy system.

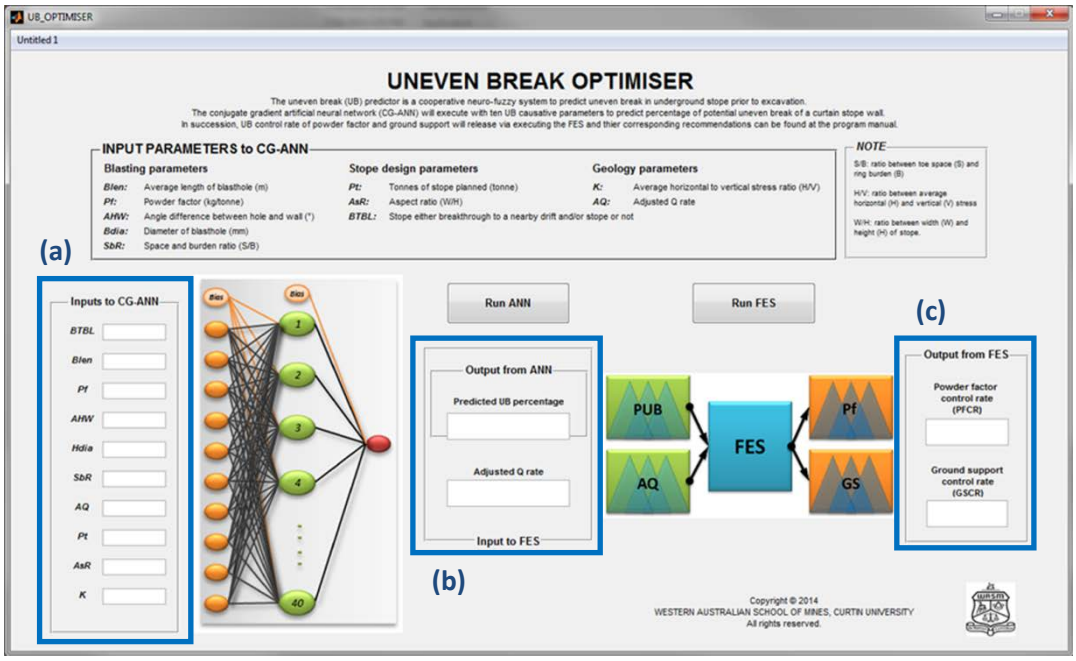

Figure 7-7 Graphical user interface (*GUI*) of integrated UB management cooperative neuro-fuzzy system (called an '*uneven break optimiser*')

7.4.1 *Instruction of uneven break optimiser*

The purpose of an 'uneven break optimiser' is to help mining engineers minimise unplanned dilution and ore-loss (i.e., an uneven break, UB) in stope production. The integral UB prediction artificial neural network (ANN) system allows for the prediction of a potential uneven break (UB) before actual production blasting. Furthermore, the connected UB consultation fuzzy expert system (FES) shows the direction and intensity of the approach that would minimise an unfavourable potential uneven break (UB) based on the powder factor (Pf) and the ground

support (GS) control rate (PFCR and GSCR). To aid the user, simplified sequential instructions for an uneven break optimiser are listed below.

1) Prepare the requisite ten input parameters by referring to the planned stope design.
2) Type the ten input parameters into the boxes in area (a) in Figure 7-7.
3) Click the 'Run-ANN' button to activate the UB prediction ANN.
4) Check the computed potential uneven break (PUB) percentage in the upper box in area (b) in Figure 7-7. (The inputted AQ value will simultaneously appear in the lower box in area (b).)
5) Click the 'Run FES' button to activate the UB consultation FES.
6) Check the computed Pf and GS control rates (PFCR and GSCR) in area (c) in Figure 7-7.
7) Make a decision that minimises the predicted potential UB by referring to the UB consultation map (Figure 7-6, Table 7-4, and Table 7-5).

7.5 SUMMARY AND DISCUSSION

In this chapter, an uneven break (UB) consultation system was developed using a fuzzy expert system (FES). The predicted uneven break (PUB) from the UB prediction ANN and adjusted Q-value (AQ) were set as inputs, and two new parameters, the powder factor and the ground support control rate (PFCR and GSCR), were introduced and allocated to the outputs of the developed FES. The developed UB consultation FES was formulated using the Mamdani fuzzy inference system (FIS), and the membership functions and the fuzzy rules were formulated based on a survey of fifteen underground mining experts. Furthermore, uneven break (UB) consultation maps were developed to provide an intuitive understanding of the PFCR and GSCR.

The developed UB consultation FES was combined with the UB prediction ANN system using a graphic user interface (GUI) to build an integrated UB management system. Thus, an integrated UB management cooperative neuro-fuzzy system, which is known as an 'uneven break optimiser', was developed.

The uneven break optimiser will help mining engineers to predict unfavourable unplanned dilution and ore-loss (i.e., uneven break, UB) prior to actual excavation and make optimised recommendations to minimise the predicted potential uneven break (UB).

CHAPTER 8. CONCLUSIONS AND FUTURE WORK

Unplanned dilution and ore-loss (which is referred to as an uneven break, UB) are critically important to mine management because these core cost factors are often cited as the primary reasons for mine closure. Recently, an underground mine management system was improved using various statistical, empirical, and numerical modelling methods. However, most mines still suffer from severe uneven break (UB), and experienced mining engineers must largely use their own intuition to minimise uneven break (UB). Notwithstanding the numerous efforts of engineers and researchers, the exact mechanism of unplanned dilution and ore-loss remains unclear, and there is no operational practical quantitative UB prediction and consultation system.

The aim of this study is to develop a dynamic unplanned dilution and ore loss (UB) management system using uneven break (UB) prediction and consultation models. Attempts have also been made to elucidate the uneven break (UB) mechanism by investigating trends in the contributions of influential parameters to uneven break (UB). To formulate accurate UB prediction models, a total of 1,067 datasets were collected via thorough review of over 30,000 documents from three underground stoping mines in Western Australia, which consisted of ten potential UB causative factors. The following blasting-related parameters were investigated: the average length of the blasthole (Blen), the powder factor (Pf), the angle difference between the hole and the wall (AHW), the blasthole diameter (Bdia) and the space and burden ratio (SbR). The adjusted Q rate (AQ) and the average horizontal to vertical stress ratio (K) were examined consecutively, and the representative geological factors, the planned tonnes of stope (Pt), the aspect ratio (AsR), and stope either breakthrough to a nearby drift and/or stope or not (BTBL) were investigated as representative stope design parameters.

The UB prediction models were developed using conventional statistical methods and an advanced soft computing approach. The UB prediction performances were then evaluated in terms of the correlation coefficient (R) between the actual stope UB and the predicted UB from developed models. First, multiple linear and

nonlinear regression analyses (MLRA and MNRA) were used as statistical tools and were found to be inadequate for UB prediction. For instance, the NLRA and MNRA models of the general dataset (GM) for UB prediction yielded correlation coefficients (R) of 0.419 and 0.438, respectively. Then, a conjugate gradient type artificial neural network (CG-ANN) was applied as a soft computing approach. The optimised CG-ANN exhibited a reliable UB prediction performance because the correlation coefficient (R) was 0.719, which was superior to that of the multiple regression models. The current UB prediction performance for the investigated three mines only exhibited a correlation coefficient (R) of 0.088: the prediction performance of the developed CG-ANN model was outstanding, showing that this method could be used in actual mines.

In fact, the uneven break (UB) is an inevitable phenomenon when ore is extracted using a drilling and blasting method. Despite the efforts of numerous engineers and scholars, the exact mechanism remains unclear. Thus, attempts were made to elucidate the contributions of different parameters to the UB phenomenon based on UB prediction models of the general model (GM). Although the multiple linear and nonlinear regression analyses (MLRA and MNRA) demonstrated poor and moderate validities, trends in the effects of the parameters could be determined. The AHW, AQ, and Blen were negatively correlated with the uneven break (UB), whereas the other parameters were positively correlated with the UB. The parameter contributions for the optimised CG-ANN model were analysed using weight- and sensitivity-based algorithms. First, the connection weight algorithm (CWA) was applied as a weight-based algorithm, where the AQ was the most influential parameter with a contribution of 22.40%. K also exhibited a relatively high contribution of 19.49%, and the remaining eight parameters had contributions of less than 10%. As for the MNRA results, the AQ, Blen, Pt, and AHW were negatively correlated with the UB phenomenon. The profile method (PM) was also applied as a sensitivity-based algorithm. As in the CWA analysis, the AQ and K exhibited strong influences on the UB phenomenon with contributions of 20.48% and 18.12%. Applying the PM revealed the following essential trends: the magnitude of the overbreak decreases for a higher rock quality, a deeper, narrower

or larger stope, a shorter ring burden, a lower powder factor, a smaller blasthole diameter, a longer blasthole, a stope breakthrough to another space, and a fanned drilling pattern. In addition, the contributions of the three core categories, i.e., the geology, the blasting, and the stope design, to the uneven break (UB) were calculated using the profile method (PM) application. The geology was found to be the most significant contributor with a contribution of 38.79%, whereas the blasting and stope design categories contributed 37.17% and 24.04%, respectively.

To develop an integral UB management system, an UB consultation system was built using a fuzzy expert system (FES). The FES was connected to the UB prediction CG-ANN model by importing the predicted-UB (PUB) and the adjusted Q-value (AQ) as inputs to the system. Two new parameters, the powder factor and the ground support control rate (PFCR and GSCR), were introduced to support the engineers' decision-making processes and were allocated to the FES outputs. The developed FES was established using a Mamdani fuzzy inference system (FIS), and membership functions and fuzzy rules were formulated based on a survey of fifteen underground mining experts. Uneven break (UB) consultation maps were also developed to provide engineers with an intuitive understanding of the concepts of the PFCR and the GSCR. Finally, a graphic user interface (GUI) was used to combine the UB consultation FES and the UB prediction CG-ANN system into a single integrated UB management cooperative neuro-fuzzy system, which was called an 'uneven break optimiser'. The developed uneven break optimiser will play a significant role in increasing the productivity of stope production as well as in enhancing the profitability of the entire mining processes by minimising the potential uneven break (UB) phenomenon.

In this study, a reliable UB management system was formulated but the developed system also has some limitations because of the complexity of the UB phenomenon. Mining activities always pose inherent uncertainties. The employed ten major UB causative factors also have inherent variability that may drop the accuracy of the proposed UB prediction model. The influences of input variables variability can be assessed by formulating a new hybrid stochastic model combining with ANN. The reliability of the UB prediction system hinges on the degree of coverage of the

collected dataset relative to the actual overall UB occurrence factors. Although the proposed UB management system showed outstanding performance, it cannot be used to predict the UB beyond the range of the training dataset. For instance, the system was developed for a rock quality (AQ: adjusted Q-value) range between 6.30 and 93.30. Thus, the system cannot be applied if the quality of the rock mass on the site is above or below this range. Fortunately, this limitation can be improved straightforwardly by re-training the CG-ANN with additional dataset ranges. Another limitation of the developed UB management system is that it was developed using only historical information. Thus, the human error factor cannot be directly included in the system. Possible remedies for these limitations will be left for future work on updating the UB management system. For instance, the reliability of the proposed system can be improved by composing a real-time data collection system in mines which will improve the quality and quantity of the datasets. In this way, the coverage of the UB management system will be broader and the human error factor can also be directly included as a UB causative factor.

REFERENCES

Aghajani Bazzazi, A., Osanloo, M., & Karimi, B. (2011). Deriving preference order of open pit mines equipment through MADM methods: Application of modified VIKOR method. *Expert Systems with Applications, 38*(3), 2550-2556.

Alimoradi, A., Moradzadeh, A., Naderi, R., Salehi, M. Z., & Etemadi, A. (2008). Prediction of geological hazardous zones in front of a tunnel face using TSP-203 and artificial neural networks. *Tunnelling and Underground Space Technology, 23*(6), 711-717.

Álvarez-Vigil, A., González-Nicieza, C., López Gayarre, F., & Álvarez-Fernández, M. (2012). Predicting blasting propagation velocity and vibration frequency using artificial neural networks. *International Journal of Rock Mechanics and Mining Sciences, 55*, 108-116.

Alvarez Grima, M., & Babuška, R. (1999). Fuzzy model for the prediction of unconfined compressive strength of rock samples. *International Journal of Rock Mechanics and Mining Sciences, 36*(3), 339-349.

Amirkhanian, S. N., & Baker, N. J. (1992). Expert system for equipment selection for earth-moving operations. *Journal of Construction Engineering and Management, 118*(2), 318-331.

Antony, J. (2003). *Design of experiments for engineers and scientists* (Vol. 26): Butterworth-Heinemann.

Ataei, M., Jamshidi, M., Sereshki, F., & Jalali, S. (2008). Mining method selection by AHP approach. *Journal of the Southern African Institute of Mining and Metallurgy, 108*, 741-749.

Ataei, M., & Kamali, M. (2012). Prediction of blast-induced vibration by adaptive neuro-fuzzy inference system in Karoun 3 power plant and dam. *Journal of Vibration and Control*.

Austrade. (2013). *Underground Mining*. GPO Box 5301, Sydney NSW: Commonwealth of Australia.

Aydin, A. (2004). Fuzzy set approaches to classification of rock masses. *Engineering Geology, 74*(3–4), 227-245.

Azadeh, A., Osanloo, M., & Ataei, M. (2010). A new approach to mining method selection based on modifying the Nicholas technique. *Applied Soft Computing, 10*(4), 1040-1061.

Azimi, Y., Osanloo, M., Aakbarpour-Shirazi, M., & Aghajani Bazzazi, A. (2010). Prediction of the blastability designation of rock masses using fuzzy sets. *International Journal of Rock Mechanics and Mining Sciences, 47*(7), 1126-1140.

Bahrami, A., Monjezi, M., Goshtasbi, K., & Ghazvinian, A. (2011). Prediction of rock fragmentation due to blasting using artificial neural network. *Engineering with Computers, 27*(2), 177-181.

Bandopadhyay, S. (1987). Partial ranking of primary stripping equipment in surface mine planning. *International Journal of Surface Mining, Reclamation and Environment, 1*(1), 55-59.

Bandopadhyay, S., & Venkatasubramanian, P. (1987). Expert systems as decision aid in surface mine equipment selection. *International Journal of Surface Mining, Reclamation and Environment, 1*(2), 159-165.

Bandopadhyay, S., & Venkatasubramanian, P. (1988). A rule-based expert system for mining method selection. *CIM Bulletin, 81*(919), 84-88.

Barton, N. (1974). Engineering classification of rock masses for the design of tunnel support. *Rock mechanics, 6*(4), 189.

Barton, N., Lien, R., & Lunde, J. (1974). Engineering classification of rock masses for the design of tunnel support: Rock Mechanics, v. 6. *southern Nevada: Geological Society of America Bulletin, 88*, 943-959.

Bascetin, A. (2004). Technical note: an application of the analytic hierarchy process in equipment selection at Orhaneli open pit coal mine. *Mining Technology, 113*(3), 192-199.

Bascetin, A., & Kesimal, A. (1999). The study of a fuzzy set theory for the selection of an optimum coal transportation system from pit to the power plant. *International Journal of Surface Mining, Reclamation and Environment, 13*(3), 97-101.

Beiki, M., Bashari, A., & Majdi, A. (2010). Genetic programming approach for estimating the deformation modulus of rock mass using sensitivity analysis by neural network. *International Journal of Rock Mechanics and Mining Sciences, 47*(7), 1091-1103.

BFP Consultants Pty Ltd. (2004). *Rock stress measurements by overcoring at Timor TF 1710 SOD and Baltic BD 3835 WOD, Plutonic Gold Mine*. Unpublished manuscript.

Bieniawski, Z. (1973). Engineering classification of jointed rock masses. *Civil Engineer in South Africa, 15*(12).

Bieniawski, Z. (1974). *Geomechanics classification of rock masses and its application in tunnelling.* Paper presented at the Advances in Rock Mechanics. Proceedings of the 3rd International Society of Rock Mechanics Congress.

Bieniawski, Z. (1978). *Determining rock mass deformability: experience from case histories.* Paper presented at the International Journal of Rock Mechanics and Mining Sciences & Geomechanics Abstracts.

Bieniawski, Z., & Grandori, R. (2007). Predicting TBM Excavability-Part II. *Tunnels & Tunnelling International*.

Bitarafan, M., & Ataei, M. (2004). Mining method selection by multiple criteria decision making tools. *The Journal of The South African Institute of Mining and Metallurgy, 104*(9), 493-498.

Black, M. (1937). Vagueness. *Philosophy of science*.

Blackwell, G. (1999). Estimation of large open pit haulage truck requirements. *CIM bulletin, 92*(1028), 143-149.

Brady, T., Martin, L., & Pakalnis, R. (2005). Empirical approaches for opening design in weak rock masses. *Mining Technology, 114*(1), 13-20.

Brown, E., & Hoek, E. (1978). *Trends in relationships between measured< i> in-situ</i> stresses and depth.* Paper presented at the International Journal of Rock Mechanics and Mining Sciences & Geomechanics Abstracts.

Bryson, A. H., & Ho, Y. C. (1969). *Applied Optimal Control*: Blaisdell.

Butler, A., & Franklin, J. (1990). *Classex: an expert system for rock mass classification.* Paper presented at the ISRM International Symposium.

Cagliostro, D., & Romander, C. (1975). Experiments on the Response of Hexagonal Subassembly Ducts to Radial Loads. *SRI Project PYD-1960, Third Interim Report, 18*.

Cankaya, S. (2009). A comparative study of some estimation methods for parameters and effects of outliers in simple regression model for research on small ruminants. *Tropical animal health and production, 41*(1), 35-41.

Carver, R. P. (1978). The case against statistical significance testing. *Harvard Educational Review, 48*(3), 378-399.

Cepuritis, P., Villaescusa, E., Beck, D., & Varden, R. (2010). *Back Analysis of Over-break In a Longhole Open Stope Operation Using Non-linear Elasto-Plastic Numerical Modelling.* Paper presented at the 44th US Rock Mechanics Symposium and 5th US-Canada Rock Mechanics Symposium.

Chakraborty, A., Guha, P., Chattopadhyay, B., Pal, S., & Das, J. (2004). *A fusion neural network for estimation of blasting vibration.* Paper presented at the Neural Information Processing.

Clark, L., & Pakalnis, R. (1997). *An empirical design approach for estimating unplanned dilution from open stope hangingwalls and footwalls.* Paper presented at the Presentation at 99th Canadian Institute of Mining annual conference, Vancouver, BC.

Clark, L. M. (1998). Minimizing dilution in open stope mining with a focus on stope design and narrow vein longhole blasting.

Clarke, M., Denby, B., & Schofield, D. (1990). Decision making tools for surface mine equipment selection. *Mining Science and Technology, 10*(3), 323-335.

Darabi, A., Ahangari, K., Noorzad, A., & Arab, A. (2012). Subsidence estimation utilizing various approaches – A case study: Tehran No. 3 subway line. *Tunnelling and Underground Space Technology, 31*(0), 117-127.

Deere, D. (1964). Technical description of rock cores for engineering purposes. *Rock Mechanics and Engineering Geology, 1*(1), 17-22.

Dehghani, H., & Ataee-Pour, M. (2011). Development of a model to predict peak particle velocity in a blasting operation. *International Journal of Rock Mechanics and Mining Sciences, 48*(1), 51-58.

Denby, B., & Schofield, D. (1990). Applications of expert systems in equipment selection for surface mine design. *International Journal of Surface Mining, Reclamation and Environment, 4*(4), 165-171.

Deng, J., & Lee, C. (2001). Displacement back analysis for a steep slope at the Three Gorges Project site. *International journal of rock mechanics and mining sciences, 38*(2), 259-268.

Diederichs, M., & Kaiser, P. (1999). Tensile strength and abutment relaxation as failure control mechanisms in underground excavations. *International Journal of Rock Mechanics and Mining Sciences, 36*(1), 69-96.

Diederichs, M. S., & Kaiser, P. K. (1996). Rock instability and risk analyses in open stope mine design. *Canadian geotechnical journal, 33*(3), 431-439.

Dimopoulos, I., Chronopoulos, J., Chronopoulou-Sereli, A., & Lek, S. (1999). Neural network models to study relationships between lead concentration in grasses and permanent urban descriptors in Athens city (Greece). *Ecological Modelling, 120*(2), 157-165.

Dimopoulos, Y., Bourret, P., & Lek, S. (1995). Use of some sensitivity criteria for choosing networks with good generalization ability. *Neural Processing Letters, 2*(6), 1-4.

Durbin, J., & Watson, G. S. (1950). Testing for serial correlation in least squares regression: I. *Biometrika, 37*(3/4), 409-428.

Einstein, H. H., & Schwartz, C. W. (1979). Simplified analysis for tunnel supports. *Journal of Geotechnical and Geoenvironmental Engineering, 105*(ASCE 14541).

Esmaeili, M., Osanloo, M., Rashidinejad, F., Bazzazi, A. A., & Taji, M. (2012). Multiple regression, ANN and ANFIS models for prediction of backbreak in the open pit blasting. *Engineering with Computers*, 1-10.

Fişne, A., Kuzu, C., & Hüdaverdi, T. (2011). Prediction of environmental impacts of quarry blasting operation using fuzzy logic. *Environmental monitoring and assessment, 174*(1-4), 461-470.

Fletcher, R., & Reeves, C. M. (1964). Function minimization by conjugate gradients. *The computer journal, 7*(2), 149-154.

Ganguli, R., & Bandopadhyay, S. (2002). Expert system for equipment selection. *International Journal of Surface Mining, Reclamation and Environment, 16*(3), 163-170.

García Bastante, F., Alejano, L., & González-Cao, J. (2012). Predicting the extent of blast-induced damage in rock masses. *International Journal of Rock Mechanics and Mining Sciences, 56*(0), 44-53.

Garrett, R. G. (1989). The chi-square plot: a tool for multivariate outlier recognition. *Journal of Geochemical Exploration, 32*(1–3), 319-341.

Garson, G. D. (1991). Interpreting neural-network connection weights. *AI expert, 6*(4), 46-51.

Germain, P., & Hadjigeorgiou, J. (1997). Influence of stope geometry and blasting patterns on recorded overbreak. *International Journal of Rock Mechanics and Mining Sciences, 34*(3–4), 115.e111-115.e112.

Gershon, M., Bandopadhyay, S., & Panchanadam, V. (1993). *Mining method selection: a decision support system integrating multi-attribute utility theory and expert systems.* Paper presented at the Proceedings of the 24th international symposium on the application of computers in mine planning (APCOM).

Gevrey, M., Dimopoulos, I., & Lek, S. (2003). Review and comparison of methods to study the contribution of variables in artificial neural network models. *Ecological Modelling, 160*(3), 249-264.

Gokceoglu, C., Yesilnacar, E., Sonmez, H., & Kayabasi, A. (2004). A neuro-fuzzy model for modulus of deformation of jointed rock masses. *Computers and Geotechnics, 31*(5), 375-383.

Grima, M. A. (2000). Neuro-fuzzy modeling in engineering geology.

Guray, C., Celebi, N. e., Atalay, V., & Pasamehmetoglu, A. G. (2003). Ore-age: a hybrid system for assisting and teaching mining method selection. *Expert Systems with Applications, 24*(3), 261-271.

Habibagahi, G., & Katebi, S. (1996). Rock mass classification using fuzzy sets. *Iranian journal of science and technology, 20*(3), 273-284.

Hadjigeorgiou, J., Leclair, J., & Potvin, Y. (1995). An update of the stability graph method for open stope design. *CIM Rock Mechanics and Strata Control session, Halifax, Nova Scotia*, 14-18.

Hamidi, J. K., Shahriar, K., Rezai, B., & Bejari, H. (2010). Application of fuzzy set theory to rock engineering classification systems: an illustration of the rock mass excavability index. *Rock mechanics and rock engineering, 43*(3), 335-350.

Hansen, L. K., & Salamon, P. (1990). Neural network ensembles. *Pattern Analysis and Machine Intelligence, IEEE Transactions on, 12*(10), 993-1001.

Hartman, H. (2007). *Introductory mining engineering*: John Wiley & Sons.

Hawkins, D. M. (1980). *Identification of outliers* (Vol. 11): Chapman and Hall London.

Hawkins, D. M. (2004). The problem of overfitting. *Journal of chemical information and computer sciences, 44*(1), 1-12.

Hecht-Nielsen, R. (1987). *Kolmogorov's mapping neural network existence theorem.* Paper presented at the The 1st IEEE International Conference on Neural Networks, San Diego, CA, USA.

Henning, J. G., Kaiser, E., & Mitri, H. (2001). *Evaluation of stress influences on ore dilution: a case study.* Paper presented at the DC Rocks 2001 The 38th US Symposium on Rock Mechanics (USRMS).

Henning, J. G., & Mitri, H. S. (2007). Numerical modelling of ore dilution in blasthole stoping. *International Journal of Rock Mechanics and Mining Sciences, 44*(5), 692-703.

Henning, J. G., & Mitri, H. S. (2008). Assessment and control of ore dilution in long hole mining: case studies. *Geotechnical and Geological Engineering, 26*(4), 349-366.

Hestenes, M. R., & Stiefel, E. (1952). Methods of conjugate gradients for solving linear systems: (NBS).

Hipel, K. W. (1982). *Fuzzy set methodologies in multicriteria modeling* (Vol. 279): North-Holland, New York.

Hoek, E. (1994). Strength of rock and rock masses. *ISRM News Journal, 2*(2), 4-16.

Hoek, E. (2000). Practical rock engineering: (Rocscience).

Hoek, E., & Brown, E. (1997). Practical estimates of rock mass strength. *International Journal of Rock Mechanics and Mining Sciences, 34*(8), 1165-1186.

Holland, J. (1975). *Adaptation in Natural and Artificial Systems*: University of Michigan Press.

Hooker, V. E., & Bickel, D. L. (1974). *Overcoring equipment and techniques: used in rock stress determination* (Vol. 8618): US Bureau of Mines.

Hughes, R., Mitri, H., & Lecomte, E. (2010). *Examining the influence of stope strike length on unplanned ore dilution in narrow vein longitudinal mining.* Paper presented at the 44th US Rock Mechanics Symposium and 5th US-Canada Rock Mechanics Symposium.

Hutchinson, D. J., & Diederichs, M. S. (1996). *Cablebolting in underground mines*: BiTech Publishers.

Hwang, C., & Yoon, K. (1981). *Multiple attribute decision making*: Springer.

IBM. (2012). IBM SPSS Statistics for Windows, Version 21.0. Armonk, NY: IBM Corp.

Iglewicz, B., & Martinez, J. (1982). Outlier detection using robust measures of scale. *Journal of Statistical Computation and Simulation, 15*(4), 285-293.

Iphar, M., & Goktan, R. (2006). An application of fuzzy sets to the diggability index rating method for surface mine equipment selection. *International journal of rock mechanics and mining sciences, 43*(2), 253-266.

Itasca. (2002). Fast Lagrangian Analysis of Continua, Version 4.0 User's Guide. *Itasca Consulting Group, Inc., Thrasher Square East, 708*.

Itasca Consulting Group, I. (2013). *Software.* Retrieved from http://itascacg.com/software

Jang, H., & Topal, E. (2013). Optimizing overbreak prediction based on geological parameters comparing multiple regression analysis and artificial neural network. *Tunnelling and Underground Space Technology, 38*(0), 161-169.

Jang, J. (1993). ANFIS: adaptive-network-based fuzzy inference system. *Systems, Man and Cybernetics, IEEE Transactions on, 23*(3), 665-685.

Jing, L. (2003). A review of techniques, advances and outstanding issues in numerical modelling for rock mechanics and rock engineering. *International Journal of Rock Mechanics and Mining Sciences, 40*(3), 283-353.

Juang, C., & Lee, D. (1989). Development of an expert system for rock mass classification. *Civil Engineering Systems, 6*(4), 147-156.

Juang, C., & Lee, D. (1990). *Rock mass classification using fuzzy sets.* Paper presented at the Proceedings of the 10th Southeast Asian Geotechnical Conference, Chinese Institute of Civil and Hydraulic Engineering, Taipei, Taiwan.

Kaastra, L., & Boyd, M. (1996). Designing a Neural Network for Forecasting Financial and Economic Time Series. *Neurocomputing*, 215 - 236.

Karnin, E. D. (1990). A simple procedure for pruning back-propagation trained neural networks. *Neural Networks, IEEE Transactions on, 1*(2), 239-242.

Kayabasi, A., Gokceoglu, C., & Ercanoglu, M. (2003). Estimating the deformation modulus of rock masses: a comparative study. *International Journal of Rock Mechanics and Mining Sciences, 40*(1), 55-63.

Kim, C., Bae, G., Hong, S., Park, C., Moon, H., & Shin, H. (2001a). Neural network based prediction of ground surface settlements due to tunnelling. *Computers and Geotechnics, 28*(6–7), 517-547.

Kim, C. Y., Bae, G. J., Hong, S. W., Park, C. H., Moon, H. K., & Shin, H. S. (2001b). Neural network based prediction of ground surface settlements due to tunnelling. *Computers and Geotechnics, 28*(6–7), 517-547.

Krajcinovic, D. (1983). Creep of Structures - a Continuous Damage Mechanics Approach. *Journal of Structural Mechanics, 11*(1), 1-11.

Kulatilake, P., Qiong, W., Hudaverdi, T., & Kuzu, C. (2010). Mean particle size prediction in rock blast fragmentation using neural networks. *Engineering Geology, 114*(3), 298-311.

Lang, B. D. A. (1994). *Span design for entry-type excavations.* University of British Columbia.

Lee, C., & Sterling, R. (1992). *Identifying probable failure modes for underground openings using a neural network.* Paper presented at the International journal of rock mechanics and mining sciences & geomechanics abstracts.

Lek, S., Belaud, A., Dimopoulos, I., Lauga, J., & Moreau, J. (1995). Improved estimation, using neural networks, of the food consumption of fish populations. *Marine and Freshwater Research, 46*(8), 1229-1236.

Lek, S., Delacoste, M., Baran, P., Dimopoulos, I., Lauga, J., & Aulagnier, S. (1996). Application of neural networks to modelling nonlinear relationships in ecology. *Ecological Modelling, 90*(1), 39-52.

Levenberg, K. (1944). A method for the solution of certain problems in least squares. *Quarterly of Applied Mathematics, 2*, 164-168.

Li, W., Dai, L.-F., Hou, X.-B., & Lei, W. (2007). Fuzzy genetic programming method for analysis of ground movements due to underground mining. *International Journal of Rock Mechanics and Mining Sciences, 44*(6), 954-961.

Li, W., Liu, S.-J., Li, J.-F., Ji, Z.-H., Wang, Q., & Yin, X. (2013). Ground movement analysis in deep iron mine using fuzzy probability theory. *Applied Mathematical Modelling, 37*(1–2), 345-356.

Li, W., Mei, S., Zai, S., Zhao, S., & Liang, X. (2006). Fuzzy models for analysis of rock mass displacements due to underground mining in mountainous areas. *International journal of rock mechanics and mining sciences, 43*(4), 503-511.

Liu, L., & Katsabanis, P. D. (1997). Development of a continuum damage model for blasting analysis. *International Journal of Rock Mechanics and Mining Sciences, 34*(2), 217-231.

Liu, Y.-C., & Chen, C.-S. (2007). A new approach for application of rock mass classification on rock slope stability assessment. *Engineering Geology, 89*(1–2), 129-143.

Lu, Y. (2005). Underground blast induced ground shock and its modelling using artificial neural network. *Computers and Geotechnics, 32*(3), 164-178.

Lukasiewicz, J. (1920). Philosophical remarks on many-valued systems of propositional logic. *Polish Logic, 1939*, 40-63.

Mahalanobis, P. C. (1936). On the generalized distance in statistics. *Proceedings of the National Institute of Sciences (Calcutta), 2*, 49-55.

Mahdevari, S., & Torabi, S. R. (2012). Prediction of tunnel convergence using Artificial Neural Networks. *Tunnelling and Underground Space Technology, 28*(0), 218-228.

Majdi, A., & Beiki, M. (2010). Evolving neural network using a genetic algorithm for predicting the deformation modulus of rock masses. *International Journal of Rock Mechanics and Mining Sciences, 47*(2), 246-253.

Mamdani, E. H., & Assilian, S. (1975). An experiment in linguistic synthesis with a fuzzy logic controller. *International journal of man-machine studies, 7*(1), 1-13.

Mandal, S., & Singh, M. (2009). Evaluating extent and causes of overbreak in tunnels. *Tunnelling and Underground Space Technology, 24*(1), 22-36.

Manoj, K., & Singh, T. (2005). Prediction of blast induced air overpressure in opencast mine. *Noise & Vibration Worldwide, 36*(2), 7-16.

Manoj, K., & Singh, T. (2009). Prediction of blast-induced ground vibration using artificial neural network. *International Journal of Rock Mechanics and Mining Sciences, 46*(7), 1214-1222.

Marquardt, D. W. (1963). An algorithm for least-squares estimation of nonlinear parameters. *Journal of the Society for Industrial & Applied Mathematics, 11*(2), 431-441.

Martin, C., Tannant, D., Yazici, S., & Kaiser, P. (1999). *Stress path and instability around mine openings.* Paper presented at the Proc. 9th, ISRM Congress on Rock Mechanics.

Mathews, K., Hoek, E., Wyllie, D., & Stewart, S. (1981). Prediction of stable excavation spans for mining at depths below 1000 m in hard rock. *CANMET DSS Serial No: 0sQ80-00081., Ottawa*.

MathWorks, I. (2013). R2013a Natick, Massachusetts, United States.

McCulloch, W. S., & Pitts, W. (1943). A logical calculus of the ideas immanent in nervous activity. *The Bulletin of Mathematical Biophysics, 5*(4), 115-133.

McHugh, S. (1983). Crack extension caused by internal gas pressure compared with extension caused by tensile stress. *International Journal of Fracture, 21*(3), 163-176.

Meulenkamp, F., & Grima, M. A. (1999). Application of neural networks for the prediction of the unconfined compressive strength (UCS) from Equotip hardness. *International Journal of rock mechanics and mining sciences, 36*(1), 29-39.

Miller, F., & Jacob, D. (1993). Cavity monitoring system: (Google Patents).

Møller, M. F. (1993). A scaled conjugate gradient algorithm for fast supervised learning. *Neural Networks, 6*(4), 525-533.

Monjezi, M., Ahmadi, M., Sheikhan, M., Bahrami, A., & Salimi, A. (2010). Predicting blast-induced ground vibration using various types of neural networks. *Soil Dynamics and Earthquake Engineering, 30*(11), 1233-1236.

Monjezi, M., Amini, K., & Yazdian, V. (2011a). Optimization of open pit blast parameters using genetic algorithm. *International Journal of Rock Mechanics and Mining Sciences, 48*(5), 864-869.

Monjezi, M., & Dehghani, H. (2008). Evaluation of effect of blasting pattern parameters on back break using neural networks. *International Journal of Rock Mechanics and Mining Sciences, 45*(8), 1446-1453.

Monjezi, M., Ghafurikalajahi, M., & Bahrami, A. (2011b). Prediction of blast-induced ground vibration using artificial neural networks. *Tunnelling and Underground Space Technology, 26*(1), 46-50.

Monjezi, M., Khoshalan, H., & Varjani, A. (2012). Prediction of flyrock and backbreak in open pit blasting operation: a neuro-genetic approach. *Arabian Journal of Geosciences, 5*(3), 441-448.

Monjezi, M., Singh, T., Khandelwal, M., Sinha, S., Singh, V., & Hosseini, I. (2006). Prediction and analysis of blast parameters using artificial neural network. *Noise & Vibration Worldwide, 37*(5), 8-16.

Morgan, H. (1961). A contribution to the analysis of stress in a circular tunnel. *Geotechnique, 11*(1), 37-46.

Morgan, N., & Bourlard, H. (1989). *Generalization and parameter estimation in feedforward nets: Some experiments.* Paper presented at the NIPS.

Mubita, D. (2005). Recent initiatives in reducing dilution at Konkola Mine, Zambia. *Journal of the South African Institute of Mining and Metallurgy, 105*(2), 107-112.

Namin, F., Shahriar, K., Bascetin, A., & Ghodsypour, S. (2011). FMMSIC: a hybrid fuzzy based decision support system for MMS (in order to estimate interrelationships between criteria). *Journal of the Operational Research Society, 63*(2), 218-231.

Negnevitsky, M. (2005). *Artificial intelligence: a guide to intelligent systems*: Pearson Education.

Nguyen, V. (1985). *Some fuzzy set applications in mining geomechanics.* Paper presented at the International Journal of Rock Mechanics and Mining Sciences & Geomechanics Abstracts.

Nicholas, D. E. (1992). Seclection procedure. In H. L. Hartman (Ed.), *SME Mining Engineering Handbook.* (Vol. 2). Littleton, : SME.

Nicholson, G., & Bieniawski, Z. (1990). A nonlinear deformation modulus based on rock mass classification. *International Journal of Mining and Geological Engineering, 8*(3), 181-202.

Nickson, S. D. (1992). *Cable support guidelines for underground hard rock mine operations.* University of British Columbia.

Ning, Y. J., Yang, J., Ma, G. W., & Chen, P. W. (2011). Modelling Rock Blasting Considering Explosion Gas Penetration Using Discontinuous Deformation Analysis. *Rock Mechanics and Rock Engineering, 44*(4), 483-490.

Nourani, V., & Sayyah Fard, M. (2012). Sensitivity analysis of the artificial neural network outputs in simulation of the evaporation process at different climatologic regimes. *Advances in Engineering Software, 47*(1), 127-146.

Olden, J. D., & Jackson, D. A. (2002). Illuminating the “black box”: a randomization approach for understanding variable contributions in artificial neural networks. *Ecological modelling, 154*(1), 135-150.

Olden, J. D., Joy, M. K., & Death, R. G. (2004). An accurate comparison of methods for quantifying variable importance in artificial neural networks using simulated data. *Ecological Modelling, 178*(3), 389-397.

Osborne, M. R. (1992). Fisher's method of scoring. *International Statistical Review/Revue Internationale de Statistique*, 99-117.

Paine, A. S., & Please, C. P. (1994). AN IMPROVED MODEL OF FRACTURE PROPAGATION BY GAS DURING ROCK BLASTING - SOME ANALYTICAL RESULTS. *International Journal of Rock Mechanics and Mining Sciences & Geomechanics Abstracts, 31*(6), 699-706.

Pakalnis, R. (1986). Empirical stope design at Ruttan mine. *Vancouver, Canada, Department of Mining and Minerals Processing, University of British Columbia*, 90-95.

Pakalnis, R., Poulin, R., & Hadjigeorgiou, J. (1996). *Quantifying the cost of dilution in underground mines.* Paper presented at the International Journal of Rock Mechanics and Mining Sciences and Geomechanics Abstracts.

Pakalnis, R., Poulin, R., & Vongpaisal, S. (1995). *Quantifying dilution for underground mine operations.* Paper presented at the Annual meeting of the Canadian Institute of Mining, Metallurgy and Petroleum, Halifax.

Pal, N., & Chintalapudi, K. (1997). A connectionist system for feature selection. *NEURAL PARALLEL AND SCIENTIFIC COMPUTATIIONS, 5*, 359-382.

Perron, J. (1999). *Simple solutions and employee's involvement reduced the operating cost and improved the productivity at Langlois mine.* Paper presented at the Proceeding of the 14th CIM mine operator's conference.

Potvin, Y. (1988). Empirical open stope design in Canada.

Potvin, Y., & Hadjigeorgiou, J. (2001). The stability graph method for open-stope design. *Underground Mining Methods: Engineering Fundamentals and International Case Studies. Society of Mining, Metallurgy and Exploration, 8307 Shaffer Parkway, Littleton, CO 80127, USA, 2001.*, 513-520.

Rafiai, H., Jafari, A., & Mahmoudi, A. (2013). Application of ANN-based failure criteria to rocks under polyaxial stress conditions. *International Journal of Rock Mechanics and Mining Sciences, 59*, 42-49.

Rafiai, H., & Moosavi, M. (2012). An approximate ANN-based solution for convergence of lined circular tunnels in elasto-plastic rock masses with anisotropic stresses. *Tunnelling and Underground Space Technology, 27*(1), 52-59.

Reed, R. (1993). Pruning algorithms-a survey. *Neural Networks, IEEE Transactions on, 4*(5), 740-747.

Remennikov, A. M., & Rose, T. A. (2007). Predicting the effectiveness of blast wall barriers using neural networks. *International journal of impact engineering, 34*(12), 1907-1923.

Rezaei, M., Monjezi, M., & Yazdian Varjani, A. (2011). Development of a fuzzy model to predict flyrock in surface mining. *Safety Science, 49*(2), 298-305.

Rocscience inc. (2014). *Overview of products.* Retrieved from https://www.rocscience.com/highlights

Rosenblatt, F. (1958). The perceptron: A probabilistic model for information storage and organization in the brain. *Psychological Review, 65*(6), 386-408.

Rosenblatt, M. (1956). A central limit theorem and a strong mixing condition. *Proceedings of the National Academy of Sciences of the United States of America, 42*(1), 43.

Ross, T. J. (2009). *Fuzzy logic with engineering applications* (Third ed.): John Wiley & Sons.

Saaty, T. L. (1980). The analytic hierarchy process: planning, priority setting, resources allocation. *M cGraw-H ill*.

Scoble, M., & Moss, A. (1994). Dilution in underground bulk mining: implications for production management. *Geological Society, London, Special Publications, 79*(1), 95-108.

Seaman, L. (1980). A Computational Model for Dynamic Tensile Microfracture with Damage in One Plane. *SRI Poulter Laboratory Technical Report*, 001-080.

ShengFeng, T., Zhang, Q., & Mo, Y. (1988). *A rock classification expert system.* Paper presented at the Pattern Recognition, 1988., 9th International Conference on.

Sheorey, P. (1991). *Experiences with application of the NGI classification to coal measures.* Paper presented at the International Journal of Rock Mechanics and Mining Sciences & Geomechanics Abstracts.

Singh, T. (2004). Artificial neural network approach for prediction and control of ground vibrations in mines. *Mining Technology, 113*(4), 251-256.

Singh, T., Kanchan, R., & Verma, A. (2004). Prediction of blast induced ground vibration and frequency using an artificial intelligent technique. *Noise & Vibration Worldwide, 35*(11), 7-15.

Singh, V., Singh, D., & Singh, T. (2001). Prediction of strength properties of some schistose rocks from petrographic properties using artificial neural networks. *International Journal of Rock Mechanics and Mining Sciences, 38*(2), 269-284.

Sonmez, H., Gokceoglu, C., Nefeslioglu, H., & Kayabasi, A. (2006). Estimation of rock modulus: for intact rocks with an artificial neural network and for rock masses with a new empirical equation. *International Journal of Rock Mechanics and Mining Sciences, 43*(2), 224-235.

Sonmez, H., Tuncay, E., & Gokceoglu, C. (2004). Models to predict the uniaxial compressive strength and the modulus of elasticity for Ankara Agglomerate. *International Journal of Rock Mechanics and Mining Sciences, 41*(5), 717-729.

Stewart, P., Slade, J., & Trueman, R. (2005). *The effect of stress damage on dilution in narrow vein mines.* Paper presented at the 9th AusIMM Underground Operators Conference 2005.

Stewart, P., & Trueman, R. (2008). Strategies for Minimising and Predicting Dilution in Narrow Vein Mines–The Narrow Vein Dilution Method.

Stewart, P. C. (2005). *Minimising dilution in narrow vein mines.* Doctor of Philosophy. University of Queensland.

Stiehr, J. F., & Dean, J. (2011). ISEE blasters' handbookpp. 442-452: (International Society of Explosives, Cleveland).

Sugeno, M. (1985a). *Industrial applications of fuzzy control*: Elsevier Science Inc.

Sugeno, M. (1985b). An introductory survey of fuzzy control. *Information sciences, 36*(1), 59-83.

Suglo, R. S., & Opoku, S. (2012). An assessment of dilution in sublevel caving at Kazansi Mine. *International Journal of Mining and Mineral Engineering, 4*(1), 1-16.

Sun, S., Liu, J., & Jihong, W. (2013). Predictions of Overbreak Blocks in Tunnels Based on the Wavelet Neural Network Method and the Geological Statistics Theory. *Mathematical Problems in Engineering, 2013*.

Suorineni, F., Tannant, D., & Kaiser, P. (1999a). Determination of fault-related sloughage in open stopes. *International Journal of Rock Mechanics and Mining Sciences, 36*(7), 891-906.

Suorineni, F., Tannant, D., & Kaiser, P. (1999b). Fault factor for the stability graph method of open-stope design. *TRANSACTIONS OF THE INSTITUTION OF*

MINING AND METALLURGY SECTION A-MINING INDUSTRY, 108, A92-A104.

Takagi, T., & Sugeno, M. (1985). Fuzzy identification of systems and its applications to modeling and control. *Systems, Man and Cybernetics, IEEE Transactions on, SMC-15*(1), 116-132.

Tatman, C. (2001). Mining dilution in moderate- to narrow-width deposits. *Underground Mining Methods: Engineering Fundamentals and International Case Studies. Society of Mining, Metallurgy and Exploration, 8307 Shaffer Parkway, Littleton, CO 80127, USA, 2001.*, 615-626.

Taylor, L. M., Chen, E. P., & Kuszmaul, J. S. (1986). MICROCRACK-INDUCED DAMAGE ACCUMULATION IN BRITTLE ROCK UNDER DYNAMIC LOADING. *Computer Methods in Applied Mechanics and Engineering, 55*(3), 301-320.

Verma, A., & Singh, T. (2013). A neuro-fuzzy approach for prediction of longitudinal wave velocity. *Neural Computing and Applications*, 1-9.

Villaescusa, E. (1998). Geotechnical design for dilution control in underground mining. *Mine Planning and Equipment Selection*, 141-149.

Villaescusa, E., Seto, M., & Baird, G. (2002). Stress measurements from oriented core. *International Journal of Rock Mechanics and Mining Sciences, 39*(5), 603-615.

Wang, J. (2004). Influence of stress, undercutting, blasting and time on open stope stability and dilution.

Wang, J., Pakalnis, R., Milne, D., & Lang, B. (2000). *Empirical underground entry type excavation span design modification.* Paper presented at the Proceedings, 53rd Annual Conference, Canadian Geotechnical Society.

Wei, X. Y., Zhao, Z. Y., & Gu, J. (2009). Numerical simulations of rock mass damage induced by underground explosion. *International Journal of Rock Mechanics and Mining Sciences, 46*(7), 1206-1213.

Wood, A. M. (1975). The circular tunnel in elastic ground. *Geotechnique, 25*(1), 115-127.

Yager, R. R. (1978). Fuzzy decision making including unequal objectives. *Fuzzy sets and systems, 1*(2), 87-95.

Yang, R., Bawden, W. F., & Katsabanis, P. D. (1996). A new constitutive model for blast damage. *International Journal of Rock Mechanics and Mining Sciences & Geomechanics Abstracts, 33*(3), 245-254.

Yang, Y.-j., & Zhang, Q. (1998). The application of neural networks to rock engineering systems (RES). *International Journal of Rock Mechanics and Mining Sciences, 35*(6), 727-745.

Yang, Y., & Zhang, Q. (1997). A hierarchical analysis for rock engineering using artificial neural networks. *Rock mechanics and rock engineering, 30*(4), 207-222.

Yao, X., Allen, G., & Willett, M. (1999). *Dilution evaluation using Cavity Monitoring System at HBMS—Trout Lake Mine.* Paper presented at the Proceeding of the 101st CIM annual general meeting, Calgary.

Yiming, W., Guangxu, T., & Xiaohua, C. (1995). A STUDY ON THE NEURAL NETWORK BASED EXPERT SYSTEM FOR MINING METHOD SELECTION [J]. *Computer Applications and Software, 5*, 009.

Yoshikawa, S., & Mogi, K. (1989). Experimental studies on the effect of stress history on acoustic emission activity—a possibility for estimation of rock stress. *Journal of Acoustic Emission, 8*(4), 113-123.

Yu, H., & Wilamowski, B. (2011). Levenberg-marquardt training. *The Industrial Electronics Handbook, 5*, 1-15.

Yun, Q., & Huang, G. (1987). A fuzzy set Approach to the Selection of mining Method. *Mining Science and Technology, 6*(1), 9-16.

Zadeh, L. A. (1965). Fuzzy sets. *Information and control, 8*(3), 338-353.

Zadeh, L. A. (1994). Soft computing and fuzzy logic. *Software, IEEE, 11*(6), 48-56.

Zhang, Q., Mo, Y. b., & Tian, S. f. (1988). *An expert system for classification of rock masses.* Paper presented at the The 29th US Symposium on Rock Mechanics (USRMS).

Zhang, Y.-Q., Hao, H., & Lu, Y. (2003). Anisotropic dynamic damage and fragmentation of rock materials under explosive loading. *International Journal of Engineering Science, 41*(9), 917-929.

APPENDIX A: SCATTER PLOTS OF COLLECTED TEN UB CAUSATIVE FACTORS AGAINST PERCENTAGE OF ACTUAL UNEVEN BREAK (UB)

(1,067 datasets after the second filtering stage)

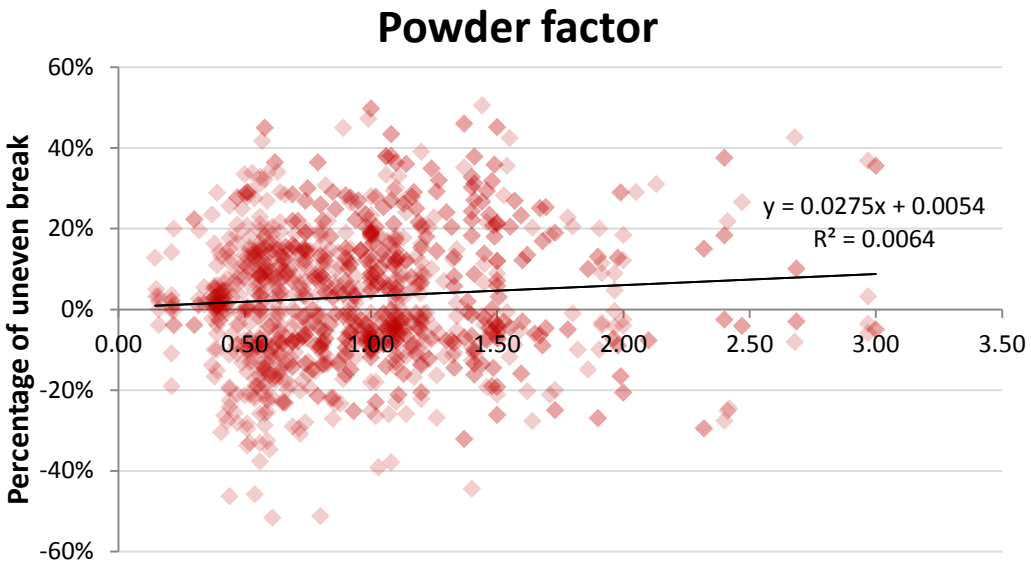

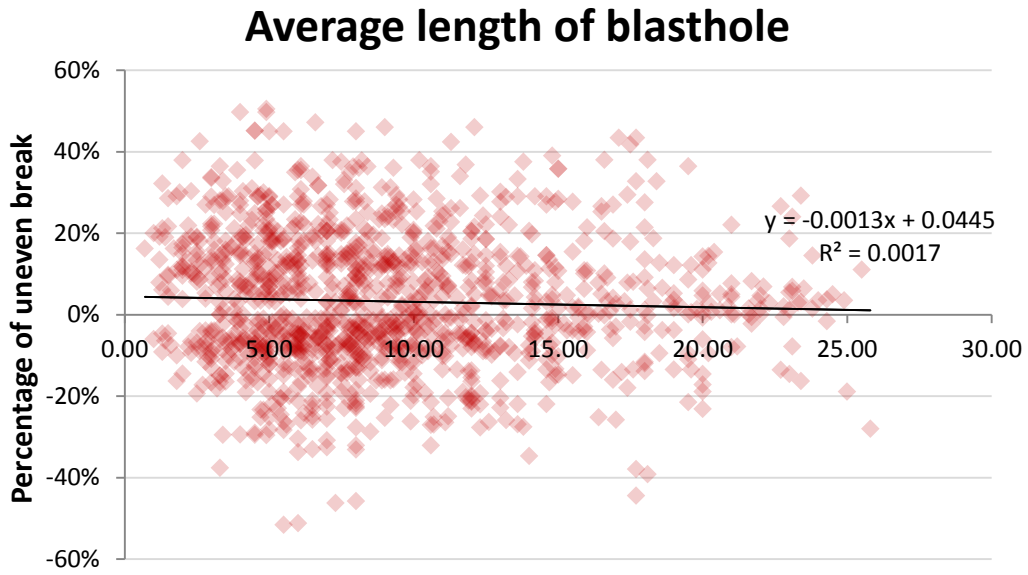

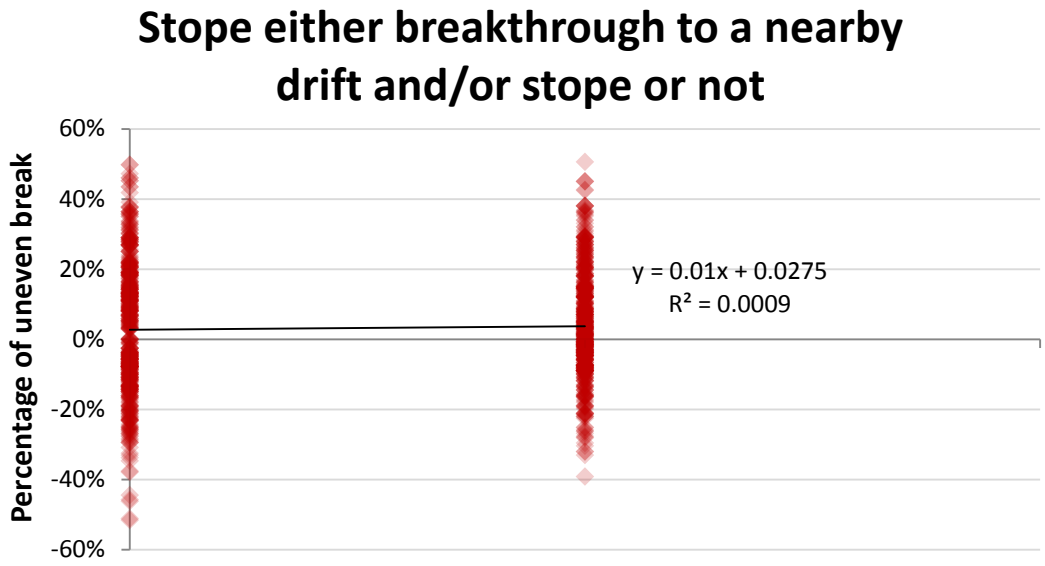
Stope either breakthrough to a nearby drift and/or stope or not
Percentage of uneven break
60%
40%
20%
0%
-20%
-40%
-60%
y = 0.01x + 0.0275
R² = 0.0009

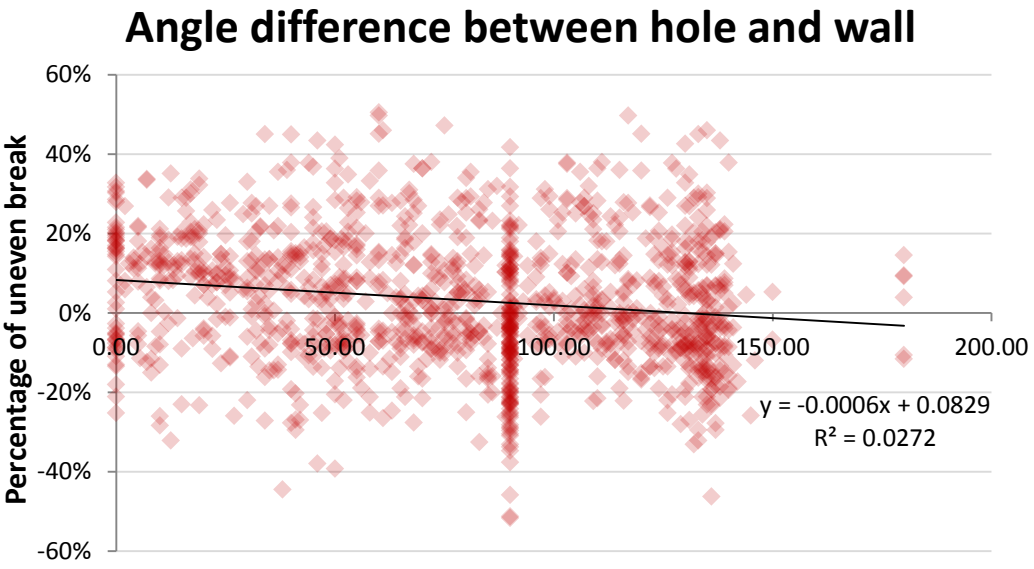
Angle difference between hole and wall
Percentage of uneven break
60%
40%
20%
0%
-20%
-40%
-60%
0.00
50.00
100.00
150.00
200.00
y = -0.0006x + 0.0829
R² = 0.0272

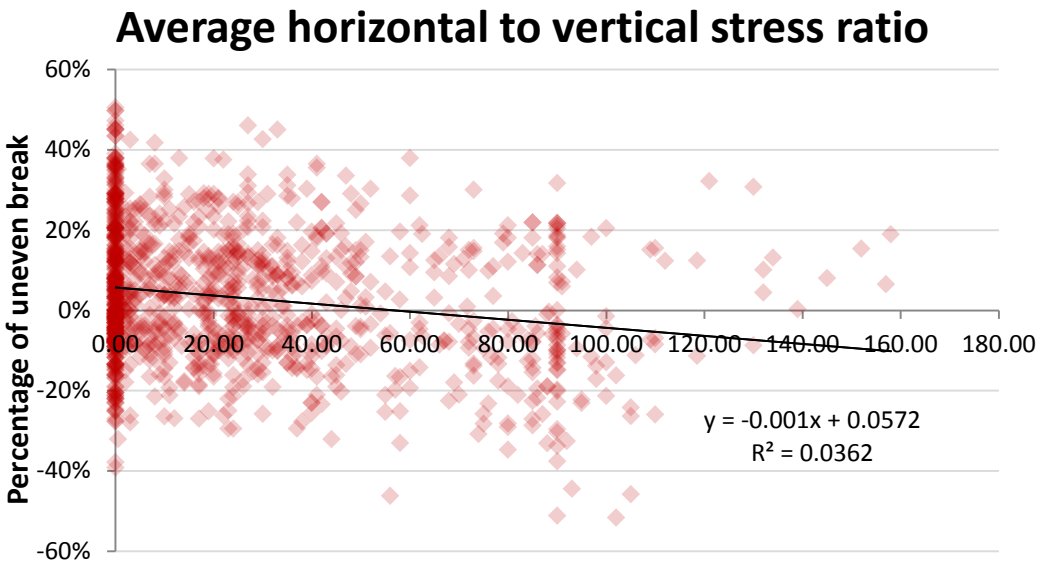
Average horizontal to vertical stress ratio
Percentage of uneven break
60%
40%
20%
0%
-20%
-40%
-60%
0.00
20.00
40.00
60.00
80.00
100.00
120.00
140.00
160.00
180.00
y = -0.001x + 0.0572
R² = 0.0362

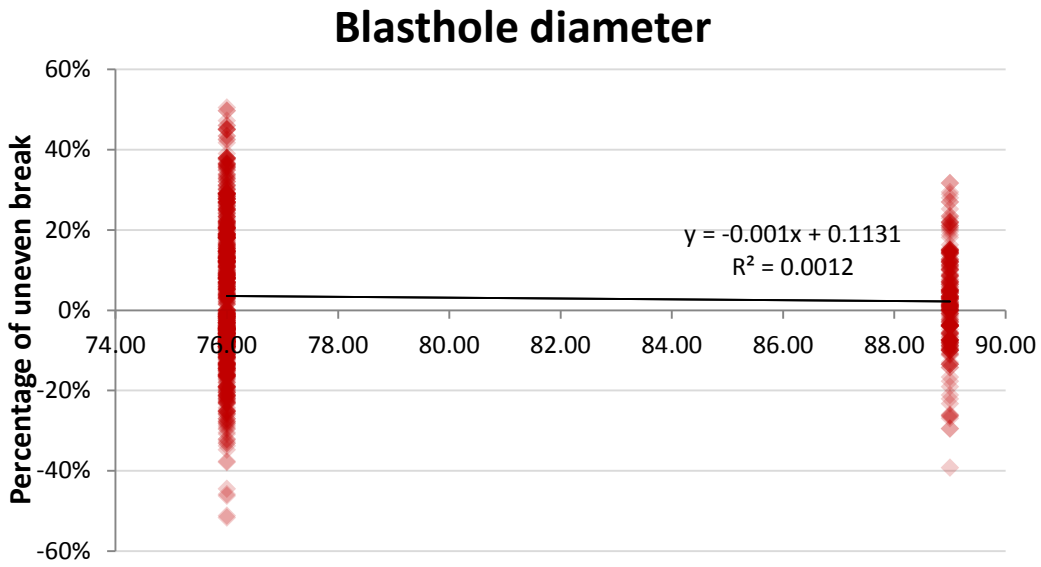
Blasthole diameter
Percentage of uneven break
60%
40%
20%
0%
-20%
-40%
-60%
74.00
76.00
78.00
80.00
82.00
84.00
86.00
88.00
90.00
y = -0.001x + 0.1131
R² = 0.0012

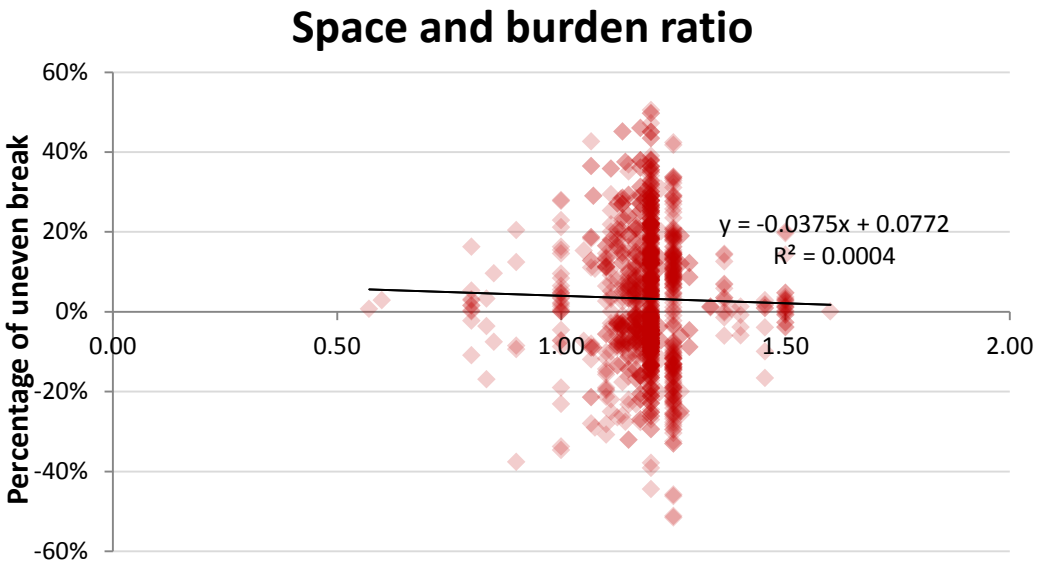
Space and burden ratio
Percentage of uneven break
60%
40%
20%
0%
-20%
-40%
-60%
0.00
0.50
1.00
1.50
2.00
y = -0.0375x + 0.0772
R² = 0.0004

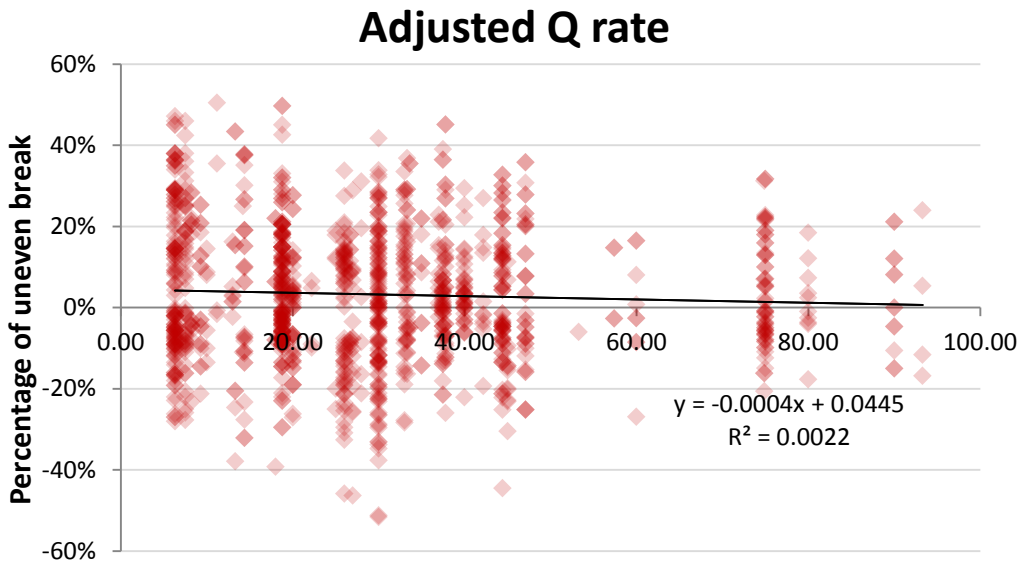
Adjusted Q rate
Percentage of uneven break
60%
40%
20%
0%
-20%
-40%
-60%
0.00
20.00
40.00
60.00
80.00
100.00
y = -0.0004x + 0.0445
R² = 0.0022

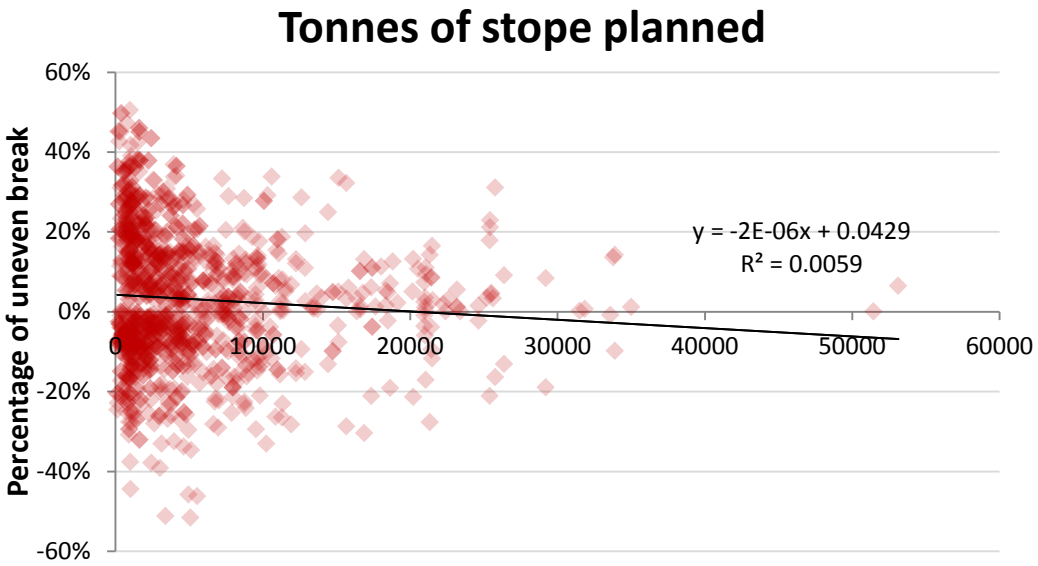
Tonnes of stope planned
Percentage of uneven break
60%
40%
20%
0%
-20%
-40%
-60%
0
10000
20000
30000
40000
50000
60000
y = -2E-06x + 0.0429
R² = 0.0059

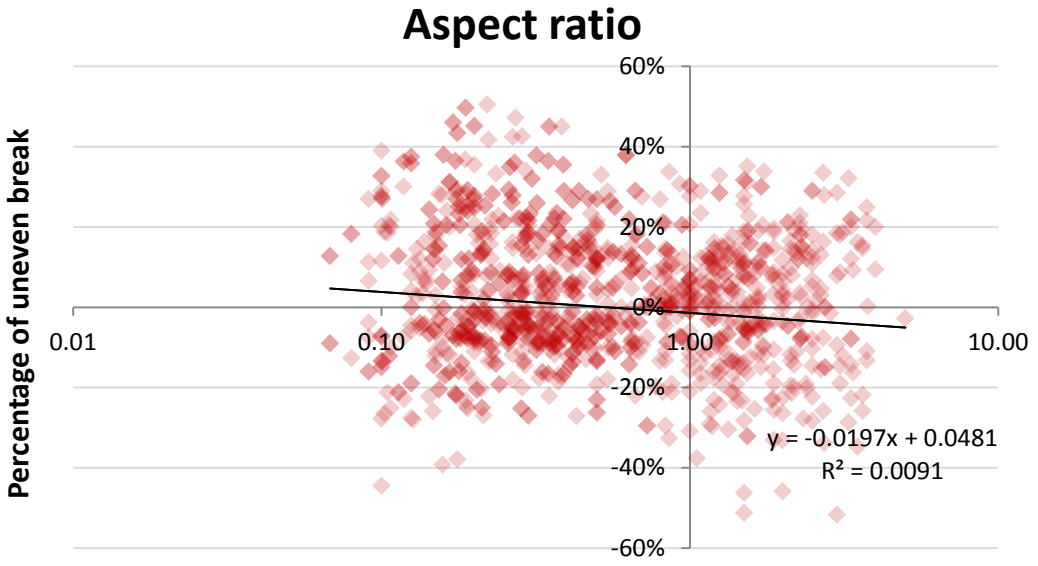
Aspect ratio
Percentage of uneven break
60%
40%
20%
0%
-20%
-40%
-60%
0.01
0.10
1.00
10.00
y = -0.0197x + 0.0481
R² = 0.0091

APPENDIX B: SOME OF MATLAB CODES OF PROPOSED ARTIFICIAL NEURAL NETWORK

Definition of code:

Xdim: dimention of Xnorm_train

Xnorm_train: normalised dataset for training

k: iteration

traansfunc: transfer function

tanh-tanh: hyperbolic tangent function

Wij: weights matrix from j layer to i layer

Wjk: weights matrix from k layer to j layer

Wij_best: trained weights matrix from j layer to i layer

Wjk_best: trained weights matrix from k layer to j layer

J_record: Jacobian matrix

ANN Training function

```
function        [Wij_best,Wjk_best,k,corref_train,corref_valid,corref_test]        =
train_neural_network_with_SCPG(Xnorm_train,Ynorm_train,...
Xnorm_valid,Ynorm_valid,Xnorm_test,Ynorm_test,N_hidden_neuron,N_output_neuron,
regLambda, reps, maxiter )
%TRAIN_NEURAL_NETWORK_WITH_CPG


%% parameter setup


Xdim = size(Xnorm_train,1);   % dimention of Xnorm_train


k = 1;


transfunc = 'tanh-tanh';


sigma0 = 1e-6;
lambda = 1;
lambda_bar = 0;


Wij = (rand(N_hidden_neuron, Xdim+1)-0.5);
Wjk = (rand(N_output_neuron, N_hidden_neuron+1 )-0.5);
Wij_best = Wij;
Wjk_best = Wjk;


J_record = zeros(1,maxiter);
```

```
Jvalid_record =  zeros(1,maxiter);


%%

 J_record(1)  =  evaluate_objective_function(Xnorm_train,  Ynorm_train,  Wij,  Wjk,
transfunc, regLambda);

Jvalid_record(1) = evaluate_objective_function(Xnorm_valid, Ynorm_valid, Wij, Wjk,
transfunc, regLambda);


w = reshape_weight_matrix_to_vector(Wij, Wjk);


p  =  -1  *  evaluate_gradient_of_objective_function(Xnorm_train,  Ynorm_train,  Wij,
Wjk, transfunc, regLambda);


N = size(p,1);


r = p;

[Pij, Pjk] = reshape_weight_vector_to_matrix(p, Xdim, N_hidden_neuron);


success = true;


while k < maxiter



    if success == true

        sigma = sigma0/norm(p);


        s =(  evaluate_gradient_of_objective_function(Xnorm_train,  Ynorm_train,  Wij
+ sigma *Pij, Wjk +sigma * Pjk, transfunc, regLambda) ...

               -  evaluate_gradient_of_objective_function(Xnorm_train,  Ynorm_train,
Wij, Wjk, transfunc, regLambda))/sigma;

        delta = p' * s;

    end


    delta

    lambda

    lambda_bar


    norm(p)



    s = s + (lambda - lambda_bar) * p;

    delta = delta + (lambda - lambda_bar) * (p'*p);




    if delta <= 0

        s = s + (lambda - 2 * delta / (p'*p) ) * p;

        lambda_bar = 2 * (lambda - delta / (p'*p) );
```

```
        delta = - delta + lambda *  (p'*p);
        lambda = lambda_bar;
    end


    mu = p' * r;
    alpha = mu / delta;


    Delta = 2 * delta * (evaluate_objective_function(Xnorm_train, Ynorm_train, Wij,
Wjk, transfunc, regLambda) ...
                        - evaluate_objective_function(Xnorm_train, Ynorm_train, Wij
+ alpha *Pij, Wjk +alpha * Pjk, transfunc, regLambda) ) / (mu^2);


    if Delta >= 0
        disp('update');
        w = w + alpha * p;
        [Wij, Wjk] = reshape_weight_vector_to_matrix(w, Xdim, N_hidden_neuron);
        r_prev = r;
        r = -1 * evaluate_gradient_of_objective_function(Xnorm_train, Ynorm_train,
Wij, Wjk, transfunc, regLambda);
        lambda_bar = 0;
        success = true;


        if mod(k,N) == 0
            p = r;
        else
            beta = (r'*r - r'*r_prev) / mu;
            p = r + beta * p;
            [Pij, Pjk] = reshape_weight_vector_to_matrix(p, Xdim, N_hidden_neuron);
        end


        if Delta >= 0.75
                lambda = lambda/2;
        end


    else
        lambda_bar = lambda;
        success = false;
    end



    if Delta < 0.25
        lambda = 4 * lambda;
    end


    if norm(r) < reps
        disp(' norm(r) is less than reps');
        break;
```

```
    end


    [Wij, Wjk] = reshape_weight_vector_to_matrix(w, Xdim, N_hidden_neuron);


    figure (1);


    subplot(2,2,1); title('Training Error');
    J_record(k) = evaluate_objective_function(Xnorm_train, Ynorm_train, Wij, Wjk,
transfunc, regLambda);
    plot(1:(k-1), J_record(1:(k-1))/size(Xnorm_train,2));


    subplot(2,2,2); title('Validation Error');
    Jvalid_record(k) = evaluate_objective_function(Xnorm_valid, Ynorm_valid, Wij,
Wjk, transfunc, regLambda);
    plot(Jvalid_record(1:(k-1))/size(Xnorm_valid,2));


    subplot(2,2,3); title('Trainining');
      corref_train = plot_performance_of_neural_network(Xnorm_train, Ynorm_train,
Wij, Wjk, transfunc);


    subplot(2,2,4);title('Validation');
      corref_valid = plot_performance_of_neural_network(Xnorm_valid, Ynorm_valid,
Wij, Wjk, transfunc);




drawnow;


    k = k + 1


end


[Wij_best, Wjk_best] = reshape_weight_vector_to_matrix(w, Xdim, N_hidden_neuron);



% % performance index figure
%
% figure (2);
% plot (Ynn, 'linewidth',2, 'color', [0,0,1])
% hold on
% plot (Yss, 'linewidth',2, 'color', [0,1,0], 'linestyle', ':')
% title('Comparison between measured & predicted uneven break', 'fontsize', 12,
'fontweight','bold');
% xlabel('PATTERNS','fontsize',11);
% ylabel('UNEVEN BREAK','fontsize',11);
%
% figure(4);
% plotregression(Yn, Yk)
```

ANN forward process(Run ANN) function

```
function [z_out, h_out, x_out] = run_neural_network(x_in,Wij,Wjk, ~)


 transfunc = 'tanh-tanh';   % changing code part

N_datasets = size(x_in,2);

x_out = [x_in;ones(1,N_datasets)];

h_in = Wij*x_out;
h_out = [tanh(h_in);ones(1,N_datasets)];

z_in = Wjk*h_out;


if strcmp(transfunc, 'tanh-tanh')
    z_out = tanh(z_in);
elseif strcmp(transfunc, 'tanh-x')
    z_out = (z_in);

end
```

APPENDIX C: GRAPHICAL VIEW OF SURVEY RESULTS FOR UB CONSULTATION FUZZY EXPERT SYSTEM

MO, O, A, U, and MU represent massive overbreak, overbreak, acceptable range, underbreak, massive underbreak.

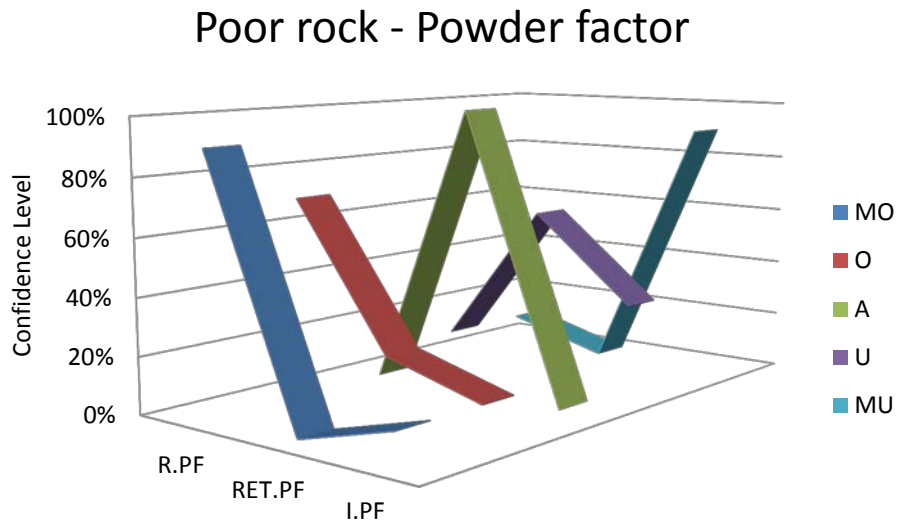

Appendix C-1 Survey results in condition of poor rock subject to powder factor

R, RET, and I.PF represent reduce, retain, and increase powder factor

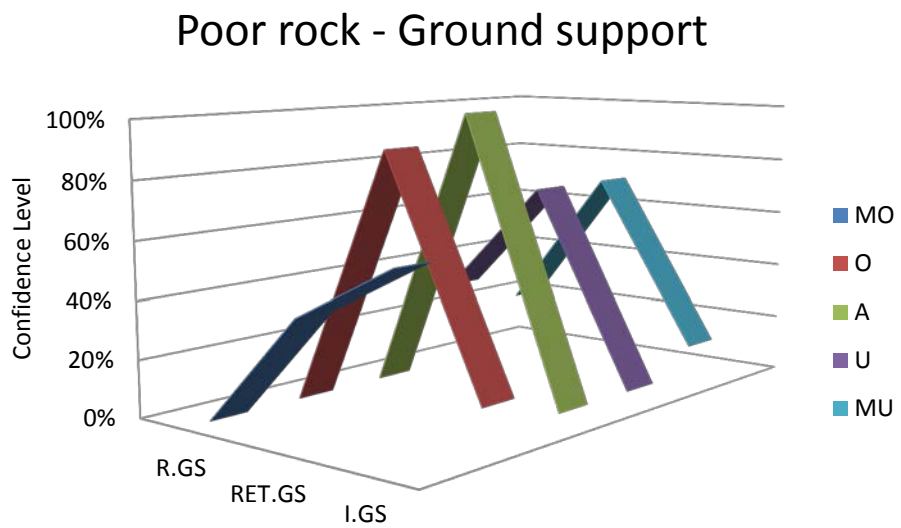

Appendix C-2 Survey results in condition of poor rock subject to ground support

R, RET, and I.GS represent reduce, retain, and increase ground support

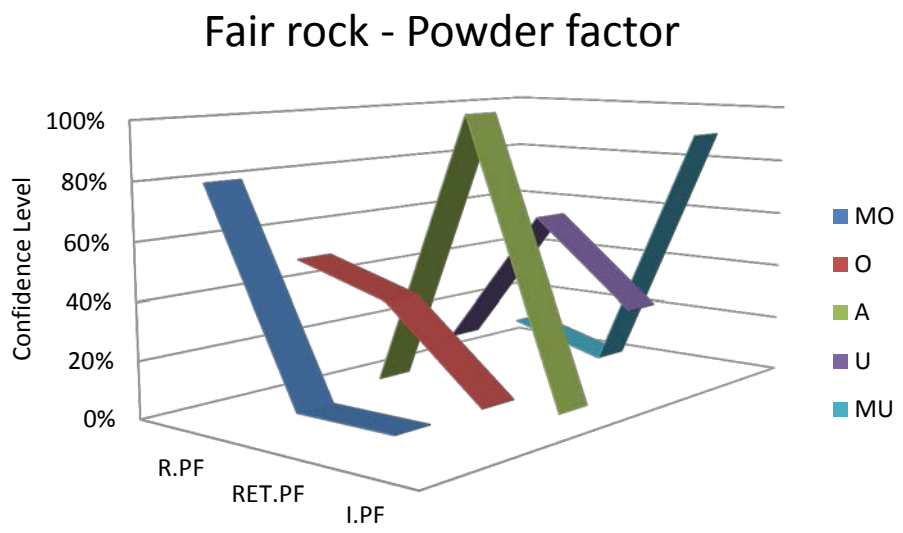

Appendix C-3 Survey results in condition of fair rock subject to powder factor

R, RET, and I.PF represent reduce, retain, and increase powder factor

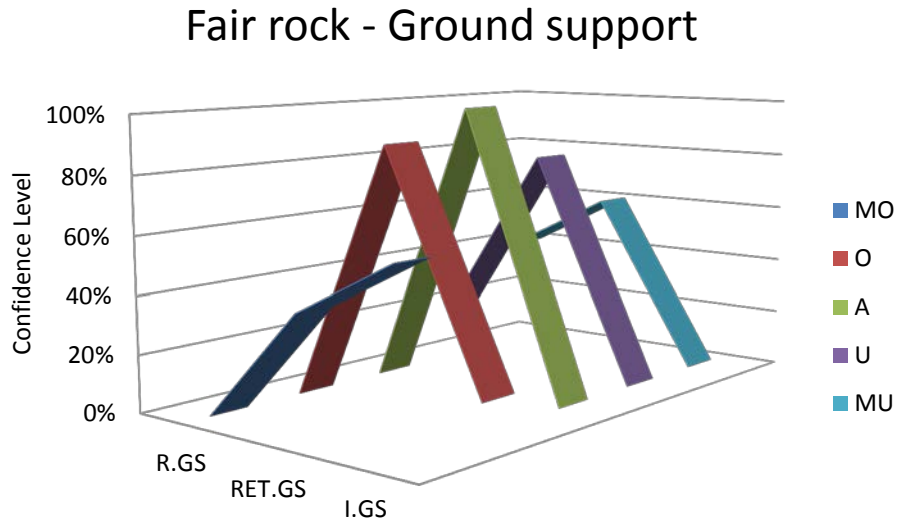

Appendix C-4 Survey results of in condition fair rock subject to ground support

R, RET, and I.GS represent reduce, retain, and increase ground support

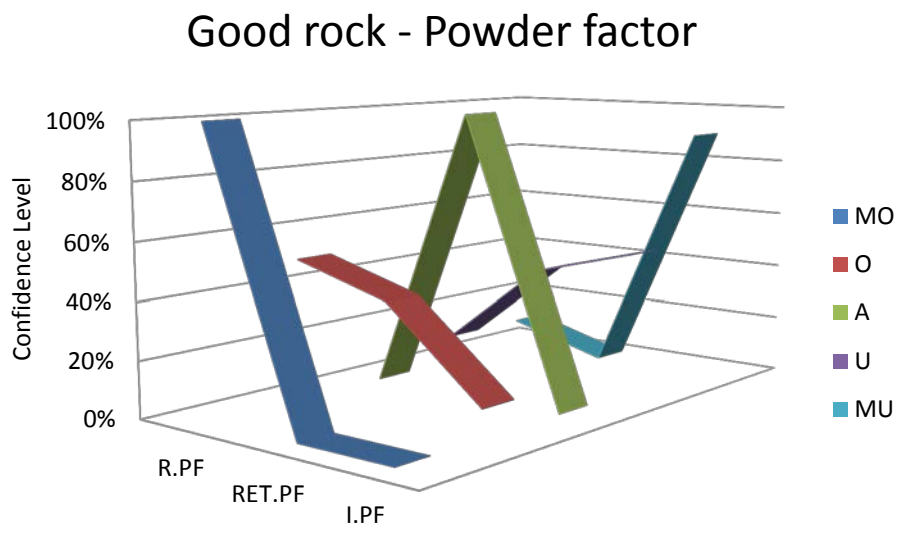

Appendix C-5 Survey results in condition of good rock subject to powder factor

R, RET, and I.PF represent reduce, retain, and increase powder factor

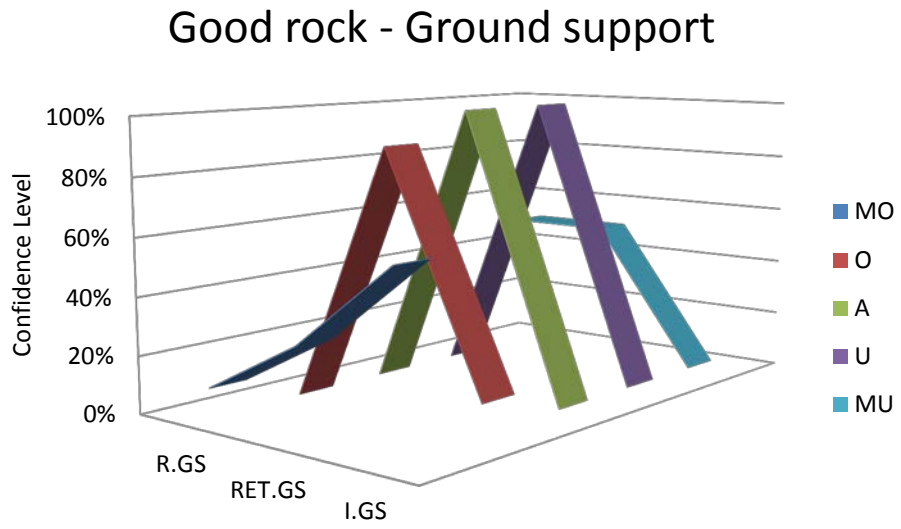

Appendix C-6 Survey results in condition of good rock subject to ground support

R, RET, and I.GS represent reduce, retain, and increase ground support

APPENDIX D: INFORMATION OF MULTIPLE LINIER AND NONLINEAR REGRESSION MODELS OF MINE-A, MINE-B, MINE-C, AND GM MODEL

Table-appendix D
Details of ten UB causative factors employed in multiple linear and nonlinear regression models

Category			Abbr.	Unit	Range	Note
Input (independent variables)	Controllable	Blasting	*Blen*	m	0.70 ~ 25.80	Average length of blasthole
			Pf	Kg/t	0.15~ 3.00	Powder factor
			AHW	°	0.00 ~ 170.20	Angle difference between hole and wall
			Bdia	mm	76 ~ 89	Blasthole diameter
			SbR	(S/B)[1]	0.57 ~ 1.50	Space and burden ratio
		Stope design	*Pt*	T	130 ~ 51,450	Tonnes of stope planned
			AsR	(W/H)[3]	0.07 ~ 4.17	Aspect ratio
			BTBL	-	Breakthrough (0) ~ Blind (1)	Stope either breakthrough to a nearby drift and/or stope or not
	uncontrollable	Geology	*AQ*	-	6.30 ~ 93.30	Adjusted Q rate
			K	(H/V)[2]	1.74 ~ 14.38	Average horizontal to vertical stress ratio
Output (dependent variable)			*UB*	%	-65.40 ~ 92.00	Percentage of uneven stope break (over and under breaks)

*[1]**S/B:** ratio between toe space (S) and ring burden (B); [2]**H/V:** ratio between average horizontal (H) and vertical (V) stress; [3]**W/H:** ratio between width (W) and height (H) of stope*

Mine-A (Multiple linear regression - Enter model)

Variables Entered		
Variables Entered	Variables Removed	Method
K, AHW, AQ, SBR, BTBL, PF, ASR, PT, BLEN, BDIA	.	Enter

Dependent Variable: UB

Model Summary					
R	R Square	Adjusted R Square	Std. Error of the Estimate	Change Statistics	
				R Square Change	F Change
.581	.338	.280	.04219633	.338	5.863

Coefficients					
Variables	Unstandardized Coefficients		Standardized Coefficients	t	Sig.
	B	Std. Error	Beta		
(Constant)	.969	.636		1.523	.130
BTBL	-.018	.019	-.108	-.932	.353
BLEN	-.009	.022	-.045	-.422	.674
PF	.375	.060	.555	6.240	.000
AHW	-.067	.030	-.214	-2.212	.029
BDIA	.024	.027	.125	.898	.371
SBR	.017	.020	.081	.830	.408
AQ	-.091	.049	-.163	-1.874	.063
PT	.048	.025	.179	1.926	.057
ASR	.042	.024	.170	1.767	.080
K	.104	.622	.019	.168	.867

Mine-A (Multiple linear regression - Stepwise model)

Model Summary					
R	R Square	Adjusted R Square	Std. Error of the Estimate	Change Statistics	
				R Square Change	F Change
.567	.322	.293	.04180247	-.010	1.728

Coefficients					
Variables	Unstandardized Coefficients		Standardized Coefficients	t	Sig.
	B	Std. Error	Beta		
(Constant)	1.088	.095		11.464	.000
PF	.377	.055	.559	6.901	.000
AHW	-.048	.026	-.153	-1.826	.070
AQ	-.093	.046	-.166	-2.032	.044
PT	.039	.021	.144	1.849	.067
ASR	.044	.021	.180	2.074	.040

Excluded Variables					
Variables	Beta In	t	Sig.	Partial Correlation	Collinearity Statistics
					Tolerance
K	.013f	.136	.892	.012	.614
BLEN	-.009f	-.097	.923	-.009	.659
BDIA	.055f	.683	.496	.062	.885
BTBL	-.025f	-.313	.755	-.029	.881
SBR	.111f	1.314	.191	.120	.783

Dependent Variable: UB
Predictors in the Model: (Constant), AHW, AQ, PF, ASR, PT

Mine-A (Multiple nonlinear regression model)

MODEL PROGRAM: a=1.088 b=0.377 c=-.048 d=-.093 e=.039 f=.044.

COMPUTE_ PRED= a *(PF ** (b))*(AHW ** (c))*(AQ ** (d))*(PT ** (e))*(ASR ** (f)).

Iteration History						
Iteration Number	Residual Sum of Squares	Parameter				
		a	b	c	d	e
1.0	12.914	1.088	.377	-.048	-.093	.039
1.1	.213	1.407	.288	-.038	-.091	.035
2.0	.213	1.407	.288	-.038	-.091	.035
2.1	.211	1.407	.306	-.040	-.090	.036
3.0	.211	1.407	.306	-.040	-.090	.036
3.1	.211	1.407	.306	-.040	-.090	.035
4.0	.211	1.407	.306	-.040	-.090	.035
4.1	.211	1.407	.306	-.040	-.090	.035

- Derivatives are calculated numerically.
- Major iteration number is displayed to the left of the decimal, and minor iteration number is to the right of the decimal.
- Run stopped after 12 model evaluations and 6 derivative evaluations because the relative reduction between successive residual sums of squares is at most SSCON = 1.00E-008.

ANOVA			
Source	Sum of Squares	df	Mean Squares
Regression	260.274	6	43.379
Residual	.211	120	.002
Uncorrected Total	260.485	126	
Corrected Total	.309	125	

- Dependent variable: UB
- R squared = 1 - (Residual Sum of Squares) / (Corrected Sum of Squares) = .317.

Mine-B (Multiple linear regression - Enter model)

Variables Entered		
Variables Entered	Variables Removed	Method
K, AHW, BLEN, PF, BTBL, SBR, ASR, PT, AQ	.	Enter

Dependent Variable: UB

Model Summary					
R	R Square	Adjusted R Square	Std. Error of the Estimate	Change Statistics	
				R Square Change	F Change
.590	.348	.322	.10683669	.348	13.127

Coefficients					
Variables	Unstandardized Coefficients		Standardized Coefficients	t	Sig.
	B	Std. Error	Beta		
(Constant)	-.651	1.509		-.432	.666
BTBL	.005	.016	.019	.333	.740
BLEN	-.162	.044	-.211	-3.718	.000
PF	.123	.154	.047	.802	.424
AHW	-.137	.033	-.237	-4.110	.000
SBR	-.052	.080	-.037	-.644	.520
AQ	-.756	.105	-.436	-7.224	.000
PT	.018	.057	.019	.318	.751
ASR	-.037	.036	-.059	-1.030	.304
K	3.229	1.460	.137	2.212	.028

Mine-B (Multiple linear regression - Stepwise model)

Model Summary					
R	R Square	Adjusted R Square	Std. Error of the Estimate	Change Statistics	
				R Square Change	F Change
.584	.341	.330	.10622956	-.004	1.460

Coefficients					
Variables	Unstandardized Coefficients		Standardized Coefficients	t	Sig.
	B	Std. Error	Beta		
(Constant)	.114	1.391		.082	.935
BLEN	-.158	.042	-.206	-3.777	.000
AHW	-.144	.032	-.250	-4.476	.000
AQ	-.756	.104	-.436	-7.304	.000
K	2.528	1.366	.107	1.850	.066

Excluded Variables					
Variables	Beta In	t	Sig.	Partial Correlation	Collinearity Statistics
					Tolerance
PT	-.007f	-.130	.897	-.009	.941
BTBL	.020f	.360	.719	.024	.946
SBR	-.037f	-.663	.508	-.044	.945
PF	.043f	.778	.438	.052	.978
ASR	-.068f	-1.208	.228	-.080	.929

Dependent Variable: UB
Predictors in the Model: (Constant), K, AHW, BLEN, AQ

Mine-B (Multiple nonlinear regression model)

MODEL PROGRAM: a=0.114 b=-.158 c=-.144 d=-.756 e=2.528.

COMPUTE_ PRED=a * (BLEN ** (b))*(AHW ** (c))*(AQ ** (d))*(K ** (e)).

Iteration History

Iteration Number	Residual Sum of Squares	Parameter				
		a	b	c	d	e
1.0	394.482	.114	-.158	-.144	-.756	2.528
1.1	50.420	1.669	-.245	-.405	.714	-14.250
2.0	50.420	1.669	-.245	-.405	.714	-14.250
2.1	7.981	1.472	-.133	-.056	-1.405	10.145
3.0	7.981	1.472	-.133	-.056	-1.405	10.145
3.1	2.464	1.637	-.163	-.149	-.746	2.264
4.0	2.464	1.637	-.163	-.149	-.746	2.264
4.1	2.446	1.669	-.164	-.162	-.652	1.348
5.0	2.446	1.669	-.164	-.162	-.652	1.348
5.1	2.446	1.669	-.164	-.163	-.652	1.359
6.0	2.446	1.669	-.164	-.163	-.652	1.359
6.1	2.446	1.669	-.164	-.163	-.652	1.359

- Derivatives are calculated numerically.
- a. Major iteration number is displayed to the left of the decimal, and minor iteration number is to the right of the decimal.
- b. Run stopped after 12 model evaluations and 6 derivative evaluations because the relative reduction between successive residual sums of squares is at most SSCON = 1.00E-008.

ANOVA

Source	Sum of Squares	df	Mean Squares
Regression	453.593	5	90.719
Residual	2.446	226	.011
Uncorrected Total	456.040	231	
Corrected Total	3.871	230	

- Dependent variable: UB
- R squared = 1 - (Residual Sum of Squares) / (Corrected Sum of Squares) = .368.

Mine-C (Multiple linear regression - Enter model)

Variables Entered		
Variables Entered	Variables Removed	Method
K, PF, BLEN, SBR, BDIA, BTBL, AQ, AHW, ASR, PT	.	Enter

Dependent Variable: UB

Model Summary					
R	R Square	Adjusted R Square	Std. Error of the Estimate	Change Statistics	
				R Square Change	F Change
.422	.178	.166	.11684428	.178	15.126

Coefficients					
Variables	Unstandardized Coefficients		Standardized Coefficients	t	Sig.
	B	Std. Error	Beta		
(Constant)	1.129	.195		5.791	.000
BTBL	.034	.009	.132	3.655	.000
BLEN	-.125	.033	-.155	-3.823	.000
PF	.140	.031	.170	4.532	.000
AHW	-.138	.027	-.211	-5.146	.000
BDIA	-.026	.013	-.079	-1.924	.055
SBR	.123	.090	.048	1.369	.171
AQ	-.133	.019	-.267	-6.876	.000
PT	.135	.111	.052	1.213	.226
ASR	.203	.035	.241	5.740	.000
K	.021	.035	.022	.600	.549

Mine-C (Multiple linear regression - Stepwise model)

Model Summary					
R	R Square	Adjusted R Square	Std. Error of the Estimate	Change Statistics	
				R Square Change	F Change
.412	.170	.163	.11706927	-.003	2.501

Coefficients					
Variables	Unstandardized Coefficients		Standardized Coefficients	t	Sig.
	B	Std. Error	Beta		
(Constant)	1.489	.087		17.043	.000
BTBL	.033	.009	.127	3.565	.000
BLEN	-.127	.030	-.157	-4.177	.000
PF	.134	.030	.163	4.499	.000
AHW	-.143	.026	-.218	-5.408	.000
AQ	-.125	.019	-.252	-6.575	.000
ASR	.190	.034	.226	5.544	.000

Excluded Variables					
	Beta In	t	Sig.	Partial Correlation	Collinearity Statistics
					Tolerance
K	.031e	.888	.375	.033	.941
PT	.020e	.501	.616	.019	.759
SBR	.053e	1.545	.123	.058	.986
BDIA	-.059e	-1.581	.114	-.060	.833

Dependent Variable: UB
Predictors in the Model: (Constant), PF, BLEN, BTBL, AQ, AHW, ASR

Mine-C (Multiple nonlinear regression model)

MODEL PROGRAM: a=1.489 b=.033 c=-.127 d=.134 e=-.143 f=-.125 g=.190.

COMPUTE_ PRED= a * (BTBL ** (b))*(BLEN ** (c))*(PF ** (d))*(AHW ** (e))*(AQ ** (f))*(ASR ** (g)).

Iteration History

Iteration Number	Residual Sum of Squares	Parameter				
		a	b	c	d	e
1.0	10.561	1.489	.033	-.127	.134	-.143
1.1	9.513	1.455	.033	-.129	.129	-.126
2.0	9.513	1.455	.033	-.129	.129	-.126
2.1	9.513	1.455	.033	-.129	.129	-.126
3.0	9.513	1.455	.033	-.129	.129	-.126
3.1	9.513	1.455	.033	-.129	.129	-.126

- Derivatives are calculated numerically.
- Major iteration number is displayed to the left of the decimal, and minor iteration number is to the right of the decimal.
- Run stopped after 6 model evaluations and 3 derivative evaluations because the relative reduction between successive residual sums of squares is at most SSCON = 1.00E-008.

ANOVA

Source	Sum of Squares	df	Mean Squares
Regression	1501.466	7	214.495
Residual	9.513	703	.014
Uncorrected Total	1510.979	710	
Corrected Total	11.608	709	

- Dependent variable: UB
- R squared = 1 - (Residual Sum of Squares) / (Corrected Sum of Squares) = .181.

GM (Multiple linear regression - Enter model)

Variables Entered		
Variables Entered	Variables Removed	Method
K, SBR, AHW, BDIA, AQ, BTBL, PT, ASR, BLEN, PF	.	Enter

Dependent Variable: UB

Model Summary					
R	R Square	Adjusted R Square	Std. Error of the Estimate	Change Statistics	
				R Square Change	F Change
.423	.179	.171	.1125870	.179	22.989

Coefficients					
Variables	Unstandardized Coefficients		Standardized Coefficients	t	Sig.
	B	Std. Error	Beta		
(Constant)	1.521	.099		15.297	.000
BTBL	.029	.008	.117	3.783	.000
BLEN	-.119	.022	-.188	-5.374	.000
PF	.123	.026	.168	4.715	.000
AHW	-.152	.019	-.262	-7.923	.000
BDIA	.013	.009	.046	1.430	.153
SBR	.015	.034	.013	.445	.657
AQ	-.113	.017	-.198	-6.592	.000
PT	.023	.036	.022	.635	.526
ASR	.069	.021	.117	3.291	.001
K	.039	.032	.037	1.220	.223

GM (Multiple linear regression - Stepwise model)

Model Summary					
R	R Square	Adjusted R Square	Std. Error of the Estimate	Change Statistics	
				R Square Change	F Change
.419	.175	.171	.1126026	-.002	2.362

Coefficients					
Variables	Unstandardized Coefficients		Standardized Coefficients	t	Sig.
	B	Std. Error	Beta		
(Constant)	1.595	.069		23.263	.000
BTBL	.031	.007	.125	4.165	.000
BLEN	-.105	.020	-.166	-5.281	.000
PF	.122	.024	.166	4.973	.000
AHW	-.149	.019	-.258	-7.815	.000
AQ	-.106	.017	-.187	-6.346	.000
ASR	.073	.020	.124	3.629	.000

Excluded Variables					
Variables	Beta In	t	Sig.	Partial Correlation	Collinearity Statistics
					Tolerance
SBR	.015e	.518	.605	.016	.969
PT	.022e	.640	.522	.020	.647
K	.035e	1.163	.245	.036	.873
BDIA	.049e	1.537	.125	.047	.756

Dependent Variable: UB
Predictors in the Model: (Constant), AHW, AQ, PF, ASR, PT

GM (Multiple nonlinear regression model)

MODEL PROGRAM: a=1.595 b=.031 c=-.105 d=.122 e=-.149 f=-.106 g=.073.

COMPUTE_ PRED= a * (BTBL ** (b))*(BLEN ** (c))*(PF ** (d))*(AHW ** (e))*(AQ ** (f))*(ASR ** (g)).

Iteration History						
Iteration Number	Residual Sum of Squares	Parameter				
		a	b	c	d	e
1.0	30.571	1.595	.031	-.105	.122	-.149
1.1	13.176	1.473	.031	-.115	.108	-.145
2.0	13.176	1.473	.031	-.115	.108	-.145
2.1	13.176	1.473	.031	-.116	.107	-.144
3.0	13.176	1.473	.031	-.116	.107	-.144
3.1	13.176	1.473	.031	-.116	.107	-.144

- Derivatives are calculated numerically.
- Major iteration number is displayed to the left of the decimal, and minor iteration number is to the right of the decimal.
- Run stopped after 6 model evaluations and 3 derivative evaluations because the relative reduction between successive residual sums of squares is at most SSCON = 1.00E-008.

ANOVA			
Source	Sum of Squares	df	Mean Squares
Regression	2214.328	7	316.333
Residual	13.176	1060	.012
Uncorrected Total	2227.504	1067	
Corrected Total	16.300	1066	

- Dependent variable: UB
- R squared = 1 - (Residual Sum of Squares) / (Corrected Sum of Squares) = .192

This page has been left as a blank by author